PB-237 425

ATMOSPHERIC PHOTOCHEMICAL SMOG MEASUREMENTS OVER SAN FRANCISCO BAY. APPENDICES

L. A. Cavanagh, et al

Stanford Research Institute

Prepared for:

Environmental Protection Agency
Coordinating Research Council
Air Resources Board, California

August 1973

DISTRIBUTED BY:

NTIS

National Technical Information Service
U. S. DEPARTMENT OF COMMERCE

BIBLIOGRAPHIC DATA SHEET	1. Report No. CRC-APRAC-CAPA-12-72-2	2.	PB 237 425

4. Title and Subtitle
Atmospheric Photochemical Smog Measurements Over San Francisco Bay -- Vol. II -- Appendices

5. Report Date
August 1973

6.

7. Author(s)
L. A. Cavanagh and J. H. Smith

8. Performing Organization Rept. No. SRI 2098

9. Performing Organization Name and Address
Stanford Research Institute
Menlo Park, California 94025

10. Project/Task/Work Unit No.
CRC-APRAC-CAPA-12

11. Contract/Grant No.

12. Sponsoring Organization Name and Address
Coordinating Research Council, Inc.,30 Rockefeller Plaza, N.Y., N.Y.; Environmental Protection Agency, Research Triangle Park, N.C. and Air Resources Board, 1025 P St., Sacramento, Cal.

13. Type of Report & Period Covered
Final

14.

15. Supplementary Notes
Not releasable to the public until October 1974

16. Abstracts

In a research program to measure composition and concentration of smog constituents in a moving air parcel, SRI outfitted a houseboat for use as a mobile laboratory and used a helicopter as an airborne laboratory. From these laboratories a research team made measurements over San Francisco Bay in the autumn of 1972. Four sampling days were analyzed extensively, and the observed measurements were correlated. A data tape containing all of the air quality measurements is available. The data from the four selected days were analyzed to determine the correlation of the ratio $\frac{[NO][O_3]}{[NO_2]}$ to solar intensity and NO concentrations.

17. Key Words and Document Analysis. 17a. Descriptors

Air Pollution
Pollutants
Aerosol
Particulates
Photochemical
Aerometric
Carbon Monoxide
Air Parcel
Air Mass
Hydrocarbons
Ozone
Nitrogen Oxides
Aldehydes
Peroxyacyl Nitrates (PAN)

17b. Identifiers/Open-Ended Terms

San Francisco Bay, California

Reproduced by
NATIONAL TECHNICAL
INFORMATION SERVICE
U.S. Department of Commerce
Springfield VA 22151

17c. COSATI Field/Group 13B; 14B; 07E

18. Availability Statement	19. Security Class (This Report)	21. No. of Pages
Releasable to the General Public. I	UNCLASSIFIED	136
	20. Security Class (This Page) UNCLASSIFIED	22. Price $5.75

STANFORD RESEARCH INSTITUTE
Menlo Park, California 94025 · U.S.A.

Final Report Appendices *August 1973*

ATMOSPHERIC PHOTOCHEMICAL SMOG MEASUREMENTS OVER SAN FRANCISCO BAY

By: L. A. CAVANAGH and J. H. SMITH

Prepared for:

COORDINATING RESEARCH COUNCIL
30 ROCKEFELLER PLAZA
NEW YORK, N.Y. 10020

ENVIRONMENTAL PROTECTION AGENCY
DIVISION OF METEOROLOGY
RESEARCH TRIANGLE PARK, NORTH CAROLINA 27711

CRC APRAC CONTRACT CAPA-12-72 and EPA CONTRACT 68-02-1009

AIR RESOURCES BOARD
1025 P STREET
SACRAMENTO, CALIFORNIA 95814

CONTRACT 2-021

SRI Projects 2092 and 2098

Approved by:

R. T. H. COLLIS, *Director*
Atmospheric Sciences Laboratory

R. L. LEADABRAND, *Executive Director*
Electronics and Radio Sciences Division

Appendix A

THE CLIMATOLOGY OF THE SAN FRANCISCO BAY AREA

Appendix A

THE CLIMATOLOGY OF THE SAN FRANCISCO BAY AREA

1. Introduction

The pollution climate of an area is the product of all the meteorological factors that affect atmospheric transport and dispersion, including wind, atmospheric stability, and precipitation. The meteorological factors are disrupted and modified by topographical and geographical features so that very important local effects are observed. Figure A-1 shows the topography of the region. It is characterized by a large body of water and an encircling range of hills. The "Bay" (San Pablo and San Francisco Bays) is the world's largest natural harbor, covering approximately 1000 square kilometers. High densities of population and industrial activity have settled on the low lands surrounding the Bay. Modification of the natural surface is very extensive and is likely to continue or accelerate.

2. Topographic and Geographic Factors

The San Francisco Bay area centers about an elongated body of water enclosed by various mountains and hills that comprise the Coast Ranges. The Golden Gate is one sea level entrance to the Bay; the other is at Carquinez Strait, where the Sacramento River empties into the northeast end of the Bay. The effect of the barrier of hills is to restrict air flow, giving rise to certain typical mesoscale circulation patterns that are governed by the gradient wind field, the thermal stability, and the topography. The effectiveness of the topographic barriers in determining airflow barriers is dependent on weather regime, with summer and fall months providing the greater frequencies of topographically controlled

Preceding page blank

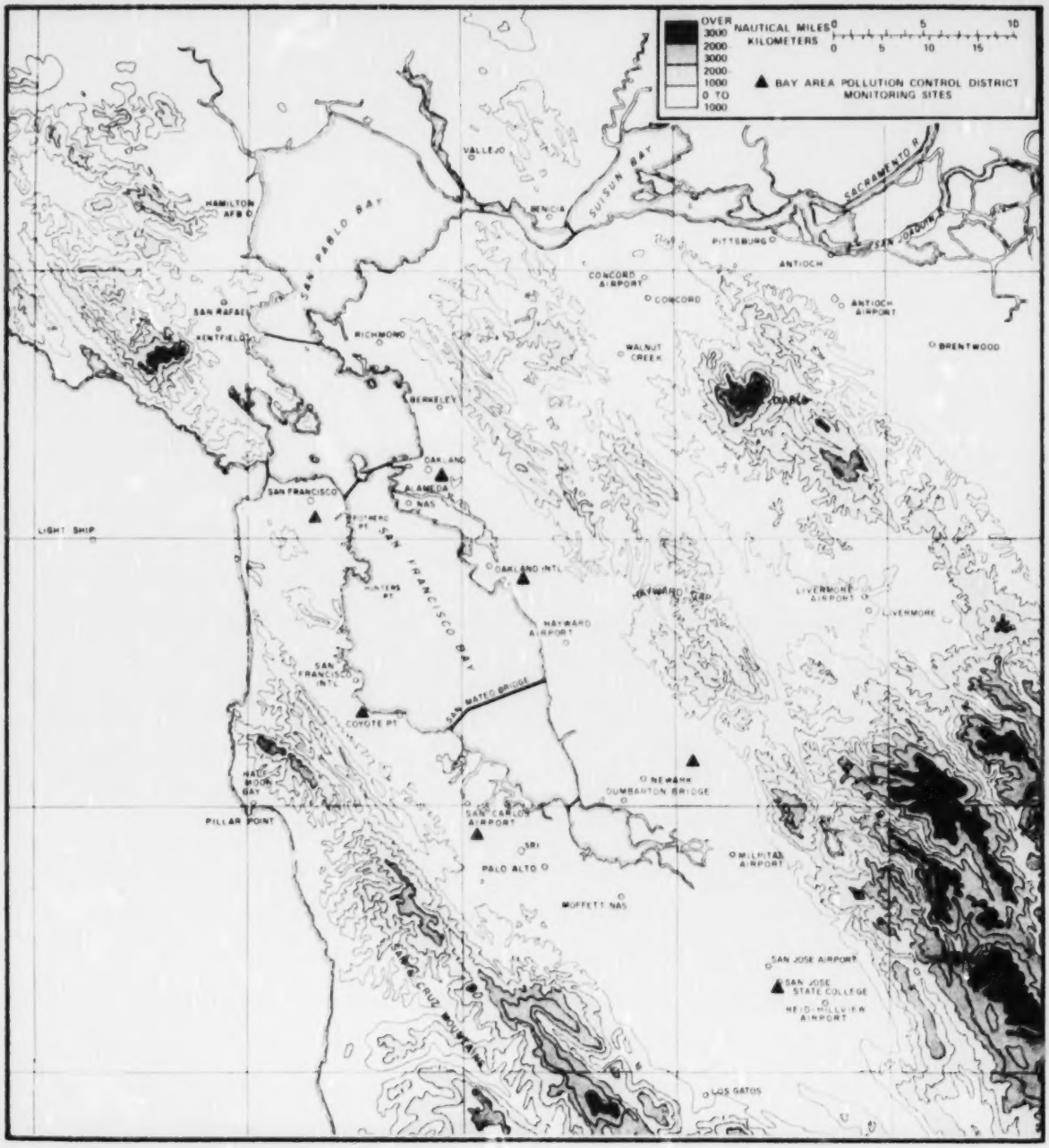

FIGURE A-1 THE SAN FRANCISCO BAY AREA

situations. Typically, during these seasons, there is limited sea-level flow to the east through the narrow Carquinez Strait. There is also some flow into the Livermore area through the Hayward Gap and Niles Canyon. The geography provides a nearly closed system with a uniform base surface.

3. Meteorological Factors

a. Winds

The semipermanent Pacific high that dominates the summer climate of the Bay area reaches its maximum intensity in August. Characteristic features of the high are the persistent west-northwest flow and the strong subsidence inversions above a cold marine layer with its attendant stratus cloud system. Large-scale temperature gradients are at their maximum because a thermal low pressure area develops over the Central Valley of California. During the fall, the Pacific high moves southeastward, merging occasionally with continental high cells to form large, stagnant, blocking systems. Wind speeds decrease, become northerly or northeasterly, and in turn drastically reduce the onshore movement of the cold marine layer. Shorter days and clear nights contribute to the lessening of the large-scale thermal gradient between the ocean and Central California. This, in turn, brings about a seasonal reduction of the onshore wind patterns that, in the summer, carry cool marine air throughout much of the Bay area.

Within the Bay area, wind flow distortion arises when air is channeled by terrain features and forced to rise above or move around hills. Wind observations in the Bay area often show patterns of confluence and diffluence, caused by physical features in the terrain. Differential heating also plays a large role in determining Bay area wind patterns because the total water surface is not much less than the total land surface. The familiar patterns of land-sea breezes is strongest in the summer, but with decreasing solar radiation over the land area in the fall, the onshore sea breeze flow weakens accordingly. Light and variable wind con-

ditions are prevalent favoring air pollution accumulation. Highest frequency of light and variable surface winds occurs during November, as evidenced by Smalley's findings shown in Table A-1.[8]

Table A-1

PERCENTAGE FREQUENCY OF LIGHT-VARIABLE SURFACE WINDS IN THE SAN FRANCISCO BAY AREA (1952 to 1955)[8]

	Time of Day (PST)				
Month	0400 (%)	1000 (%)	1600 (%)	2200 (%)	All Hours (%)
Jan	39	32	30	35	34
Feb	41	29	20	43	33
Mar	31	30	4	26	23
Apr	33	19	1	13	16
May	31	14	2	14	15
Jun	17	7	0	6	7
Jul	12	5	0	4	5
Aug	9	15	0	4	7
Sep	38	38	2	22	22
Oct	52	39	5	34	32
Nov	58	44	23	51	44
Dec	35	27	22	31	29
Annual	33	24	9	24	22

Smalley's study includes a summary of prevalent surface wind flow patterns that occurred over a four-year period. Figure A-2 is an October pattern showing a wind flow typical of the transition from summertime westerly flow to a wintertime north-northeasterly flow. A more recent study by Meteorology Research Inc.[5] found airflow patterns

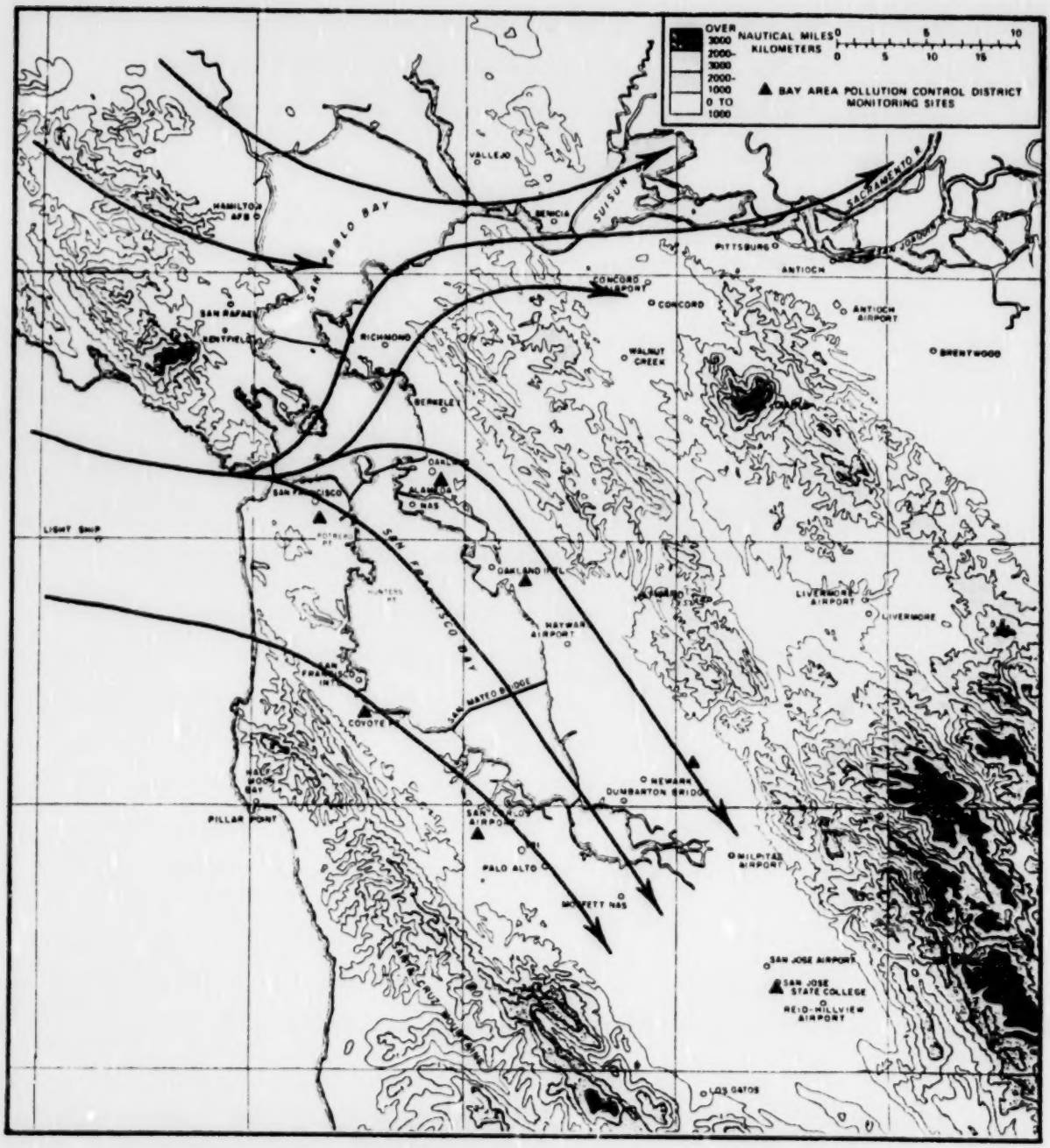

FIGURE A-2 PREVALENT SURFACE WIND FLOW PATTERN FOR OCTOBER

during October afternoons over San Francisco Bay that were essentially the same as those found by Smalley.[9] Incidence of marine air intrusions over mountain tops and passes is restricted by the lowering of the inversion. The implication of such wind patterns for air pollution problems is obvious with pollutants generated in San Francisco and western parts of the area being carried to the east and especially southeast across San Francisco Bay.

b. Temperature

The daytime temperatures in the Bay area are very strongly influenced by the topography. The airflow induced by that topography and the cold coastal waters of the Pacific Ocean (Figure A-3) shows the average maximum temperatures for July.[15] The influence of the Bay is very marked with a cooler tongue of air penetrating over the Bay and southward into San Jose and the Santa Clara Valley. This is partly due to the moderating effect of the Bay waters and partly due to the movement of air cooled by the ocean through the Golden Gate and down the Bay.

Figure A-4 shows the average October maximum temperature field.[16] The same general features are visible as in Figure A-3 for July. However, the gradients are much weaker, indicating less penetration of air from the Pacific. Further evidence of this is indicated by the fact that the average maximum temperatures are higher in San Francisco in October than in July. This is because the influx of cold Pacific air is less frequent in the latter month and lighter wind conditions generally prevail.

c. Inversions

Temperature inversions occur in the Bay area as two general types: summer subsidence inversions and winter radiation inversions. Autumn appears to be a period of transition between the seasonal extremes of a high-subsidence inversion and a low-radiation inversion. Subsidence inversions are often accompanied by stratus clouds, whereas the surface-based radiation inversions are best developed under cloudless skies. Often in the fall, both types of inversions can be found together or merged when

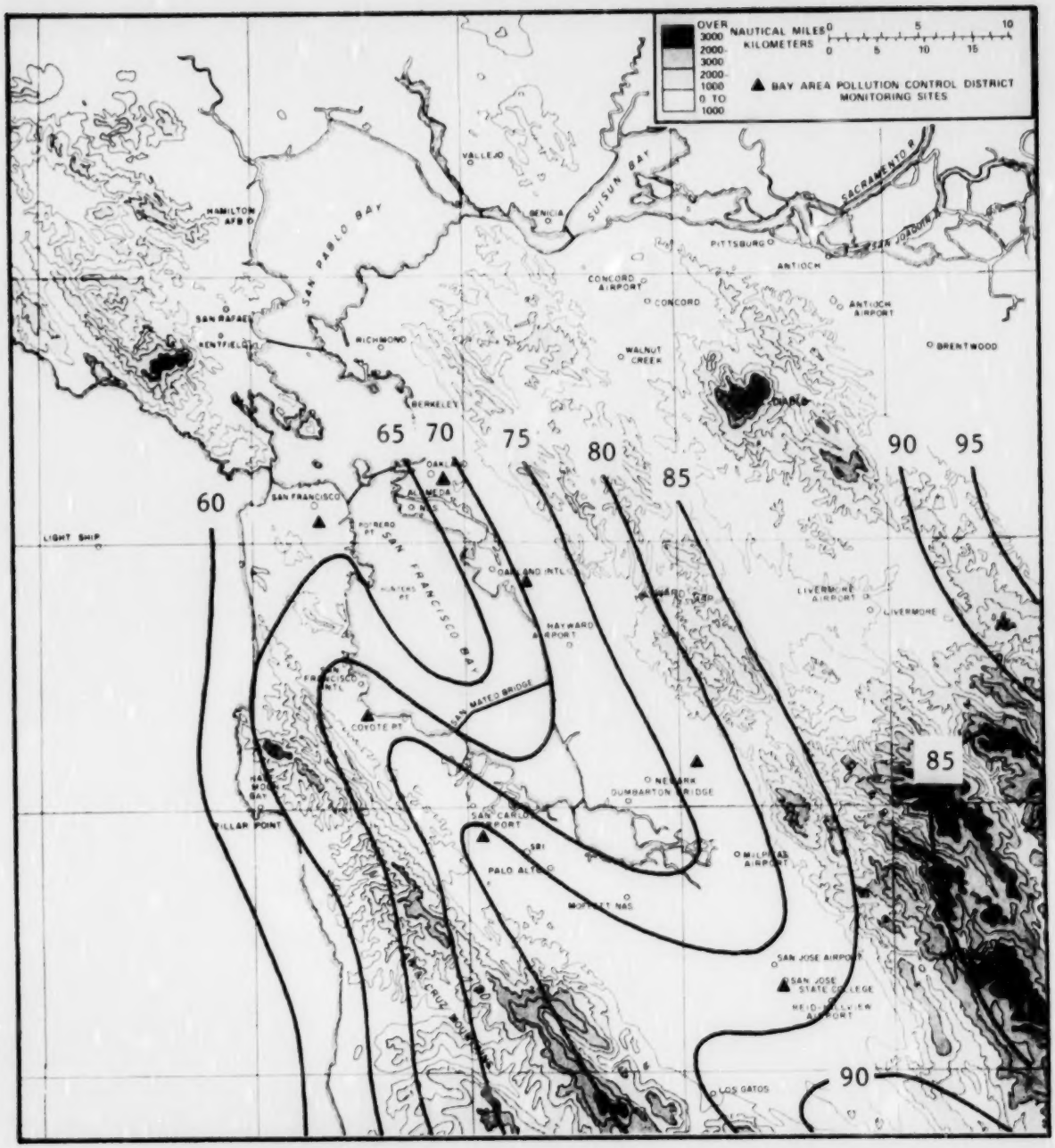

FIGURE A-3 JULY AVERAGE MAXIMUM TEMPERATURES (^{O}F)

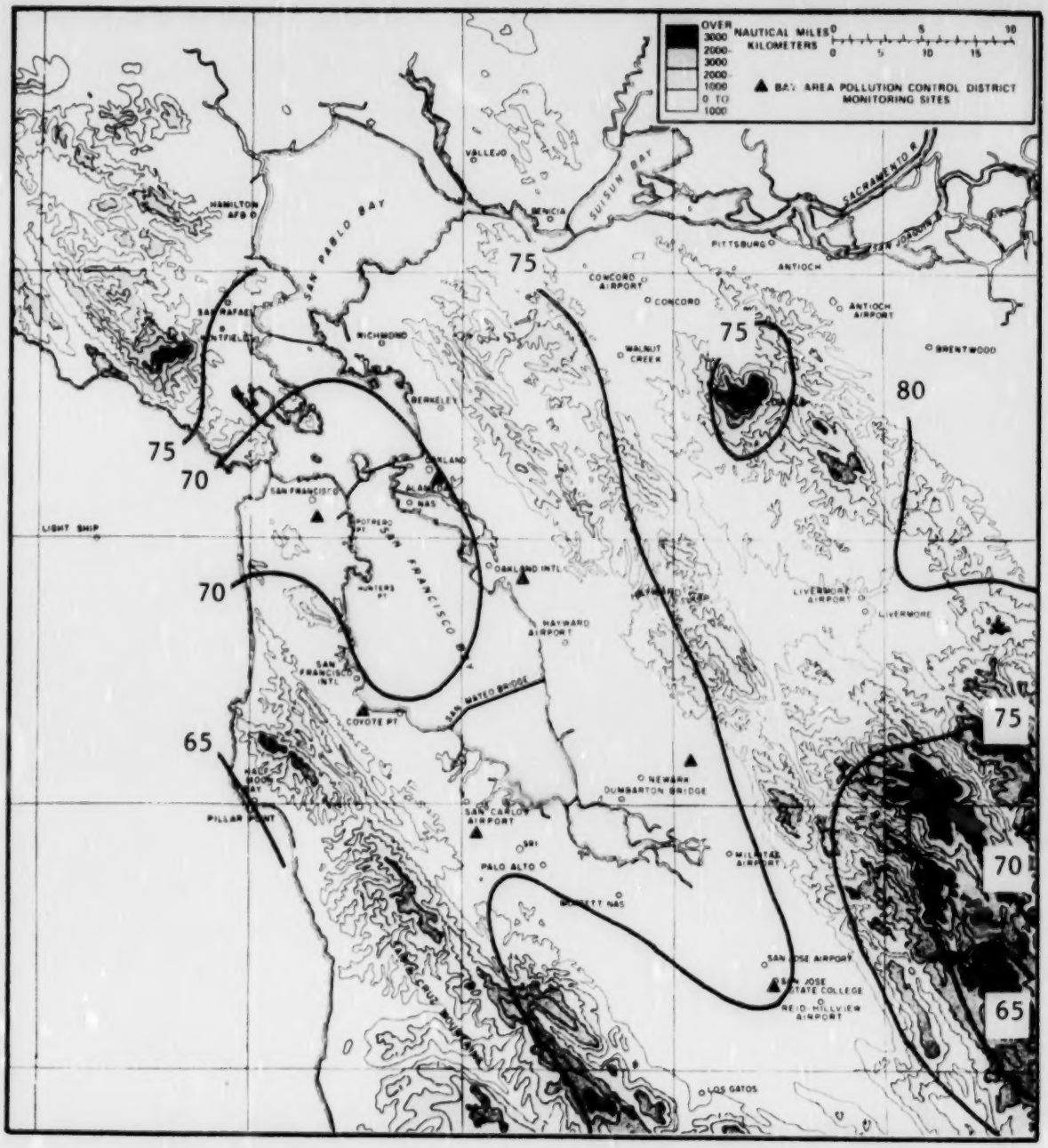

FIGURE A-4 OCTOBER AVERAGE MAXIMUM TEMPERATURE (^{o}F)

conditions favor the simultaneous development of both types. During clear northwesterly and westerly wind conditions, the inversion base averages 200 meters. When north to northeast winds prevail, the average inversion base is less than 60 meters.[17] An SRI study found the most frequently occurring inversion base height during October to be less than 100 meters.[18] The height of the inversion base is slightly lower over the South Bay than over the North Bay. More recent observations by Ahrens and Miller show that the height and the intensity of the subsidence inversion vary over the Bay area, being typically lowest over the Bay and increasing in height toward the surrounding hills.[19]

Average inversion base heights for Oakland in the fall months are listed in Table A-2. A lowering of the average height of the inversion base from September to November shows the transition from a summer subsidence to a winter radiation type. Most radiation inversions have dissipated by 1600 PST, whereas subsidence inversions tend to persist with only slight diurnal changes.

d. Cloud Cover and Precipitation

In the summer, the dominant cloud type in the Bay area is stratus. This cloud forms at the top of the marine layer, just below the inversion. Its occurrence tends to mark the flow of marine air in the region. Figure A-5 shows the percentage of occurrence of stratus during the summer forenoons of 1952.[17] The airflow patterns that have already been discussed are reflected in these frequencies. The high frequencies seem to pass through the Golden Gate and down over the Bay because typical flows of marine air and associated stratus follow this path. As these flows weaken in the fall, there is a corresponding decrease in the frequency of stratus over the Bay. Cloud amounts increase from September through November, but they are not usually of the summer stratus variety. The autumn increase of cloudiness is caused by an increasing frequency of synoptic disturbances, some of which produce precipitation.

Table A-2

FREQUENCY AND AVERAGE INVERSION BASE HEIGHTS BY MONTH FOR OAKLAND

Observation Time		0400 PST		0700 PST		1600 PST		1900 PST	
		% Frequency	Av Ht	% Frequency	Av Ht	% Frequency	Av Ht	% Frequency	Av Ht
Below 2501 feet	September	77	731	83	853	67	847	92	742
	October	76	396	74	506	47	790	79	579
	November	78	232	90	157	33	1125	85	187
Below 5001 feet	September	91	1100	97	1196	76	1164	97	912
	October	86	739	77	672	62	1481	87	905
	November	87	498	92	206	59	2155	85	187

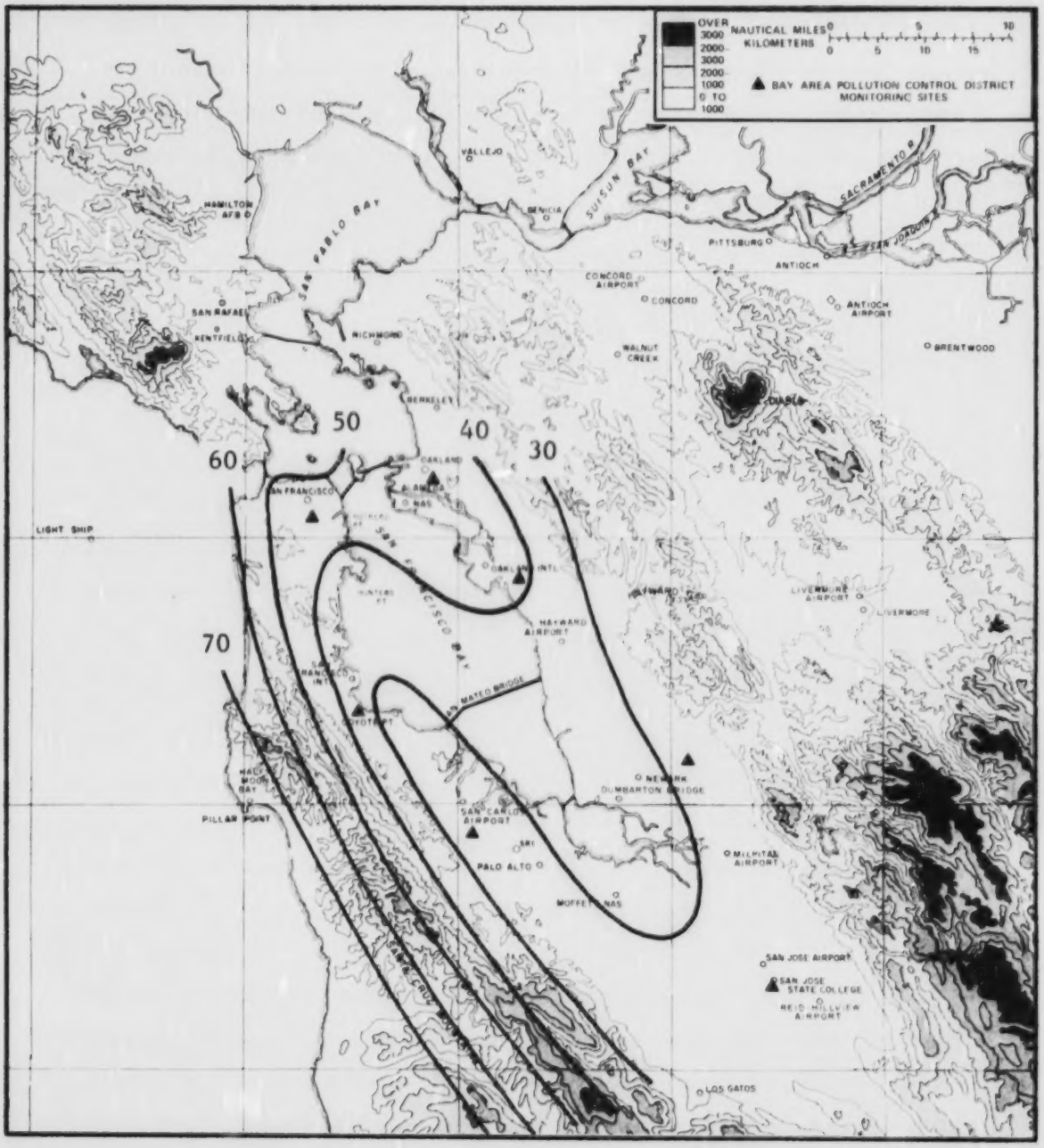

FIGURE A-5 PERCENTAGE OF OBSERVATIONS OF FOG OR STRATUS AT 1030 PST DURING SUMMER, 1952

Precipitation is also greatly affected by local terrain. Mechanical lifting is the principal mechanism, producing heavier amounts at high elevations, particularly along slopes that face the west. The sptaial pattern of average annual precipitation is shown in Figure A-6. There is considerable variation from year to year. Precipitation-producing mechanisms are synoptic in scale, with a trend in the autumn toward a gradual increase in precipitation from a summer minimum to a winter maximum.

4. Oxidant Concentrations

a. Trends in the Bay Area

The occurrence of high oxidant levels in the Bay area varies considerably from year to year. The BAAPCD has six monitoring stations* with long-term historical oxidant concentration data. Data from these stations are used to determine the oxidant concentration trends throughout the district.[20] The number of days where the high hourly average equalled or exceeded 15 pphm at one or more of the stations was 57 in 1965, 28 in 1966, 44 in 1967, 36 in 1968, 44 in 1969, 31 in 1970, 19 in 1971, and 4 in 1972.

Meteorological factors, along with the emissions of reactive organics and NO_x, play important roles in determining observed oxidant concentrations. To assess the effectiveness of control measures, the BAAPCD has objectively selected certain days from the complete data base; these days have comparable meteorological conditions of a kind that tend to occur with high oxidant concentrations. Specifically, days are only chosen for comparison when the afternoon Oakland sounding shows an inversion base below 300 meters and the maximum temperature at the benchmark station exceeds 84°F. The temperature criterion for San Francisco and San Leandro is 74°F, rather than the 84°F used for the other stations.

*Located in San Francisco, San Leandro, San Jose, Redwood City, Walnut Creek, San Rafael, and, more recently, Livermore.

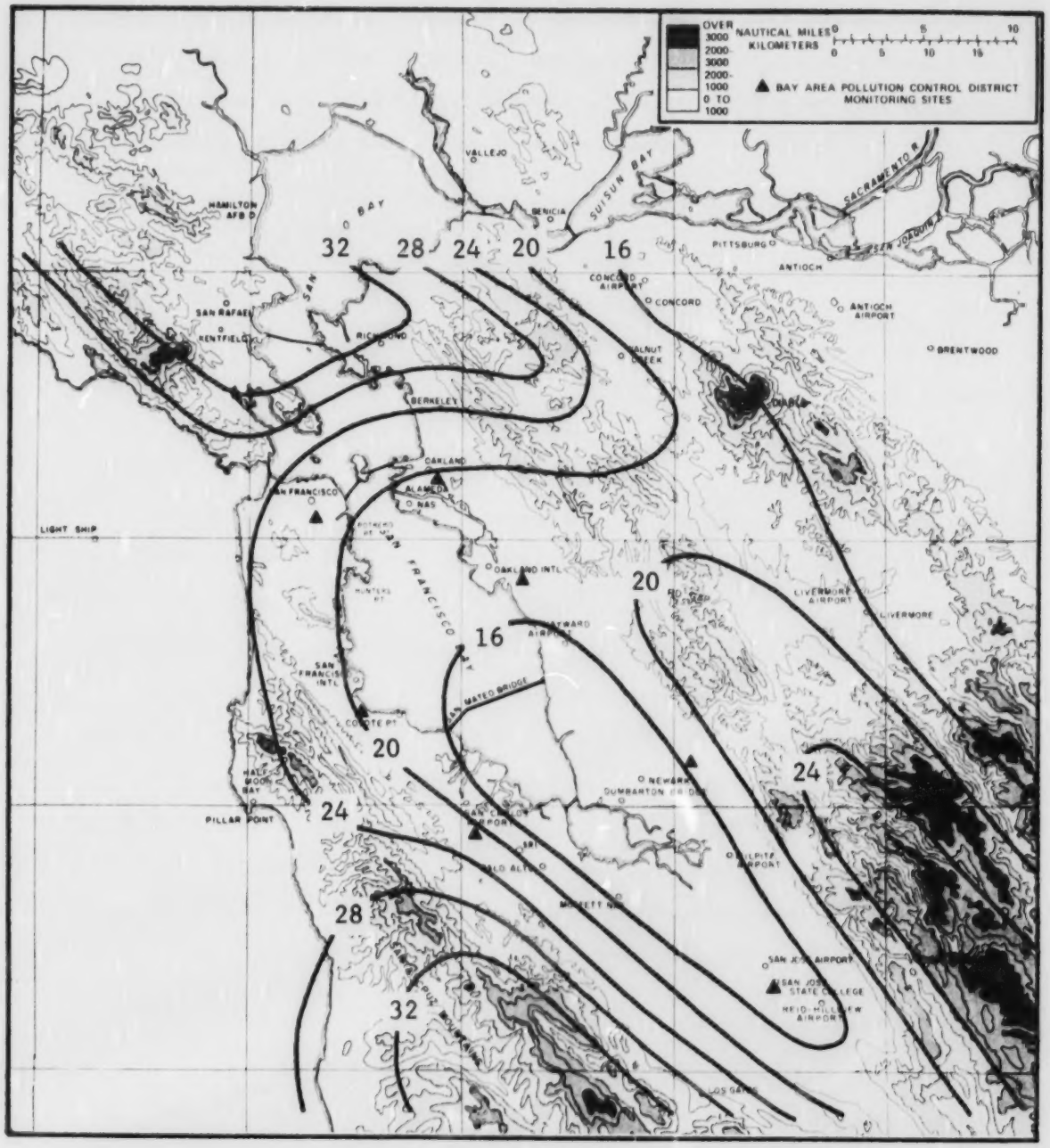

FIGURE A-6 NORMAL ANNUAL TOTAL PRECIPITATION (Inches)

The annual highest hourly average oxident concentrations for each BAAPCD station are plotted in Figure A-7. As a result of the selection process, the variations due to meteorological changes from year to year have been minimized and the trends exhibited probably reflect the results of control measures on sources of pollutants.

b. Geographical Distribution

The broad climatological patterns of the Bay area that have already been discussed indicate that the most severe oxidant episodes will be encountered in the valleys downwind of the highly urbanized districts. During the April to October smog season, airflows are such that reactive pollutants are carried from their sources in the major city areas into several of the valleys,e.g., Livermore and Santa Clara, where warmer temperatures and light winds are conducive to higher oxidant buildups. Of course, the buildups also occur as the reactants are being transported to these valleys, so that on days of high oxidant concentrations, the hour of peak oxidant concentration generally occurs sequentially from northwest to southeast on both the west and east sides of the Bay. In general, oxidant concentration levels also reflect the airflow pattern, with the more southerly stations reporting higher concentrations on a given day. The monitoring stations on the East Bay perimeter generally report higher concentrations than those on the West Bay perimeter. Sandberg and Thullier's data indicate that the oxidant concentrations at the Bay center often exceed those observed at the perimeter.[20]

5. Concluding Remarks

The preceding discussions have indicated considerable interrelationship among the various meteorological and pollution observations. The principal unifying consideration is the wind field. Large-scale climatological features, particularly the Pacific anticyclone,combine with local topography in the Bay area to produce airflows that are generally predict-

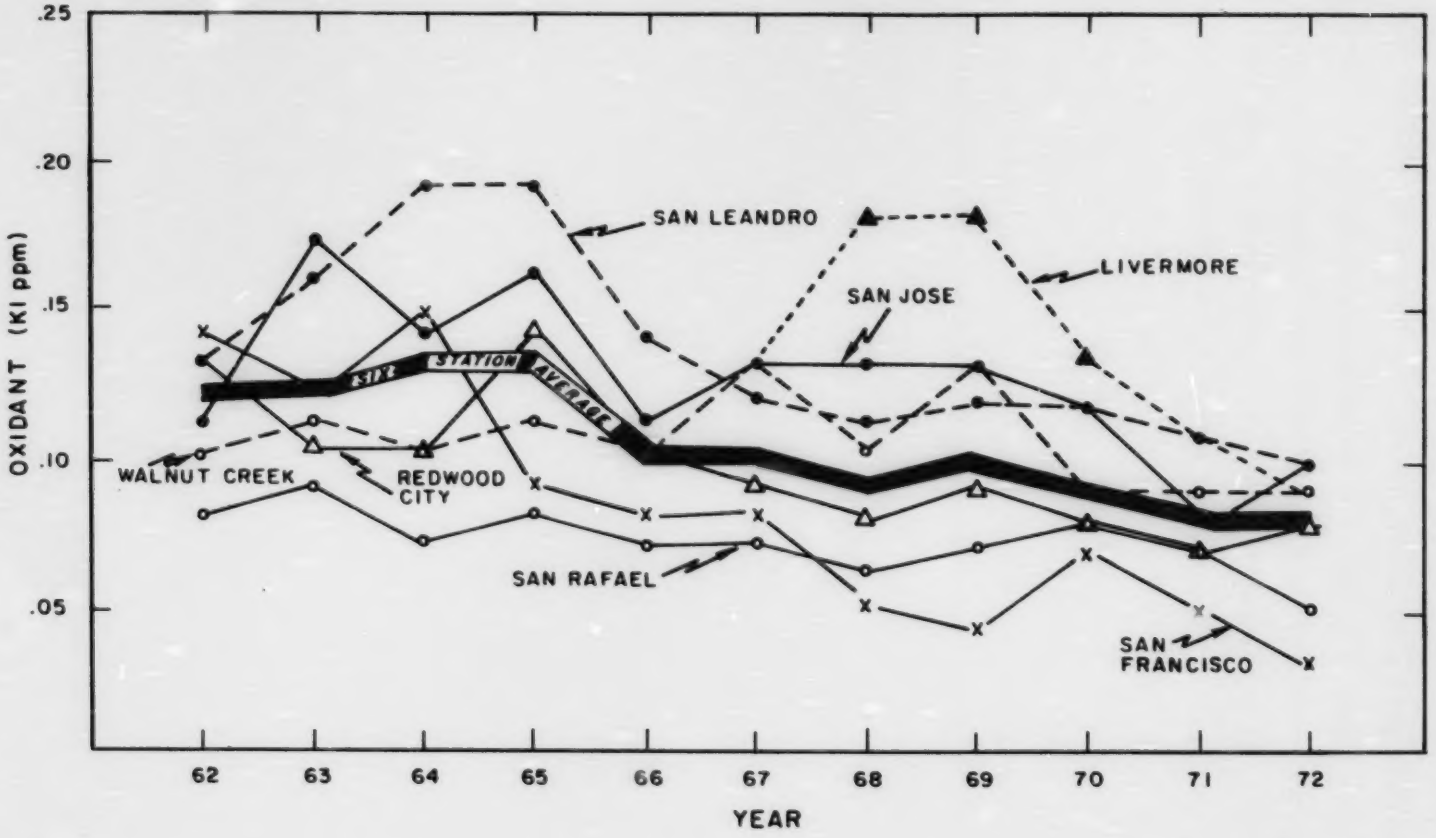

FIGURE A-7 AVERAGE OXIDANT CONCENTRATION ON COMPARABLE WARM DAYS FOR EACH BAAPCD STATION

Source: "A Study of Oxidant Concentration Trends (1962-1972)," BAAPCD Information Bulletin 1-16-73

able, especially during conditions conducive to smog formation. The inversion associated with the anticyclone generally limits surface airflow into, and out of, the Bay to the low level passes and valleys. Thus, the marine air, with its special characteristics tends to flow over San Francisco, through a few passes and spread southeastward and northward into the southern and northern part of the Bay. As it does so, it carries the cooler temperatures and stratus clouds with it. It also carries a burden of pollutants picked up from the cities over which it passes. It is not surprising that temperatures, cloudiness, and concentrations of secondary pollutants all have climatological gradients that parallel the typical streamlines of the summer and fall seasons.

Appendix B

AIR QUALITY INSTRUMENTATION AND CALIBRATION

Appendix B

AIR QUALITY INSTRUMENTATION AND CALIBRATION

1. Introduction

The instrumentation utilized during the San Francisco Bay Study is listed in Table 1, which is repeated here as Table B-1 for the reader's convenience. The details of the gas and particulate sampling inlet systems are diagrammed in Figures B-1 and B-2.

The air quality instrumentation and associated instrumentation was contained in four standard instrument mounting racks.

- Rack 1 contained the nephelometer and aerosol particle counter (APC) electronics. A coupler* (Coupler 3) was specially modified so that the computer could be used to control the start, stop, and printout of the APC. The condensation nuclei (CN) counter was mounted on top of this rack.

- Rack 2 contained the optics and pumps for the APC. It was located immediately under the particulate sampling system to minimize the number of bends in the sample tubing.

- Rack 3 held the gas sampling instruments, and the amplifiers required for the Bacharach CO analyzer, the wet and dry bulb thermistors, and the pyranometer (total solar intensity).

- Rack 4 held the NOVA computer, the three couplers,* and the reference voltage supply. The magnetic tape unit was mounted in a smaller rack on top of Rack 4.

---

*The couplers are basically digital voltmeters which, upon command from the computer, convert the analog signals from the instruments into digital form. See Appendix D for further details.

Preceding page blank

Table B-1

PROJECT INSTRUMENTATION

Measurement	Measurement Principle	Supplier and Model
Coordinating Research Council		
Ozone	Chemiluminescent	Bendix Model 8002
NO and NO_x	Chemiluminescent	Bendix Model 8101 B
Total hydrocarbon	Flame ionization detector	Beckman Model 400 A
Carbon monoxide	Mercury displacement	Bacharach Model US400L
Carbon monoxide	Nondispersive infrared	Beckman Model 315AL
Turbidity	Integrating nephelometer	Meteorological Research Model 1550
Temperature	Thermistor (dry)	
Relative humidity	Thermistor (wet)	
Solar intensity	Thermopile	Honeywell
Hydrocarbon distribution	Gas chromatography	Hewlett Packard Model 5750*
California Air Resources Board		
Total sulfur	Flame photometric	Meloy Model SA120
Condensation nuclei	Continuous reading	Environment/One, Model Rich-100
Particle size distribution	90^{o} Light scattering	SRI
Total particulate	Hi-vol filter	
Particulate distribution	Lundgren impactor	Environmental Research

*Two columns: C_1 to C_3 on 1/8 in. × 10 ft packed column on phenyl-isocyanate on Porasil C; C_3 to C_{10} on 0.02 in. × 300 ft capillary column coated with squalane. Grab samples were collected cryogenically.

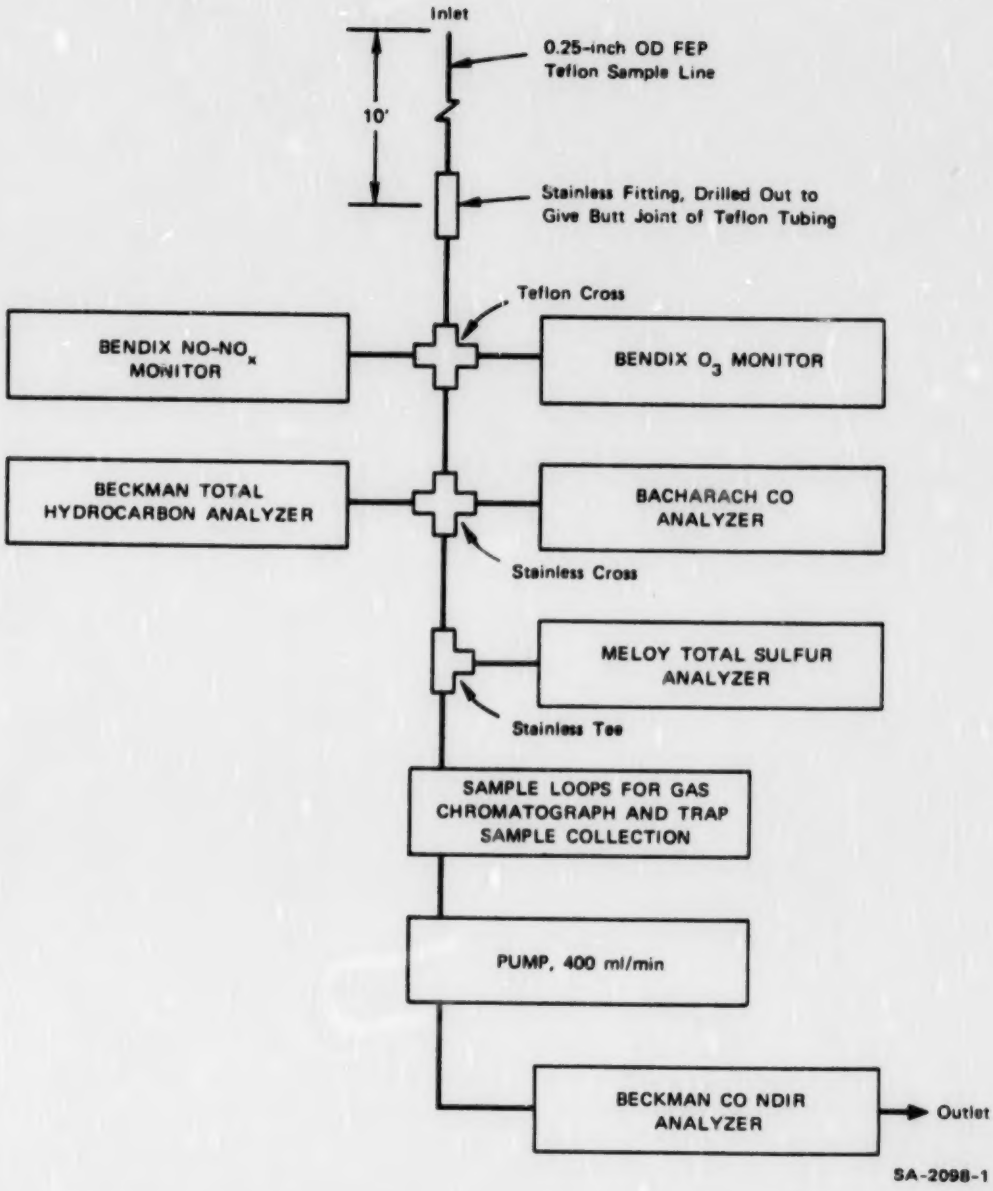

FIGURE B-1 SCHEMATIC FOR GAS SAMPLE LINES AND INSTRUMENTATION

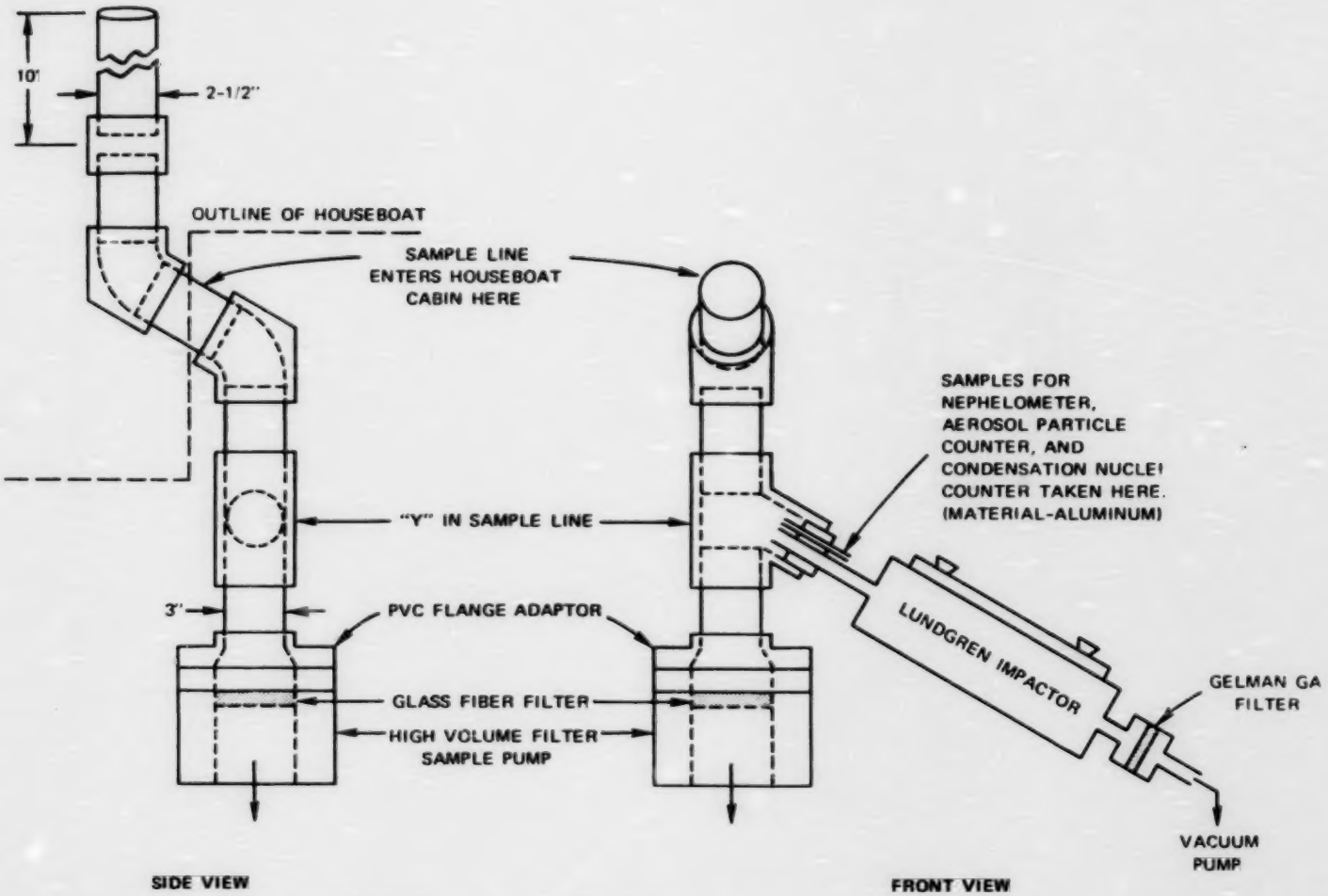

NOTE: Material for particulate sample lines is polyvinyl chloride (PVC) pipe.

SA-2098-2

FIGURE B-2 PARTICULATE SAMPLE LINE AND INLET SYSTEM

Power for the instruments was supplied from three sources. The 6-kVA generator in the houseboat did not provide sufficient power for all of the instruments and pumps. An auxiliary 4-kVA generator was mounted on the stern of the houseboat. Its power was used to operate the filter pumps and the APC only. The auxiliary generator failed midway during the research project and was replaced. The replacement generator was less well voltage regulated than the original and caused some operational difficulties in the operation of the APC.

The computer and tape deck require 60-cycle power with excellent frequency stability. The frequency stability requirements could not be met with the onboard motor generators. Therefore, we used four 12-V deep-cycle batteries and a 1-kVA inverter to provide line power for the computer and tape deck. Although the inverter provides excellent frequency stability, voltage regulation was poor. The output voltage of the inverter decreased steadily as the batteries were drained. The computer failed if the voltage dropped below 114 V, but was not voltage sensitive above this threshold voltage. Therefore, a Variac was used, as required, to maintain the output voltage above 114 V during a sampling day.

The schematic of the gas sampling system is shown in Figure B-2. All tubing connections are 0.25-inch OD FEP Teflon. Stainless steel fittings were used after the O_3 and NO/NO_x connections. The total flow through the sample line was about 3 ℓ/min, giving a residence time for the 5 meter sample line of 1.8 seconds.

The particulate sampling line was constructed of 10 cm OD polyvinyl chloride (PVC) plastic pipe and fittings. This material was selected due to its low cost, the availability of suitable fittings, and the ease with which it can be machined and sealed. The sample line passed through a window at the base of the flying bridge. Since a hole could not be cut in the roof, two bends in the sample line were required. The particulate

sample line was divided by a 3-inch PVC Y fitting* located inside the houseboat cabin. One branch of the Y connected to a PVC flange. This flange was machined to mate to a 4-inch diameter high-volume filter collector. The increase in diameter of the sample line to the filter was gradual to eliminate shoulders where particulate matter would collect. The sample flow through the filter was 10 ft^3/min (the procedures for washing and analyzing the filters are described on Page B-31).

An aluminum plug was machined with double O-ring seals to fit in the other branch of the Y. Tubes were inserted through holes in the plug to provide sample flow to particulate instrumentation. The size of the tube was determined by the sample flow requirements of the specific instrument. This particulate manifold is designed to provide near iso-kinetic sampling. The sample diameters and flow rates are given in Table B-2.

Table B-2

PARTICULATE INSTRUMENTATION SAMPLING RATES

Instrument	Sampling Rate	I.D. of Sampling Tube (in)	Flow Rate (ft/sec)
4-inch high volume filter	10 ft^3/min	3.0	3.4
APC	200 ml/min	0.19	0.6
Nephelometer	1 ft^3/min	0.65	3.8
CN counter	1 ℓ/min	0.19	3.0
Lundgren impactor	3 ft^3/min	1.38	4.8

*This fitting was not available in 2-1/2-inch pipe size.

2. Instrumentation Funded by Coordinating Research Council - Houseboat

Ozone

The Bendix Model 8002 ozone analyzer operates by the chemiluminescent reaction of O_3 with ethylene. The reaction is quantitative and there are no known interferences. The accuracy of the internal calibration system was checked using a REM Model 242 ozone generator and the reference method (neutral buffered potassium iodide).[21]

The instrument was zeroed and calibrated according to the procedure given in the Bendix manual. A sample of O_3 generated by the REM ozone generator (0.192 ppm) was passed through the instrument and through a bubbler containing neutral buffered potassium iodide. The volume passed through the bubbler was measured with a wet test meter. In duplicate runs, the instrument read 0.190 and 0.192 ppm, while the bubbler read 0.192 ppm in both cases. We concluded that the internal calibration standard was correct. The test was repeated by Barbara Wright, Air and Industrial Health Laboratories, Berkeley, California (AIHL) using a similar procedure and O_3 concentrations of 0.14 and 0.32 ppm. The analyzer results for zero and span agreed with the results from the manual samples.

NO/NO_x

The Bendix Model 8101B nitrogen oxide analyzer utilizes the chemiluminescent reaction of O_3 and NO to detect NO. The instrument is specific for NO and there are no known interferences. NO_x is determined by first passing the sample over a hot gold catalyst. While the exact chemistry is not well understood, the NO_2 is catalytically reduced to NO. NH_3 is not oxidized to NO by the gold catalyst at the temperature required for quantitative reduction of NO_2 to NO and therefore is not detected.

In the operational mode used on the houseboat, the NO signal from the photomultiplier (which detects the chemiluminescence) is integrated for

30 seconds, electronically averaged and transferred to a holding amplifier and stored for 1 minute. The instrument then automatically switches the catalyst in series with the sample stream to determine NO_x and integrates the photomultiplier signal for 30 seconds as previously described. The averaged NO_x concentration is then transferred simultaneously to a holding amplifier and to a subtractive circuit. In the subtractive circuit, the previously stored NO signal is subtracted from the NO_x signal being stored at the NO_x holding amplifier. The difference (the NO_2 concentration) is then transferred to a third holding amplifier where it is stored for 1 minute. The result is that each 30-second average of NO, NO_2 and NO_x is updated at 1-minute intervals.

External zero and calibration is required for this instrument. Two procedures were used. Primary calibrations were carried out at the beginning and end of the experimental phase of this project. Gas from a compressed cylinder of NO in N_2 was diluted into air to provide NO concentrations in the 0.2 to 1.0 ppm range. NO_2 was removed by passing the gas through triethanolamine on firebrick.[22] The sample stream was split with sample flow provided to the NO-NO_x analyzer and through an oxidizer and into Saltzman solution.[21]

Several oxidizers were used and evaluated during the project: an impinger containing acid potassium permanganate, as recommended by Saltzman;[21] potassium dichromate on glass fiber filter paper, which was folded and inserted into a glass tube; and chromium trioxide dissolved in water and adsorbed on to coarse firebrick. The first method was totally unsatisfactory because it did not give repeatable results and the conversion of NO to NO_2 was only 50 to 75 percent complete. The second method was satisfactory but the oxidizer did not last very long. The third method is most satisfactory. Since the procedure is not readily available, it is described here.

Coarse firebrick (10-12 mesh) is washed with water and decanted. It is then covered with a 17 percent aqueous CrO_3 solution. The slurry is stirred for about 15 minutes and decanted. The treated firebrick is spread out in a large dish and dried in a hood. The dried firebrick should be dark yellow; if it is too dark, it is too dry. Allow it to stand in the room to pick up more moisture. The dry CrO_3/firebrick is packed into a tube which is inserted in the gas stream. Conversion of NO to NO_2 is quantitative and the tube lasts for months.

A convenient method for zeroing the instrument was also suggested to us by AIHL. A drying tube is packed with glass wool, a layer of TEA/firebrick, a layer of glass wool, a layer of CrO_3 firebrick, and a glass wool plug. The tube is connected to the zero inlet of the instrument. The instrument zero, which may drift 2 percent/day, can easily be checked.

To determine NO and NO_2 simultaneously, air is pulled through two impingers in series; the first impinger contains Saltzman solution for direct determination of NO_2. The second impinger also contains Saltzman solution for determination of NO as NO_2. A tube containing one of the oxidizers precedes the second impinger and converts NO to NO_2. Since there is a 12 percent conversion of NO_2 to NO in Saltzman solution, the NO produced in the first impinger must be corrected in the calculation of the NO concentration determined by the second impinger.

For calibration on board the houseboat, a certified cylinder of 5 ppm NO in air was purchased from Matheson. Our analysis of this cylinder, using the above procedures, showed that the certified analysis was incorrect, but that the NO concentration did not change during the course of the experiment. This cylinder was used to span the instrument on board the houseboat, using the entire sampling inlet system as a sample line.

The instrument calibration was also checked by AIHL midway in the project. Their results suggested that the calibration of the 1.0-ppm full-scale range may be different from that of the 0.5-ppm range (the range

normally used throughout the project). Also, the results of the cylinder analyses repeated during the experimental phase suggested that the instrument calibration changed between November 8 and 20. Since we do not know when the change occurred, we have used the same calibration factors for all data collected, recognizing that the data for November 17 may be as much as 15 percent high.

The calibration data are summarized in Table B-3.

Table B-3

CALIBRATION DATA FOR HOUSEBOAT NO/NO_x ANALYZER

Date	Saltzman (ppm)		Instrument (ppm)			Remarks
	NO	NO_2	NO	NO_2	NO_x	
Aug 25	--	--	0.71	0.15	0.82	Cylinder on houseboat
Nov 8	--	--	0.72	0.16	0.77	Cylinder on houseboat
Nov 20	0.45	0.00	0.59	-0.02	0.55	Calibration on houseboat by AIHL (Range 1.0 ppm f.s.)
Nov 20	0.24	0.0	0.26	-0.01	0.24	Calibration on houseboat by AIHL (Range 0.5 ppm f.s.)
Nov 20	0.42	0.0	0.53	0.02	0.50	Calibration on houseboat by AIHL (Range 1.0 ppm)
Nov 28	--	--	0.89	0.14	0.98	Cylinder in laboratory, using span values set 25 August
Nov 28	--	--	0.70	0.13	0.84	Cylinder in laboratory, using span values set on 20 November
Nov 29	0.71	0.13	--	--	--	Average of 3 duplicate sets of analysis of span tank

Total Hydrocarbons

A Beckman Model 400A total hydrocarbon analyzer was used. The sample was pulled through the instrument by a small mechanical pump. The instrument was zeroed using Matheson Zero Gas Air. The span calibration was performed using a Matheson certified cylinder containing 1.88 ppm (v/v) of n-hexane in N_2. The calibration of this cylinder was verified by AIHL, who found 1.63 ppm. The span of this instrument was set for 10 ppm C using the 1.88 ppm calibration value. All THC values are reported as ppm C as hexane. No correction for methane was made.

Carbon Monoxide

In view of the vibration on board the houseboat, we initially decided to use the Bacharach Model US 4001 mercury displacement CO analyzer. The instrument performed well during the first runs and was switched to the helicopter instrument package. The second Bacharach analyzer was used on the houseboat but failed to operate satisfactorily. Both SRI and Bacharach technicians were unable to repair this instrument. To correct these problems a Beckman Model 315AL nondispersive analyzer (NDIR) was installed in early October. The cell was carefully located amidships and with the diaphram perpendicular to the fore and aft line of the houseboat to minimize vibrational instabilities. Shock mounts would probably have improved the instrument's performance by reducing noise, but no difficulty was experienced in zeroing or spanning the instrument when seas were calm.

A switching valve manifold was used to provide zero or span gas to the CO sensors. Nitrogen was used to zero the instruments daily (less than 1 ppm CO). A tank of about 10 ppm CO in nitrogen was made up at SRI. It was calibrated in the laboratory by comparison with Matheson certified tanks containing 20 and 40 ppm CO using another Beckman 315AL NDIR. The concentration of CO was determined to be 10.5 ppm. The spans were set to 25 ppm full scale and were checked several times during each sampling day. Instrumental drifts as great as about 10 percent can occur within a day if the span is not regularly checked.

Atmospheric Turbidity (Integrating Nephelometer)

A Meteorological Research Incorporated integrating nephelometer was used to measure the scattering coefficient of the air. The manufacturer's calibration procedures, using Freon 12 for primary calibration and the internal calibration, were used. The calibration was checked twice during the experimental phase of the project, using the internal standard.

Temperature and Relative Humidity

The temperature sensors were Veco 34D1 thermistors which served as one leg of a Wheatstone bridge network. The thermistors were mounted on brass screws which extended about 12 mm into PVC particulate sampling line. The wet bulb thermistor was covered with a wick, which passed through a 6 mm hole in the PVC pipe and into a water reservoir mounted outside the pipe.

A cable connected the thermistors to the bridge inside the houseboat. Any of three ranges could be selected: -18 to 2°C, 0 to 20°C, or 18 to 38°C. Values of the bridge resistors were chosen for optimum linearity. Low-temperature-coefficient trim potentiometers were incorporated for zero and span adjustments. Mercury batteries provided a stable bridge voltage source. The bridge output served as input to a differential amplifier located on the same chassis. The thermistors were calibrated before and after the experimental phase by comparison with an accurate thermometer in an oven. Since the output of the device was linear below the 18°C, it was not necessary to change the range when the temperature went below 18°C. The wet bulb thermistor did not perform satisfactorily; it always read high compared to readings made with a hand-held wet bulb thermometer. Presumably, the water evaporated from the wick faster than it could be carried up to the thermistor from the reservoir. Therefore, our measurements of relative humidity reported on the data tape are not reliable.

Solar Intensity

A Honeywell pyranometer, with a quartz dome and mounted in a SRI-built housing, was used to measure solar intensity aboard the houseboat. It was mounted on the port-side upper deck after-rail of the houseboat. A coaxial cable carried the millivolt signal to a temperature stabilized amplifier, where the signal was amplified by a factor of 95.

When the experimental phase of this project had been completed, a comparison calibration was made between the Honeywell pyranometer and an Eppley precision spectral pyranometer, Model PSP. When the solar angle is low, the houseboat pyranometer produced no signal due to the geometry of its housing. The sensor itself is located about 1/2 inch below the rim of the housing. Since the houseboat tetroon runs were made in the middle of the day, this effect should not cause problems. At higher light intensities, the output of the houseboat pyranometer output is linear. The calibration equation for the houseboat pyranometer was calculated from the slope and intercept of the calibration plot, the calibration factor of the Eppley pyranometer, and the amplification factor.

Gas Chromatography-Mass Spectrometry

A LKB 9000 gas chromatograph-mass spectrometer (GC-MS) was used to evaluate the applicability of the technique to the analysis of atmospheric samples collected cryogenically on the Bay. In preliminary experiments, auto exhaust samples were diluted to concentration levels similar to the concentration levels found over the Bay during the low smog conditions of this autumn. The results were found to be marginal due to the low levels of HC. A computer-tape deck peripheral system was installed during December of 1972 that improved the signal-to-noise ratio for analysis of trace constituents. The cryogenically collected samples were maintained at liquid nitrogen temperature while awaiting

the completion of the peripheral system. When the complete peripheral system was operational, the system was again evaluated with diluted auto exhaust samples.

Two outputs are available from the GS-MS during operation. The output from the total ion current monitor produces a record of total ion current versus time. This record is analogous to a gas chromatogram with detection by conventional techniques. During analysis by GC-MS, the record produced by the total ion current monitor is visually monitored and the mass spectrometer triggered into repetitive scans during the elution of each peak.

The second evaluation of the GS-MS with the computer peripheral on diluted auto exhaust samples showed improved performance but was not considered satisfactory. The sensitivity of the mass spectrometer is adequate for identification of many trace HC constituents of the simulated samples, but the sensitivity of the total ion current monitor is considerably less than can be obtained by a hydrogen flame detector under laboratory conditions.

An air sample that was cryogenically collected on 17 November 1972 was submitted for GC-MS analysis. The water vapor collected in the cryogenic traps was released more slowly than were the HC constituents upon release into the GC column of the GS-MS. Therefore, the total ion current monitor displayed a constant, large background of water over the midportion of the total ion current display. The presence of

relatively large concentrations of water required that the amplification of the total ion current display be reduced to maintain the display on scale. A zero offset (integral to the GC-MS) could not be employed since the concentration of the water was high and changed rapidly. As a result of the water interference, mass spectra were recorded every 6 seconds rather than triggering on the basis of the total ion current monitor display. Water vapor does not interfere with a GC flame ionization detector (FID), since the FID is insensitive to water vapor. In addition, the presence of GC column liquid phase bleed presents a more serious interference to GC-MS than it does to the FID. Thus special precautions must be taken to include a bleed trap for GC-MS column. The same GC column was used for both GC-MS and high resolution GC (Section 2-Hydrocarbon Distribution). Manual examination of the data in the mass spectral patterns at low mass numbers identified rare gases, methyl mercaptan, SO_2, and C_4 saturated compounds. In spectra from mass 200-350, the following compounds were present:

- Ethyl benzene
- At least one xylene
- Styrene
- n-propyl benzene
- At least one methyl ethyl benzene
- At least three trimethyl benzenes
- Dichlorobenzene
- Two unknown - MW 282 and 356

Thus, although the potential useful sensitivity of the GC-MS should be equal to the FID, in actual practice it is considerably less. Since either GC with FID or GC-MS destroys the samples during analysis, FID cannot be combined with MS detection. Under heavy smog conditions with much greater HC concentrations, the GC-MS could have provided invaluable additional information concerning the HC distribution. Since the performance of the GC-MS was marginal, only one sample was analyzed by this technique. The remainder of the cryogenically collected samples were analyzed by GC. The decision to analyze these samples by GC alone was also influenced by the marginal performance of the on-board GC.

Hydrocarbon Distribution - Gas Chromatography

The HC composition of the air was determined by gas chromatography in real time on the houseboat and from cryogenically trapped samples. The basic instrument was a Hewlett-Packard Model 5750, with flame ionization detection, modified to permit low temperature operation, direct injection of cyrogenically collected samples, and passage of the output of two columns through the same flame detector. It was necessary to use two columns, one for the C_1-C_3 hydrocarbons and one for the C_3-C_{10} hydrocarbons to provide adequate separation of all materials.

The air sample was pulled through two sample loops, one 21-ml loop for the C_1-C_3 hydrocarbons and one 200-ml loop for C_4-C_{10}

hydrocarbons, by a pump at about 1 liter per minute. Two 8-port valves permitted switching the air contained in sample loops to cryogenic traps. Each cryogenic trap was a loop of 6 inches by 1/8 inch diameter stainless tubing. The C_1-C_3 trap was packed with Porapak S; the C_3-C_{10} trap was packed with 20 percent Carbowax 20M on Chromosorb W. The general procedure for each sample was to flush the sample loops several times with air (in practice, sample air was pulled through the GC inlet system continuously), cool the trap with liquid oxygen, and pull out the appropriate 8-port valve to inject the air sample from the loop onto the trap. When three volumes of carrier gas (nitrogen for C_1-C_3, helium for C_3-C_{10}) had passed through the trap, the liquid oxygen was removed and the trap was rapidly heated with boiling water to release the sample.

The C_1-C_3 analysis was performed on a 10 foot by 1/8 inch column packed with phenylisocyanate on Porasil C, supplied by Waters Associates, using a helium carrier gas at 25 ml/min. The column was held at 20-25°C by immersion in water contained in a large dewar. Our initial experiments in the laboratory using samples of known concentration indicated that adequate separation of all C_1-C_3 compounds could be made. The relative retention times are given in Table B-4.

Table B-4

RELATIVE RETENTION TIMES OF C_1-C_3
HYDROCARBONS ON PHENYLISOCYANATE ON PORASIL C

Methane	1.00
Ethane	1.92
Ethylene	3.36
Propane	6.23
Acetylene	10.6
Propylene	21.6

It was necessary to backflush the phenylisocyante column to remove the high molecular weight hydrocarbons, whose retention time was long compared to the C_3 hydrocarbons. Otherwise, these compounds eluted as very broad peaks and had the effect of raising the background noise level. This was accomplished by means of the rotary backflush valve.

The C_3-C_{10} analyses were performed on a 200 foot by 0.02 inch capillary column. A column coated with DC-200 was used for analyses made on board the houseboat. The performance of this cloumn deteriorated during initial GC-mass spectrometer experiments (Section 2-Gas Chromatography) and a column packed with squalane was used for analyses of the cryogenically collected samples by GC-mass spectrometer and by GC.

The flow rate for the capillary column must be about 7 ml/min for optimum resolution. The time required to transfer the 200-ml air

sample to the cryogenic trap at 7 ml/min would be excessively long. Therefore, the rotary trap-column switching valve was used to isolate the trap from the column and detector, yet maintain a flow of helium carrier gas through the capillary column during sample transfer to the cryogenic trap. The 200-ml sample was transferred from the sample loop to the trap at a flow rate of 40 ml/min of helium. To inject the collected sample onto the capillary column, the trap-column switching valve was switched, the liquid oxygen was removed, and the trap was immersed in boiling water.

The GC oven was modified on an earlier SRI project to permit low temperature operation.[12] The oven was cooled with liquid CO_2 sprayed into the oven. The oven heater was used to maintain the oven temperature at -20°C during the first 5 minutes of the temperature program. Then the CO_2 was turned off and the oven temperature raised at 4°C/min on the houseboat and 2°C/min for the laboratory experiments using the squalane column. The final temperature, 90°C, was held for an additional 10 minutes. The time required for the complete cycle was about 1 hour on the houseboat.

Although some good data were obtained for C_2 and C_3 hydrocarbons aboard the houseboat, the measurements for methane were completely unsatisfactory. Peaks were observed at the methane elution time, but the calculated methane values based on the appropriate elution peak were meaningless. Although a considerable effort was made to

retrieve the methane concentrations from the chromatograms, we were not successful.

To obtain improved resolution of the HC constituents, atmospheric samples were collected and stored cryogenically for return to the SRI laboratory for analysis. We had originally proposed that these cryogenically collected samples would be submitted for analysis by gas chromatography-mass spectrometry on a LKB 900 GC-MS.

Figure B-3 illustrates a high resolution gas chromatograph of a sample cryogenically collected on October 25, 1972 over San Francisco Bay. This sample contains some 70 constituents, nearly all of which can be identified on the basis of auto exhaust constituents. A computer program developed on a previous study can identify and quantify the 80 constituents of auto exhaust. Table B-5 lists the elution order of auto exhaust constituents that have been separated and identified through high-resolution gas chromatography at SRI.

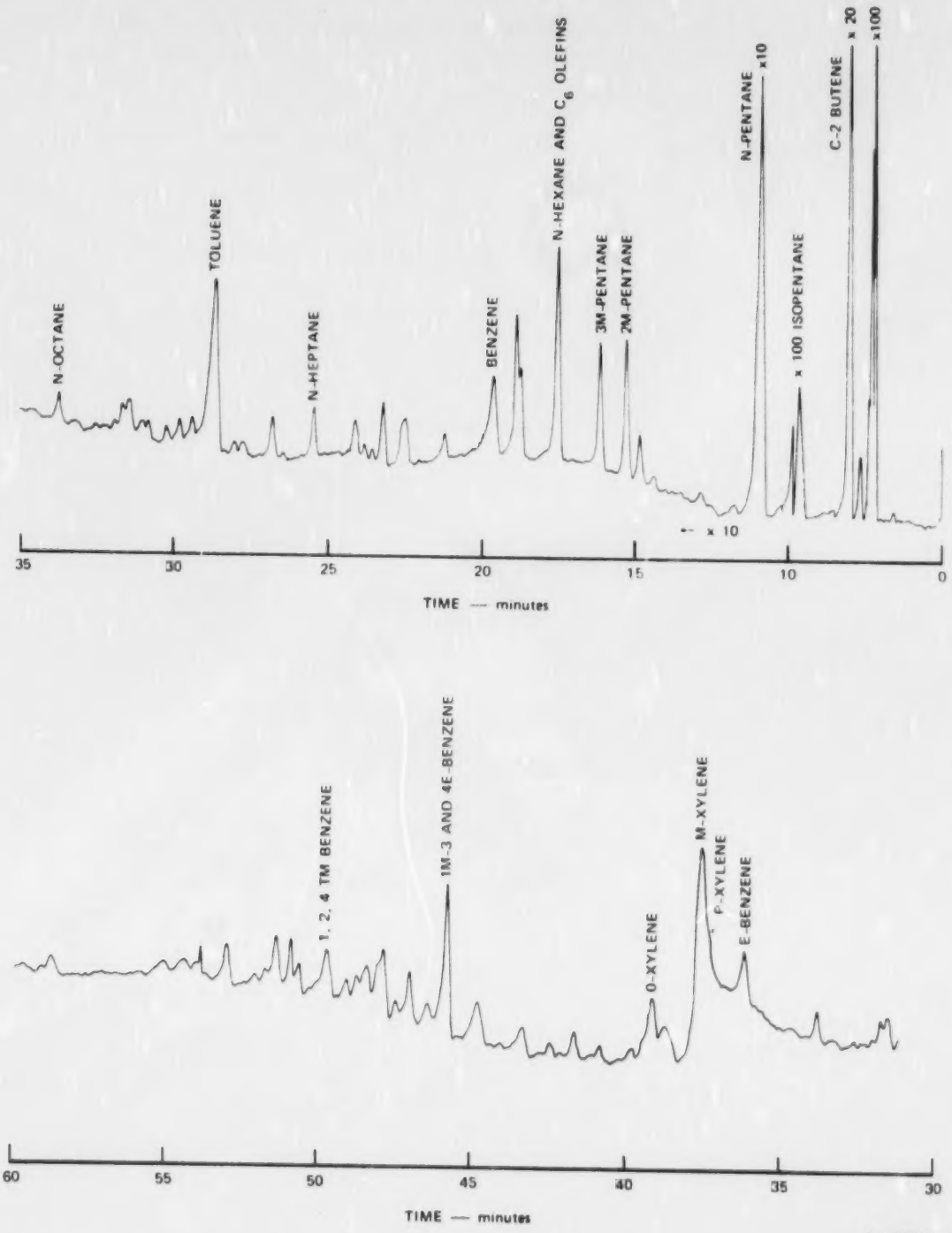

FIGURE B-3 HIGH RESOLUTION GAS CHROMATOGRAM OF HYDROCARBON DISTRIBUTION ON OCT. 25, 1972

Table B-5

ELUTION ORDER OF AUTO EXHAUST CONSTITUENTS

Column: Squalane 0.02 in. × 300 ft.
Temperature: -20 to 90°C at 2°C/min.
Initial hold: 6 min. - final hold 10 min.
Helium flow rate: 8 ml/min.

		Class*	Carbon No.
1.	C-2 hydrocarbons	--	2
2.	Propylene and propane	O	3
3.	Isobutane	P	4
4.	Isobutylene and 1-butene	O	4
5.	N-butane	P	4
6.	T-2-butene	O	4
7.	C-2-butene	O	4
8.	3-M-1-butene	O	5
9.	Isopentane	P	5
10.	2-M-1-butene	O	5
11.	N-pentane and C&T-1-pentenes	P	5
12.	2-M-2-butene	O	5
13.	2,2-DM-butane	P	6
14.	Cyclopentene	O	5
15.	3&4-M-1-pentenes	O	6
16.	Cyclopentane and 2,3-DM-1-butene	P	5
17.	2,3-DM-butane + 4M-T-2-pentene	P	6
18.	2-M-pentane	P	6
19.	3-M-pentane	P	6
20.	C&T-3-hexenes	O	6
21.	N-Hexane and C-6 olefins (4)	P	6
22.	4,4-DM-T-2-pentene and 3-M-T-2-pentene	O	7
23.	M-Cyclopentane	P	6
24.	2,4-DM-pentane	P	7
25.	Benzene	A	6
26.	1-M-cyclopentene	O	7
27.	2,3-DM-T-1-pentene and C-6 olefins (2)	O	6
28.	Cyclohexane and 3,3-DM-pentane	P	6
29.	3-M-2-E-1-butene and 5-M-T-2-hexene	O	6
30.	2-M-hexane and DM-pentanes (2)	P	7
31.	3-M-hexane and 1-C-3-DM-cyclopentane	P	7
32.	1-T-3-DM-cyclopentane	P	7
33.	3-E-pentane and 1-T-2-DM-cyclopentane	P	7
34.	2,2,4-TM-pentane and T-3-heptene	P	8

Table B-5 (Continued)

		Class*	Carbon No.
35.	3-M-C&T-hexenes and 2-M-2-hexene	O	7
36.	N-heptane and C-7 olefins	P	7
37.	1-C-2-DM-cyclopentane	P	7
38.	M-cyclohexane and 2,2-DM-hexane	P	7
39.	2,5-DM-hexane and E-cyclopentane	P	8
40.	2,4-DM-hexane	P	8
41.	1-T-2-C-4-TM-cyclopentane	P	8
42.	Toluene and 3,3-DM-hexane	A	7
43.	2,3,4-TM-pentane	P	8
44.	2,2,3-and 2,3,3-TM-pentane	P	8
45.	2,3-DM-hexane and 2-M-3-E-pentane	P	8
46.	2-M-heptane	P	8
47.	4-M-heptane	P	8
48.	3-M-heptane	P	8
49.	2,2,5-TM-hexane and 1,2,4,-TM-cyclopentane	P	8
50.	1-C-3-DM-cyclohexane	P	8
51.	1-M-T-3-E-cyclopentane	P	8
52.	2,2,4-TM-hexane and 2,3-DM-2-hexene	P	8
53.	Cycloheptane and 1-M-1-E-cyclopentane	P	8
54.	N-octane	P	8
55.	2,3,5-TM-hexane and 2,2-DM-heptane	P	9
56.	2,4-DM-heptane and 1-M-2-E-cyclopentane	P	8
57.	C-9 paraffins (4)	P	9
58.	E-cyclohexane and C-9 paraffins	P	9
59.	Ethylbenzene	A	8
60.	C-9 paraffins (4)	P	9
61.	M&P-xylenes and 3,3,4-TM-hexane	A	8
62.	2&4-M-octanes	P	9
63.	O-xylene and 2,2,4,5-TM-hexane	A	8
64.	TM-heptanes	P	10
65.	TM-heptanes	P	10
66.	N-nonane	P	9
67.	TM-heptanes	P	10
68.	TM-heptanes	P	10
69.	N-P-benzene and C-10 paraffins	A	9
70.	1-M-3&4-E-benzenes	A	9
71.	1-M-2-E-benzene and 5-M-nonane	A	9
72.	1,3,5-TM-benzene	A	9
73.	2&3-M-nonane	P	10

Table B-5 (Concluded)

		Class*	Carbon No.
74.	1,2,4-TM-benzene and butylbenzenes	A	9
75.	N-decane	P	10
76.	1,2,3-TM-benzene and 1-M-1-P-benzene	A	9
77.	1-M-3-N-P-benzene	A	10
78.	DE-benzenes	A	10
79.	1,3-DM-E-benzene	A	10
80.	DM-E-benzenes	A	10

* O - Olefins
P - Paraffins
A - Aromatics

3. Calibration of Instrumentation Supported by the California Air Resources Board

Total Sulfur

The Meloy Model SA120 flame photometric sulfur analyzer was operated according to the manufacturer's instructions. The instrument was always operated on the 10^{-8} amp range. The voltage output (V) was recorded by the data acquisition system. It was converted to concentration during the subsequent data analysis using the equation, which was taken from the manufacturer's calibration curve.

$$\log [S] = 0.611 \log V + 1.828$$

The accuracy of this calibration was checked using SO_2 generated by bubbling air through a solution of $KHSO_3$. The concentration of SO_2 was simultaneously determined by the West-Gaeke method.[23] At low concentrations (less than 50 ppb), the data reported here were shown to have an accuracy of $\pm$ 10 percent.

Condensation Nuclei

A continuously reading Environment/One Model RICH-100 condensation nuclei (CN) counter was used during this program. The instrument was rented from the manufacturer. Their calibration was used. The calibration was also checked against a General Electric Model A-518 hand operated CN counter. The readings were within 10 percent of the Environment/One furnished calibration.

An external load resistor was selected to provide a 0 to 1 volt

full-scale output. Since it was anticipated that several ranges would be used during this study, a separate voltage supply consisting of a mercury battery, a rotary switch, and several resistors was constructed. Seven voltages between 0 and 1 volt were available. The data acquisition system was programed to multiply the CN counter output by the exponential factor indicated by the voltage from the separate voltage supply.

Particle Size Distribution (Aerosol Particle Counter)

The aerosol particle counter (APC) was constructed at SRI for use on an earlier smog chamber program. Its optical design has been described before;[24] it is similar to the more familiar Royco counters. The electronics of the APC differ from the Royco counters in that particles in five size ranges are counted simultaneously.

The APC was calibrated using Dow latex spheres. Solutions of the latex spheres were prepared by dilution into distilled water. Several sources of distilled water were available within the Institute; the sample giving the lowest background count was used for all calibration runs. The particles were nebulized and spray dryed in a Collison nebulizer (Environmental Research Corporation, Aerosol Generator Model 7300). The manufacturer's calibration data permitted us to choose a dilution of the concentrated latex spheres that would yield 5.6 particles/ml in air.

The nebulized latex spheres were sampled by the APC. The sampling rate was 200 ml/min. The raw data are listed in Table B-6. An

Table B-6

APC CALIBRATION DATA

Latex Radius (μm)	Impactor	Counts Channel 1	Channel 2	Channel 3	Channel 4	Channel 5
None*	Yes	207	29	6	3	0
None*	No	132	1	0	0	0
0.109	Yes	184	1	0	0	0
0.357	Yes	1721	997	36	13	4
0.500	Yes	372	1564	491	54	10
0.714	No	760	913	582	1409	772
0.79	No	802	2868	2186	4701	2994
1.011	No	367	766	488	1079	2124

* Distilled deionized water only.

impaction filter in the nebulizer was used for the smaller particles to remove large droplets of water. The data for the large particles show a significant number of counts in channels 1, 2, and 3 due to these water droplets. Using the data for pure water, we corrected for these spurious counts. The counts for a particular size of latex spheres were assumed to be log normally distributed in the five channels.[25] Using this assumption, the cumulative relative counts were plotted on both log and normal probability paper to determine the channel index mode of the distribution. The plots for a given size particle were nearly linear. Some deviation can be expected due to the limited number of channels. The channel index modes were then plotted against the particle size. The best fit straight line was drawn through the points. Little difference could be distinguished between using a normal or a log normal distribution. This was probably due to the limited number of channels. Assuming that the division between channels was halfway between two adjacent channels, the

size range of particles counted in each channel could be determined. The results are summarized in Table B-7.

Table B-7

APC CALIBRATION DATA

Channel	Size Range (μ diameter)	Δ r (μ)
1	< 0.46	(< 0.08)
2	0.46-0.61	0.07
3	0.61-0.76	0.08
4	0.76-0.92	0.08
5	> 0.92	(> 0.1)

Total Particulate

Aerosol samples were collected on 4-inch diameter Gelman glass fiber filters as described earlier in this Appendix. It was necessary to carefully prewash the filters to reduce the background levels of NO_3^-, Cl^-, and $SO_4^=$. The following procedure was used. All glassware and equipment were washed successively in $CHCL_3$, acetone, and distilled deionized (DDi) water. A stainless steel screen was boiled in DDi water three times for 40 minutes duration each. The filters were sandwiched in the screen. Each filter was boiled in DDi water three times for 40 minutes duration each. The washed filters were dried in a stream of warm, filtered, dry nitrogen.

This type of filter absorbs considerable amounts of water when exposed to normal laboratory air. Therefore, humidifiers were constructed of pyrex jars with tight fitting lids. A screen inside the jar supported the filters midway in the jars. A saturated solution of K_2CO_3, which has an equilibrium relative humidity of 43 percent, was placed in the bottom of the jar to provide a constant humidity atmosphere. The filter was equilibrated overnight in this atmosphere and quickly weighed on a micro-

balance. After exposure, the same procedure was used to determine the weight of the filter. The weight of collected particulate was calculated by subtraction. Since the flow through the filter was 283 ℓ/min and the exposure time was known, the particle mass loading was readily calculated. The analytical methods are described in the following paragraphs.

Sample Preparation -- One-half of the filter was placed in a small extractor made from a graduated test tube connected to a small water-cooled condenser. The filter was extracted with boiling water and concentrated to 2 ml. Aliquots of this concentrated extract were used in the analysis of nitrate, sulfur (as sulfate), and chloride. The other half of the filter was ashed in a low-temperature asher to remove any organics. The ashed filter was washed twice with 8 M HNO_3 and twice with water, using enough liquid to cover the filter in each case. The extracts were combined and evaporated to about 1 ml. The concentrated extract was diluted to 10 ml in a volumetric flask.

Nitrate Analyses[26] -- An aliquot of the aqueous extract was reacted with brucine to produce a yellow compound according to the literature procedure. For concentrations between 0.05 to 0.60 mg/liter of nitrate nitrogen, the color development follows Beer's Law. The absorbance of standards and unknown solutions were measured at 410 nm on a Cary Model 14 M spectrophotometer using 1-cm cells. A standard curve was drawn, and the concentrations of unknowns were determined.

Sulfur Analyses[27] -- A 0.5-ml aliquot of the aqueous extract was placed in a platinum boat and evaporated to dryness in a heated nitrogen atmosphere. The sample and platinum boat were heated to 900°C in a hydrogen-helium atmosphere. The sulfate was reduced to H_2S which was swept from the boat into a microcoulo-

metric cell where it was treated with iodine. The change in voltage due to the change in iodine concentration was measured on a recorder. The peak areas of a set of standards in the range of 0.2 to 3.0 μg/ml of sulfur were measured and plotted on a graph. The concentration of sulfur in the unknowns was determined from this standard curve. Concentrations in μg/ml of sulfur were converted to μg/ml of sulfate by multiplying by a factor of 3.

Chloride Analyses[28] -- An aliquot of a chloride sample was introduced into a microcoulometric titration cell. The chloride was titrated with Ag^+ ion. A recorder monitored the voltage drop during titration. The peak heights for a set of standards were used to construct a calibration curve. The cell is suitable for titration of 0.1 to 1000 μg chloride per sample.

Lead Analysis[29] -- An aliquot of the 8 molar nitric acid extract was analyzed on a Perkin-Elmer Model 303 atomic absorption spectrophotometer at 2833 Å. Dilute samples (5-20 μg/ml of lead) were analyzed using the 5X scale expansion.

Particle Size Distribution (Lundgren Impactor)

A Lundgren impactor was rented from Environmental Research Corporation for this program. The device used was a prototype five-stage impactor constructed for AIHL for use on the California Aerosol Study. A 47-mm Milipore filter holder was used with Gelman GA-1 cellulose acetate after filters. A GAST Model 1022-V103-G272X pump was equipped with a large rotameter on its output, a vacuum gauge, and a bleeder valve on its input to measure and regulate the volume of air pulled through the impactor and after filter at 85 ℓ/min.

The procedures for cutting, washing, and mounting the "foils" on the impactor drums were recommended by AIHL. Mylar and Teflon foils

were supplied by AIHL and cut on their apparatus. Each foil was washed thoroughly in fresh, reagent grade acetone. They were dipped in 0.1N HNO_3 for approximately 1 minute (the 0.1N HNO_3 was prepared from DDi water). After a final wash in fresh, reagent grade acetone, the foils were dried under an infrared lamp in a stream of dried, filtered nitrogen. After drying, the foils were stored in acetate boxes, supplied by AIHL, which had previously been washed in DDi water and air dried. Each foil was weighed three times on a microbalance. A plutonium static discharger dissipated the static charge which accumulated on the foils with any motion.

Stages 1A, 2, 3, and 4 were first wrapped with a 2-inch Teflon foil. A 1-inch Mylar foil was wrapped over the Teflon foil. In each experiment the Mylar was placed on the lower half of the drum. Stage 1B was wrapped with a piece of 2-inch sticky polyethylene tape, sticky side out, which was used as supplied by AIHL.

Two batches of Gelman GA-1 filters were used. Filters 100 to 109 were washed and supplied by AIHL. Filters 200 to 203 were washed at SRI using the AIHL-recommended procedure. A stack of 15 filters was placed in a clean ceramic Buchner filter. About 1 liter of DDi water was slowly poured through the filters, using an aspirator to provide suction. The washed filters were dried in a vacuum oven and then under a stream of dry N_2. The filters were weighed before and after exposure on the microbalance and stored in individual plastic boxes. The weights of particulate collected are given in Table B-8.

Table B-8

LUNDGREN IMPACTOR SAMPLES

Date	Time (hr:min)	Impactor Data Stage	No.	Mylar (μg)	Teflon (μg)	Polyethyene Tape μg	After Filter No.	After Filter μg	Volume Sampled (m^3)
721019	1141-1220						101	151	2.8
721025	0800-1104						100	294	13.0
	1235-1320								
721026	1006-1050						102	533	3.3
721031	1352-1407								
721102	0833-1120	1A	9	75			103	970	13.2
		1B	Z			233			
	1123-1317	2	10	67	186		104	1384	9.1
		3	11	110	199				
	1633-1745	4	12	130	272		105	441	5.7
721106	1038-1201	1A	13	42	159		106	138	15.7
		1B	Y			449			
	1210-1405	2	14	0	147		108	161	4.6
		3	15	26	203				
		4	16	0	88				
721117		1A	17	0	100		200	17	1.2
		1B	X			45			
		2	18	6	195		201	~ 0	2.4
		3	19	8	151				
		4	20	0	0				

Appendix C

AIR QUALITY AND METEOROLOGICAL DATA FOR SELECTED SAMPLING DAYS

Appendix C

AIR QUALITY AND METEOROLOGICAL DATA FOR SELECTED SAMPLING DAYS

Figure C-1 is a map of the San Francisco Bay area. The insets define the area of the subsequent maps. The maps following Figure C-1 show the hourly meteorological and air quality measurements reported by all available monitoring stations in the Bay area for sampling days that were not selected for detailed analysis. The wind streamlines derived from these observations are shown as broad arrows. The houseboat course and times are also plotted on these maps. The San Jose and Oakland rawinsonde temperature-humidity profiles are included for each day data were available. Figures C-2 to C-9 show these map and vertical profiles, respectively, for selected sampling days. Detailed data are included for the following sample days: 6 October, 7 October, 19 October, and 6 November.

Helicopter flight paths for 19 October, 31 October, and 6 November are shown by Figures C-10, C-11, and C-12, respectively. The airborne measurements for these days are tabulated in Tables C-1, C-2, and C-3, respectively.

The results of chemical analysis of particulate matter collected on 19 October, 24 October, 25 October, 26 October, 31 October, 2 November, 6 November, and 17 November are shown in Table C-4.

The hydrocarbon distribution of cryogenic samples collected on 25 October, 26 October, 31 October, 2 November, and 6 November are tabulated in Table C-5. Table C-5 also shows the hydrocarbon distribution and concentration ranges of typical auto exhaust.

Preceding page blank

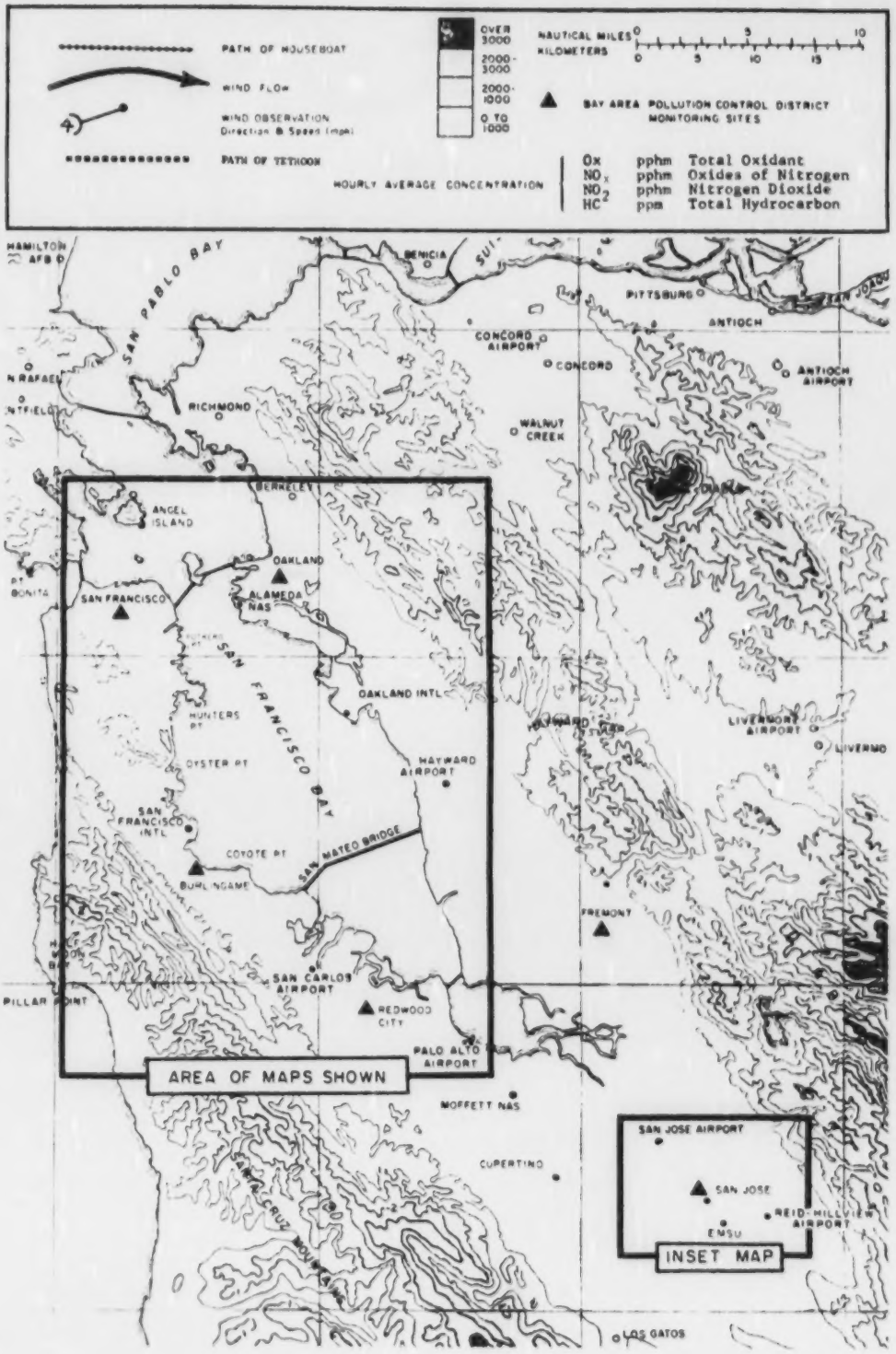

FIGURE C-1 OVERALL AREA OF SAN FRANCISCO BAY SHOWING SAMPLING AREA INSET

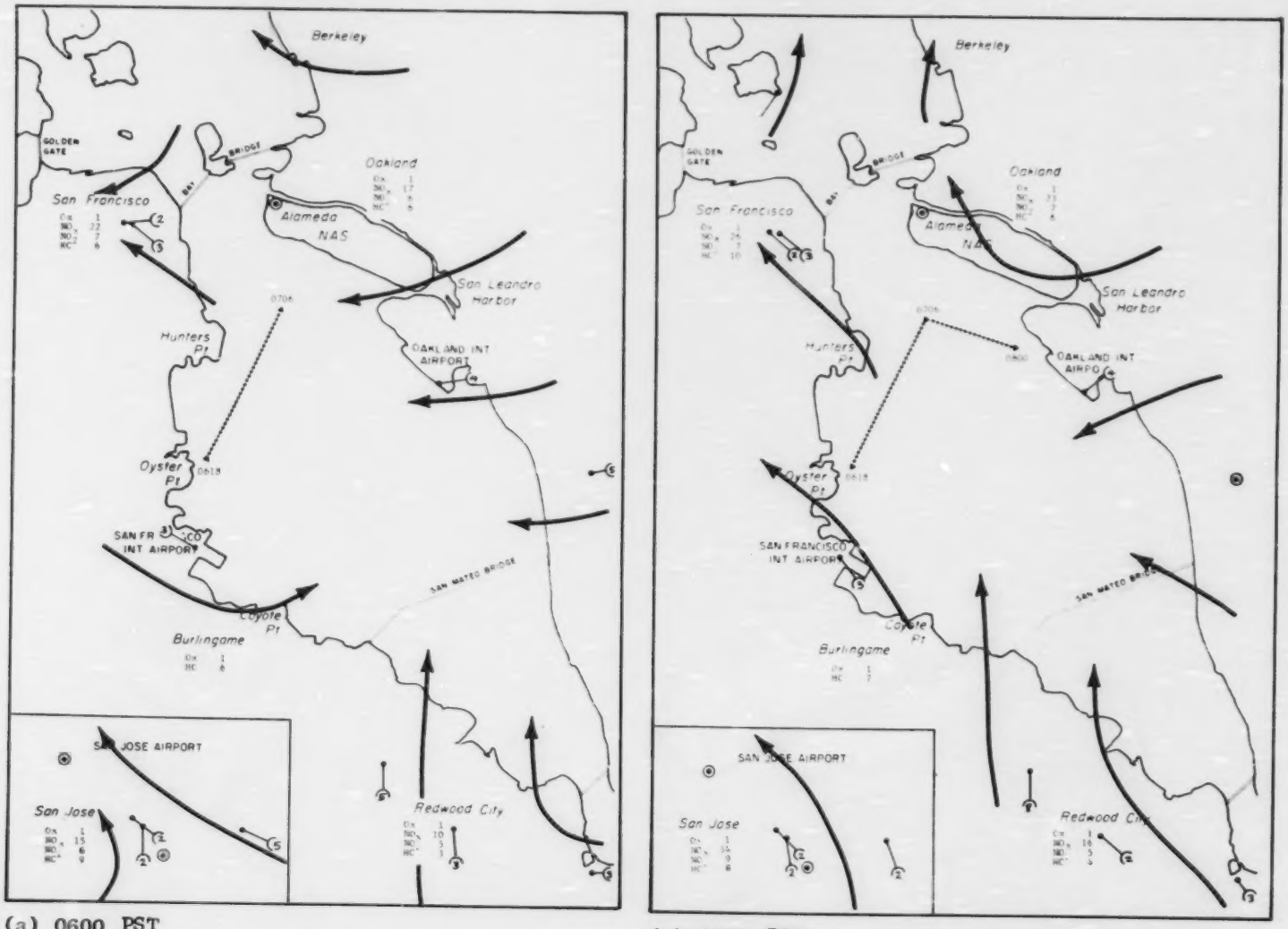

FIGURE C-2 AIR POLLUTION LEVELS, SURFACE WIND FLOW, AND HOUSEBOAT COURSE, 6 OCTOBER 1972

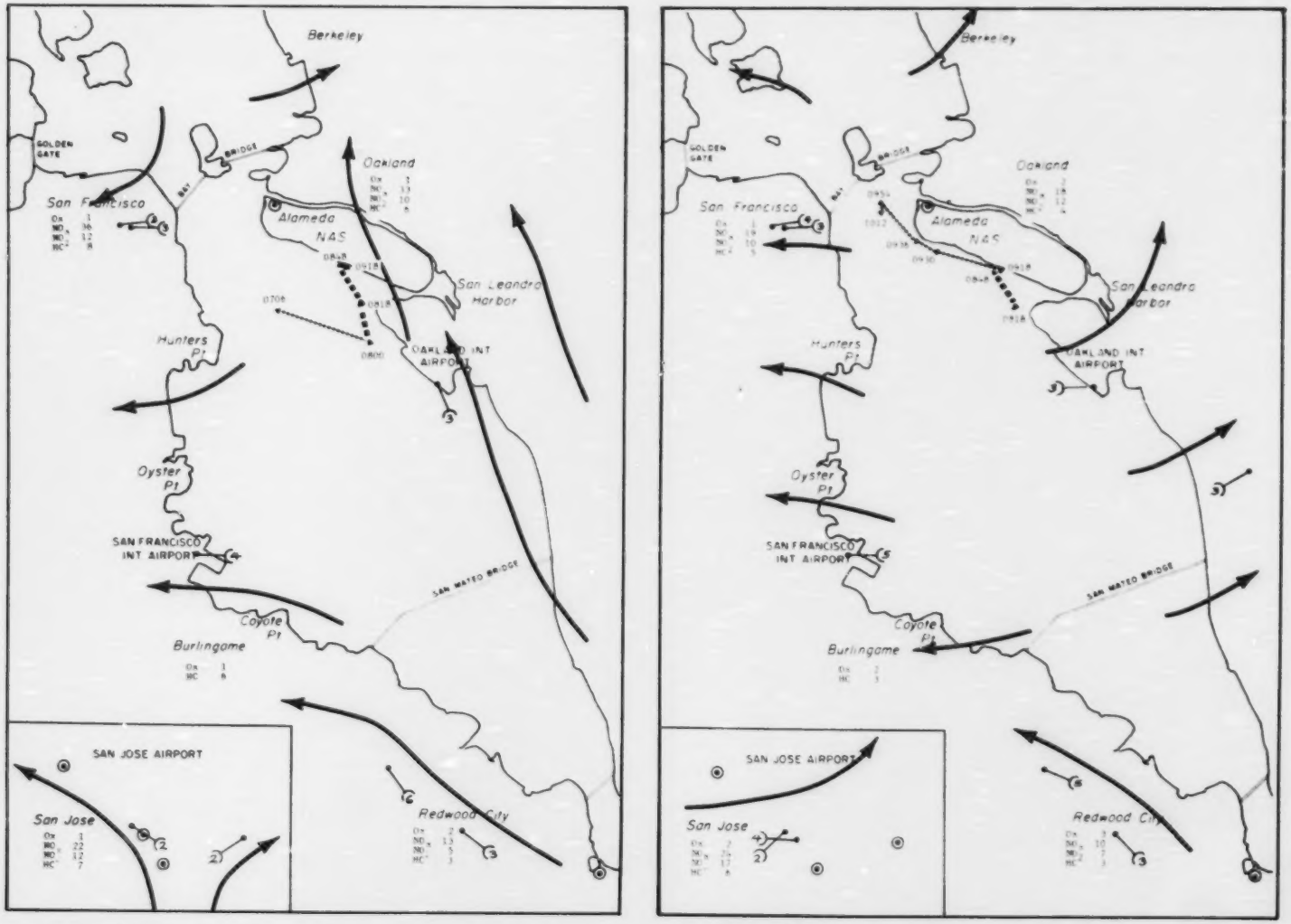

(c) 0800 PST

(d) 0900 PST

FIGURE C-2 AIR POLLUTION LEVELS, SURFACE WIND FLOW, AND HOUSEBOAT COURSE, 6 OCTOBER 1972
(Continued)

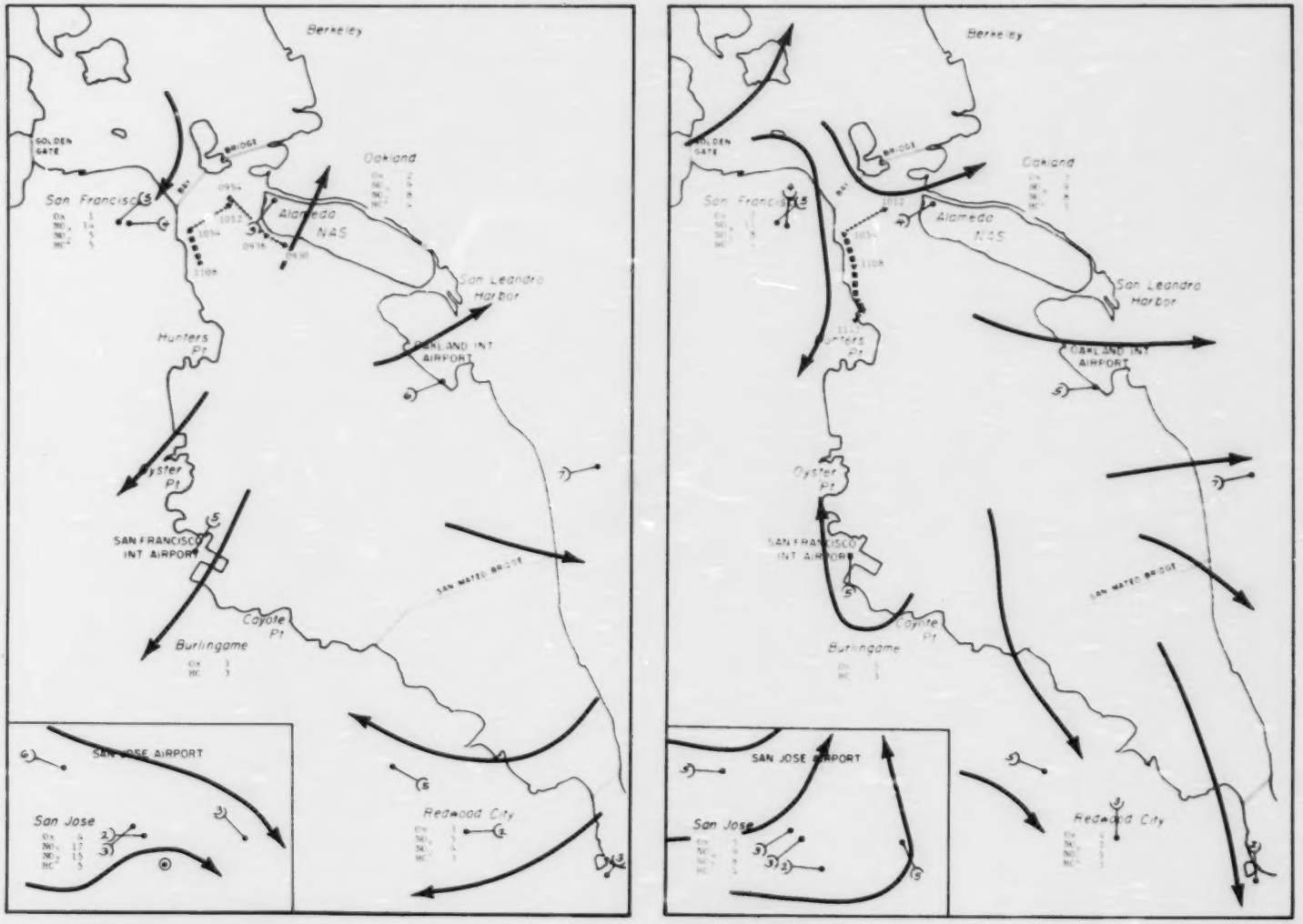

(e) 1000 PST

(f) 1100 PST

FIGURE C-2 AIR POLLUTION LEVELS, SURFACE WIND FLOW, AND HOUSEBOAT COURSE, 6 OCTOBER 1972
(Continued)

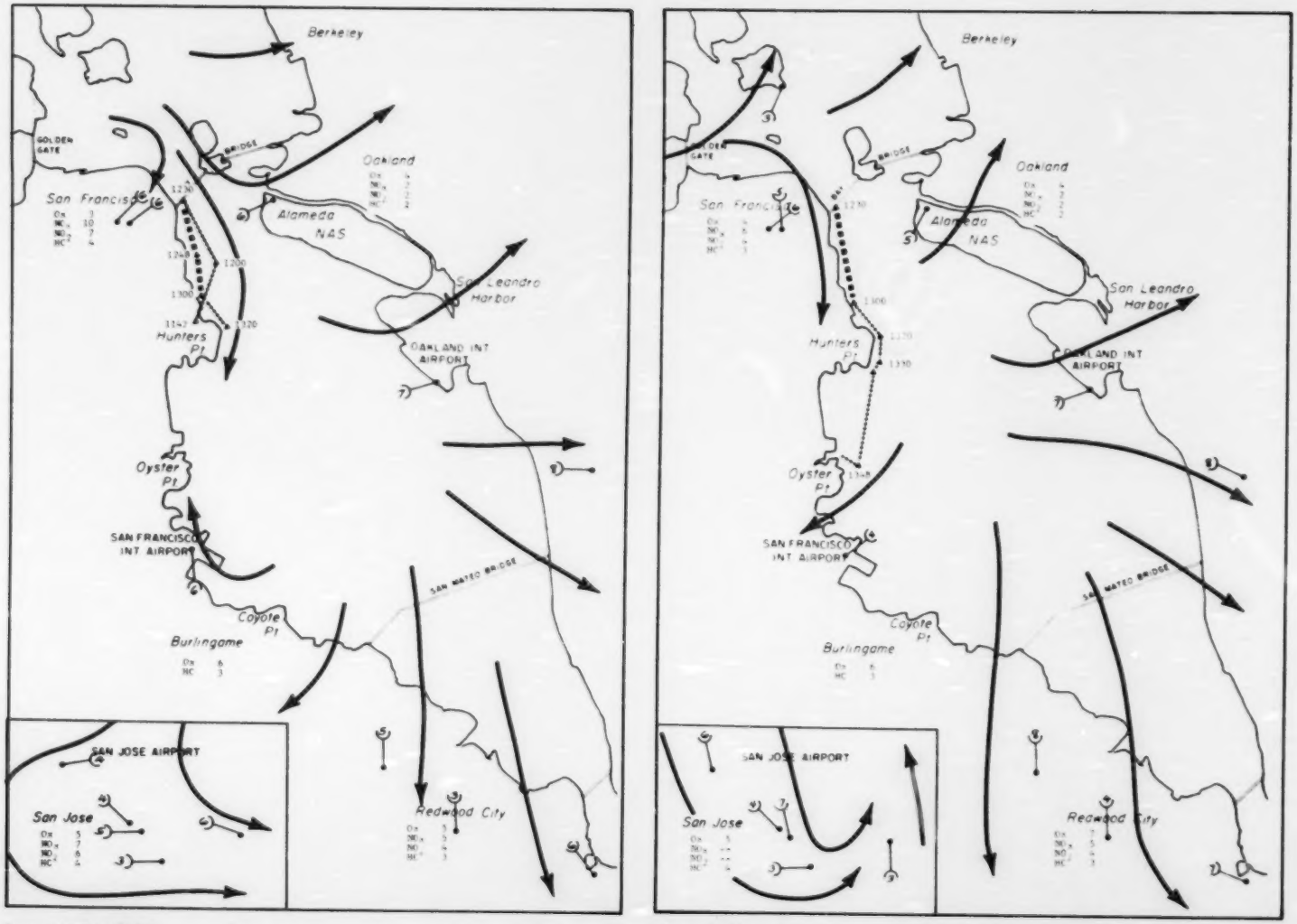

(g) 1200 PST

(h) 1300 PST

FIGURE C-2 AIR POLLUTION LEVELS, SURFACE WIND FLOW, AND HOUSEBOAT COURSE, 6 OCTOBER 1972
(Continued)

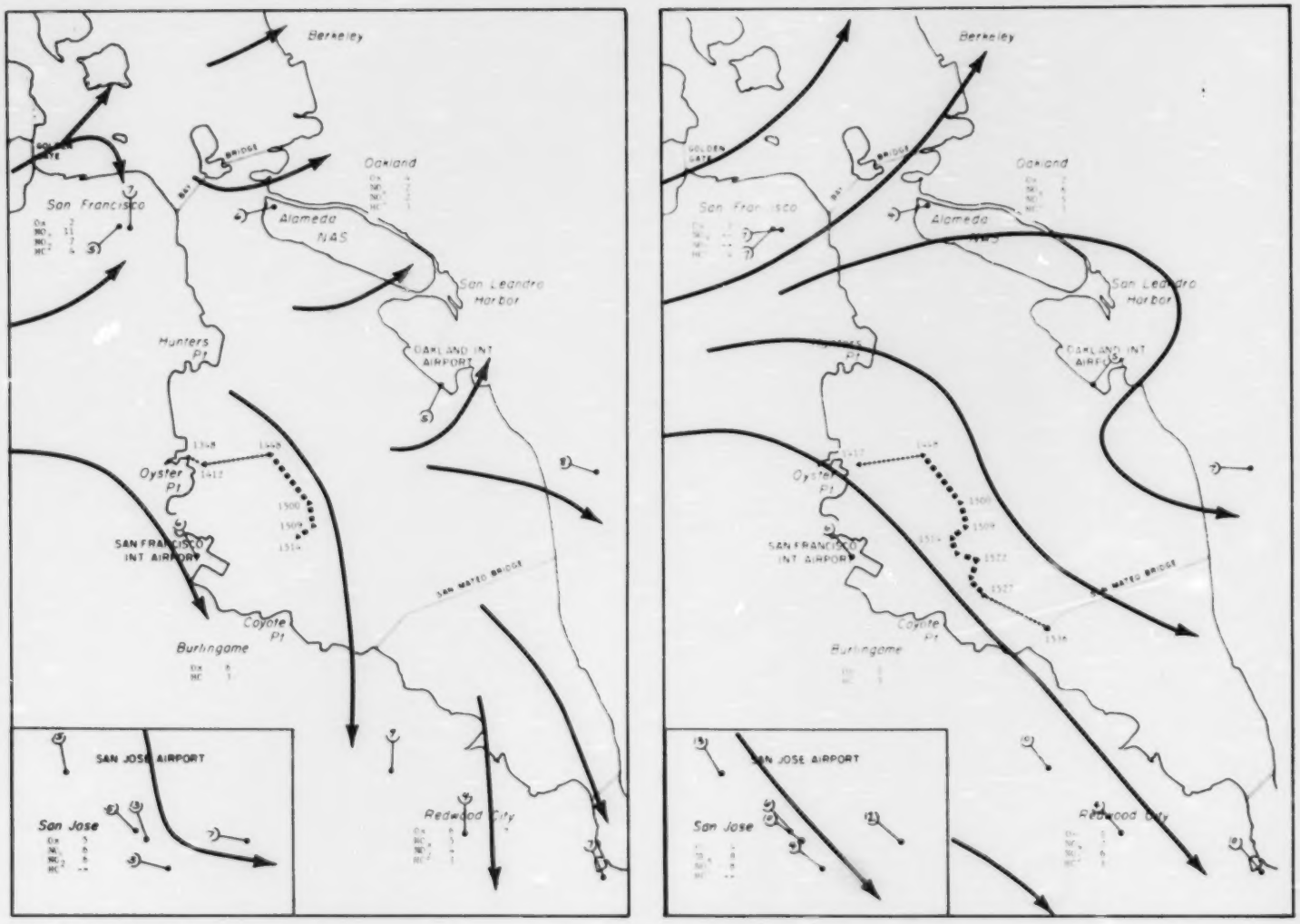

(i) 1400 PST

(j) 1500 PST

FIGURE C-2 AIR POLLUTION LEVELS, SURFACE WIND FLOW, AND HOUSEBOAT COURSE, 6 OCTOBER 1972
(Continued)

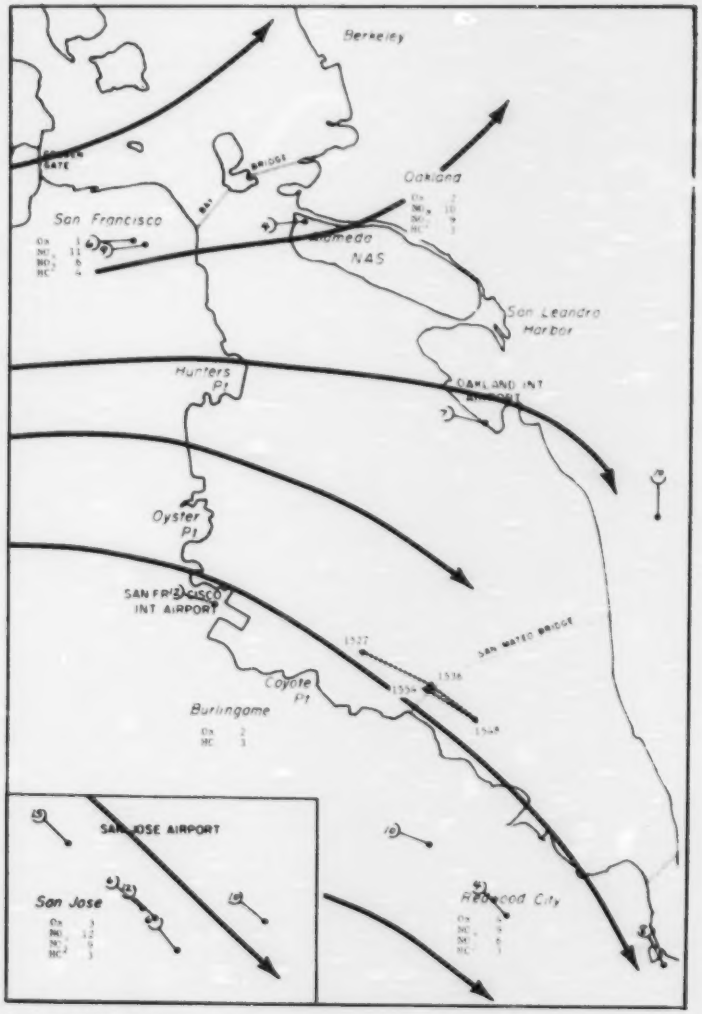

(k) 1600 PST

FIGURE C-2 AIR POLLUTION LEVELS, SURFACE WIND FLOW, AND HOUSEBOAT COURSE, 6 OCTOBER 1972
(Concluded)

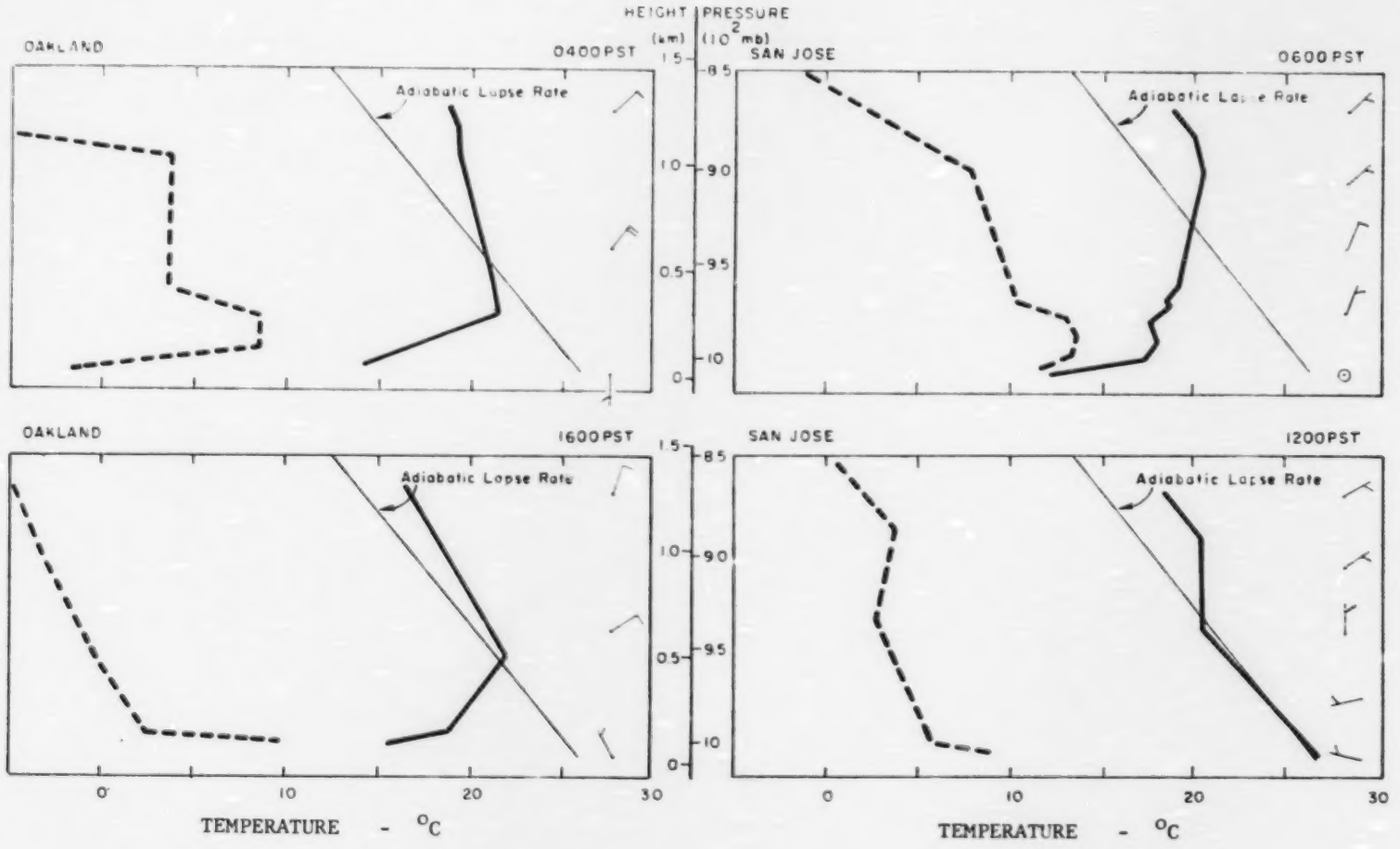

FIGURE C-3 RAWINSONDE TEMPERATURE AND DEW POINT OBSERVATIONS, 6 OCTOBER 1972
(Temperature ——, Dew Point - - - -)

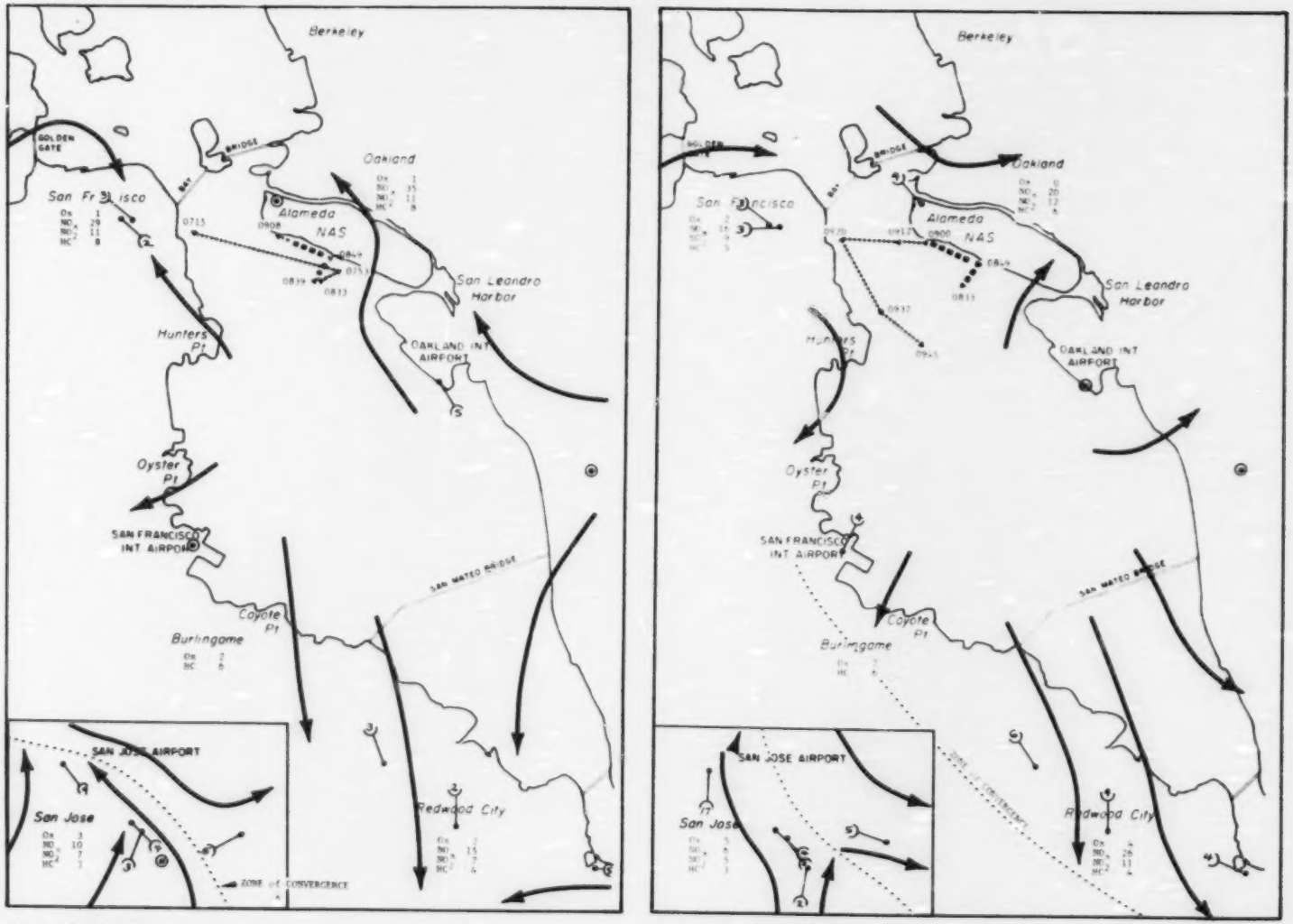

(a) 0800 PST

(b) 0900 PST

FIGURE C-4 AIR POLLUTION LEVELS, SURFACE WIND FLOW, AND HOUSEBOAT COURSE, 7 OCTOBER 1972

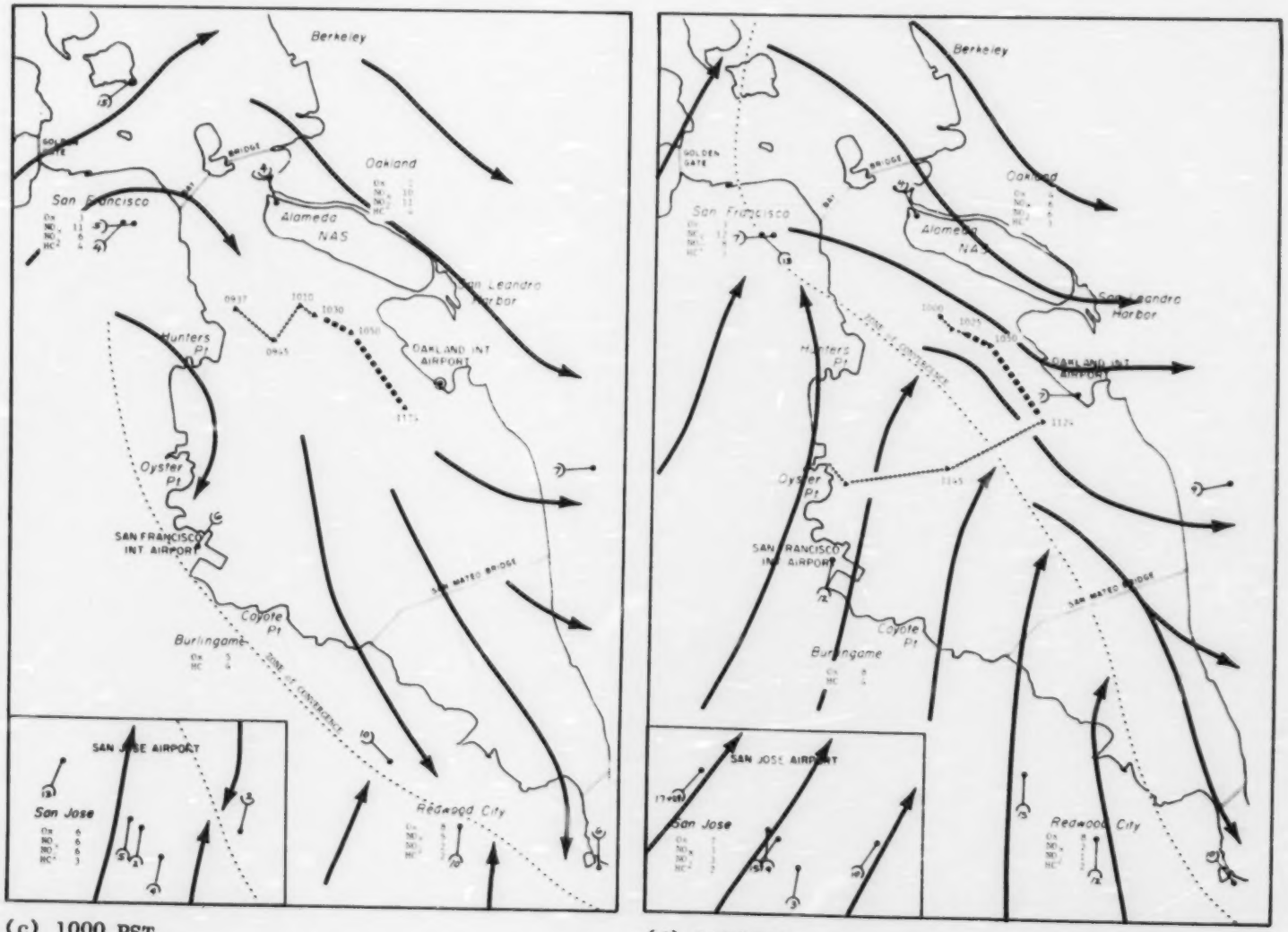

(c) 1000 PST

(d) 1100 PST

FIGURE C-4 AIR POLLUTION LEVELS, SURFACE WIND FLOW, AND HOUSEBOAT COURSE, 7 OCTOBER 1972
(Continued)

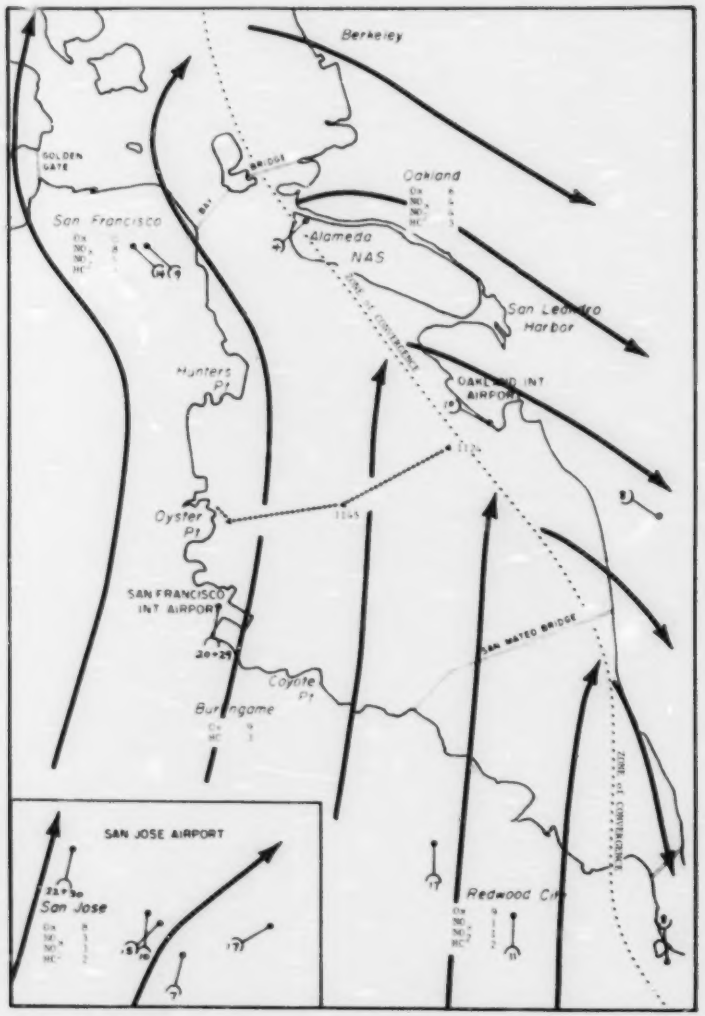

(e) 1200 PST

FIGURE C-4 AIR POLLUTION LEVELS, SURFACE WIND FLOW, AND HOUSEBOAT COURSE, 7 OCTOBER 1972 (Concluded)

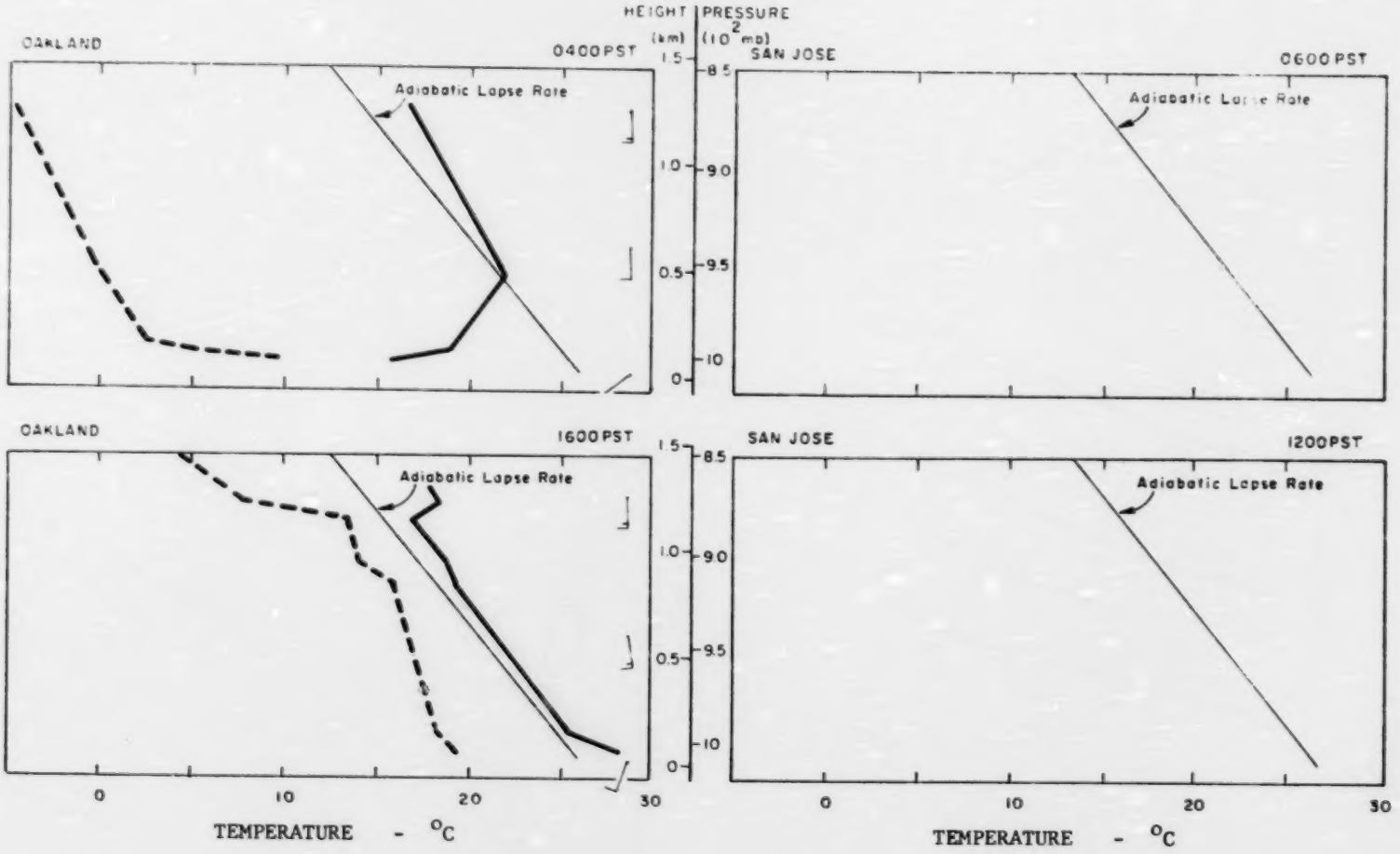

FIGURE C-5 RAWINSONDE TEMPERATURE AND DEW POINT OBSERVATIONS, 7 OCTOBER 1972

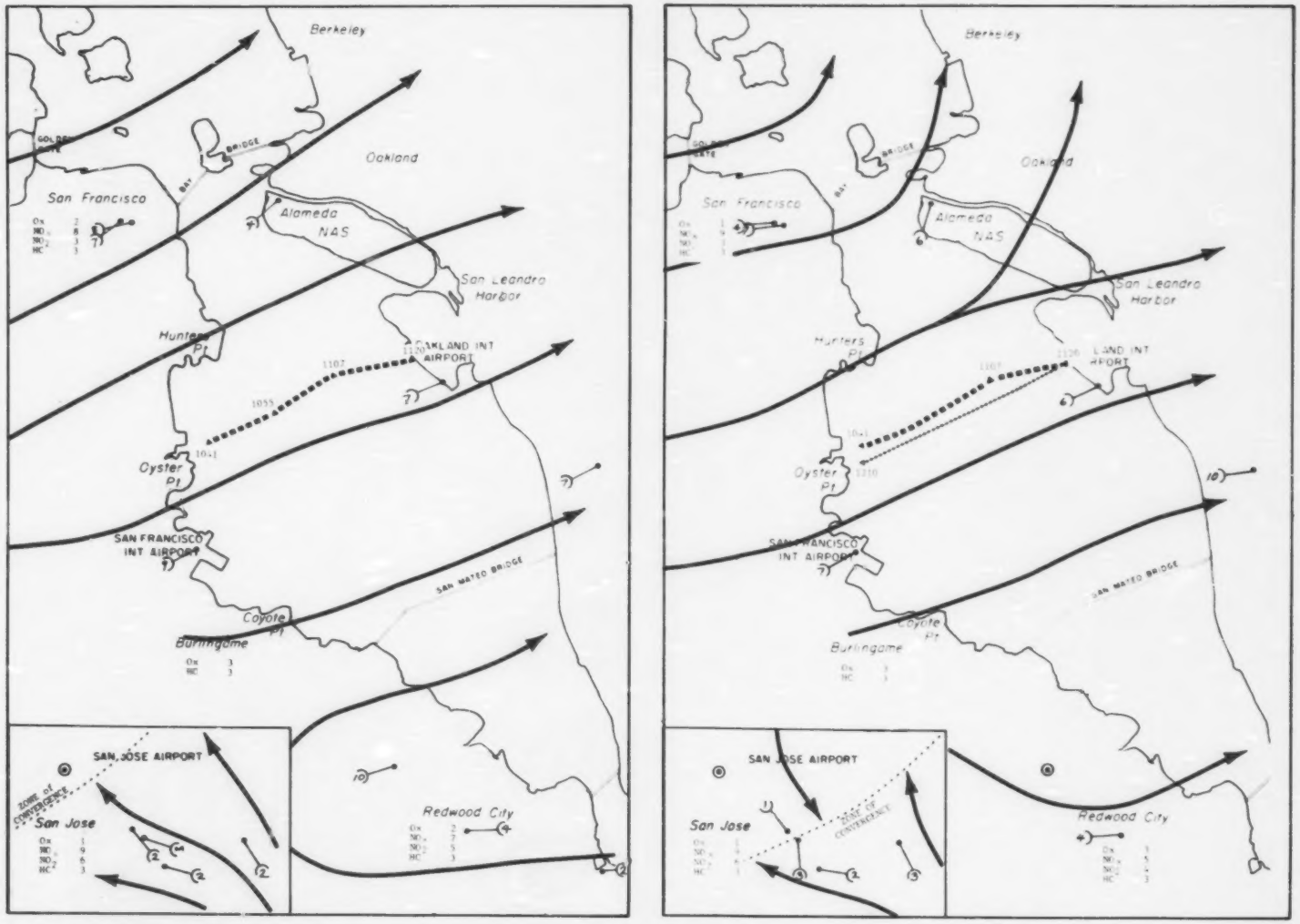

(a) 1000 PST

(b) 1100 PST

FIGURE C-6 AIR POLLUTION LEVELS, SURFACE WIND FLOW, AND HOUSEBOAT COURSE, 19 OCTOBER 1972

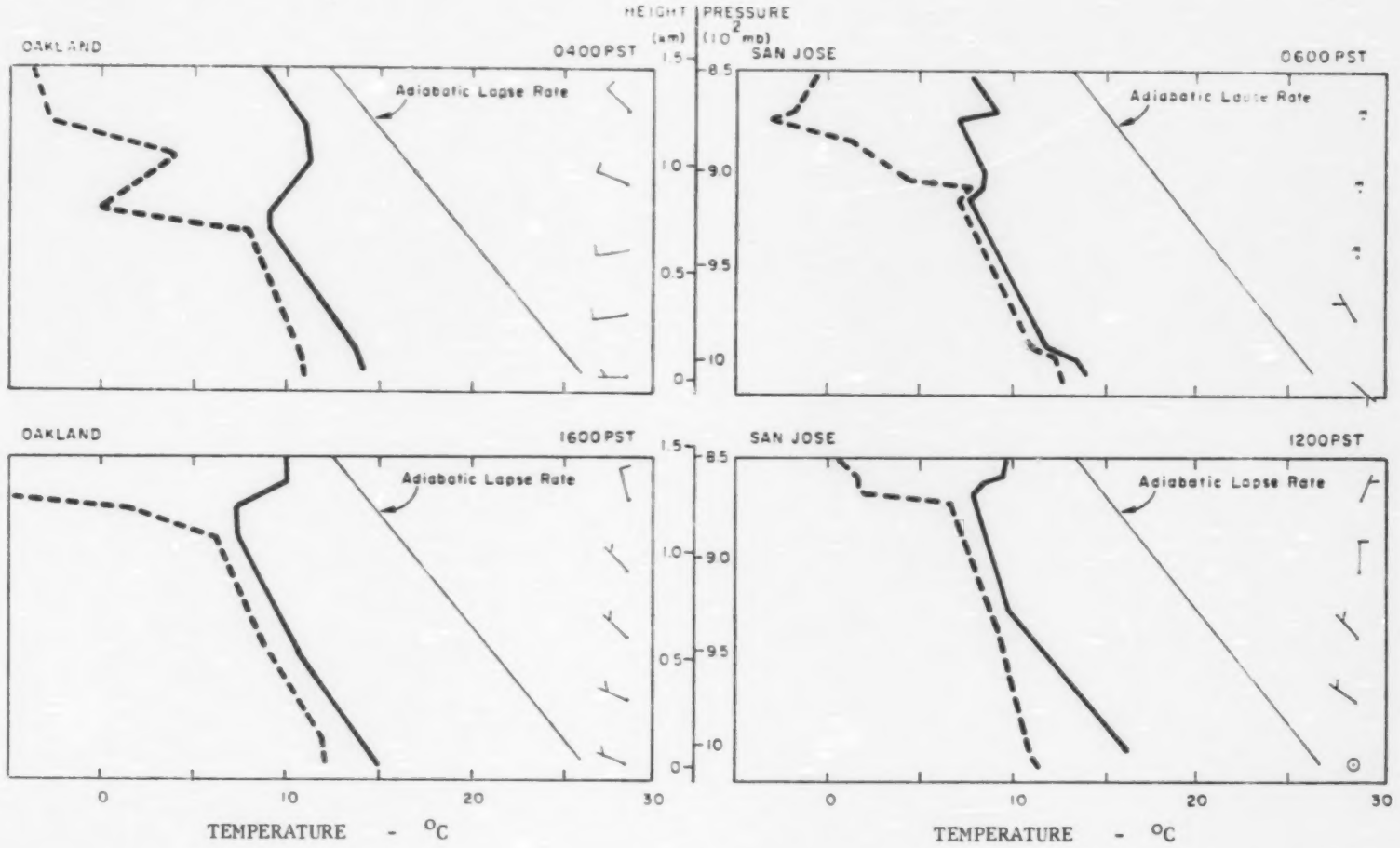

FIGURE C-7 RAWINSONDE TEMPERATURE AND DEW POINT OBSERVATIONS, 19 OCTOBER 1972
(Temperature ——, Dew Point - - - -)

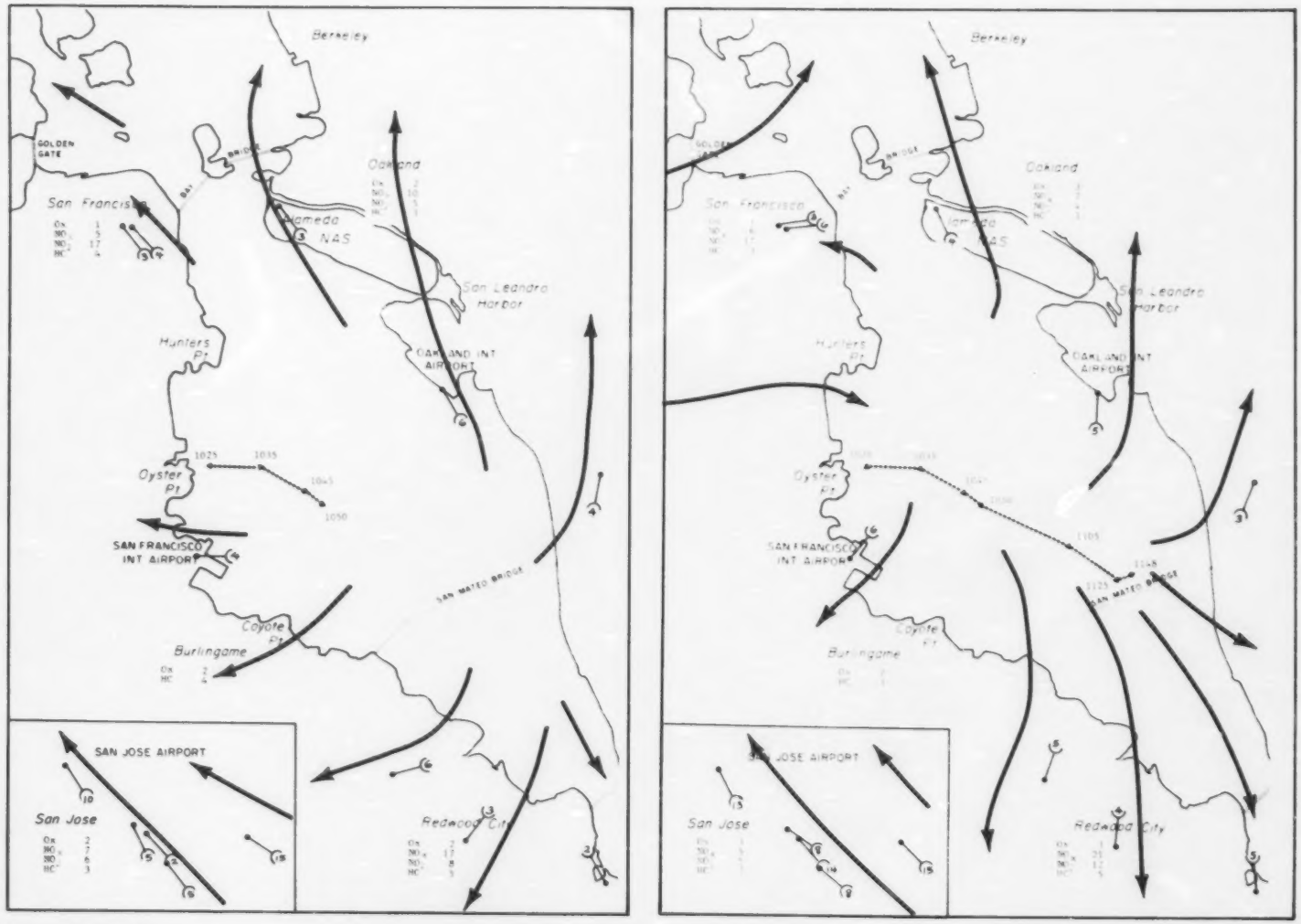

(a) 1000 PST

(b) 1100 PST

FIGURE C-8 AIR POLLUTION LEVELS, SURFACE WIND FLOW, AND HOUSEBOAT COURSE, 6 NOVEMBER 1972

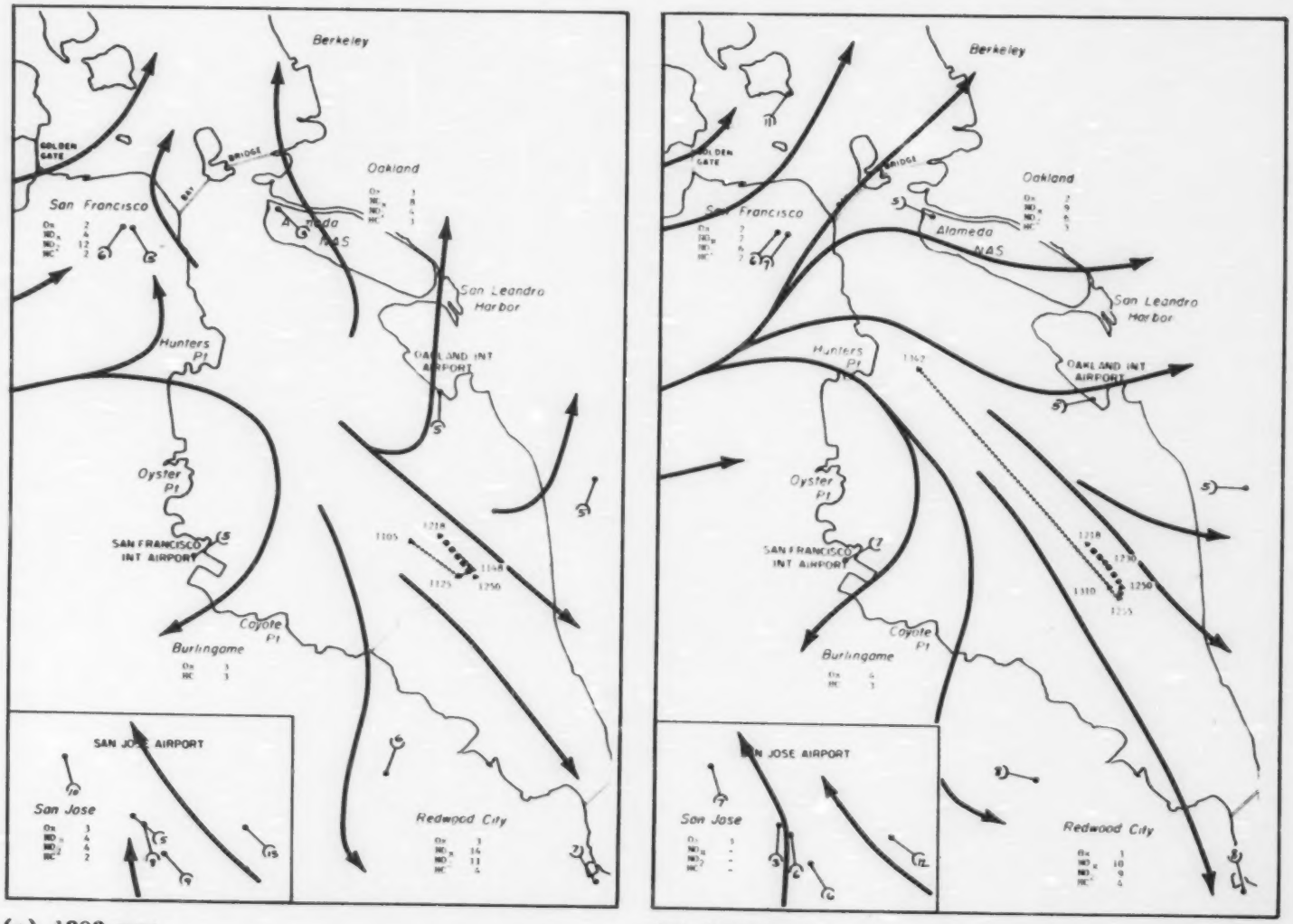

(c) 1200 PST

(d) 1300 PST

FIGURE C-8 AIR POLLUTION LEVELS, SURFACE WIND FLOW, AND HOUSEBOAT COURSE, 6 NOVEMBER 1972 (Continued)

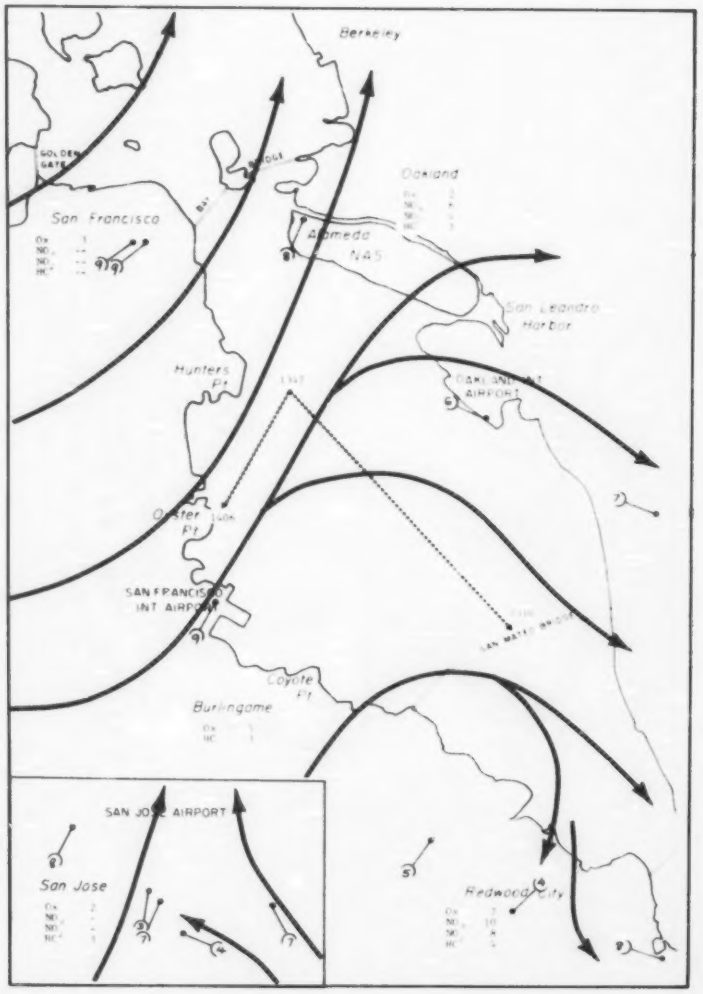

(e) 1400 PST

FIGURE C-8 AIR POLLUTION LEVELS, SURFACE WIND FLOW, AND HOUSEBOAT COURSE, 6 NOVEMBER 1972 (Concluded)

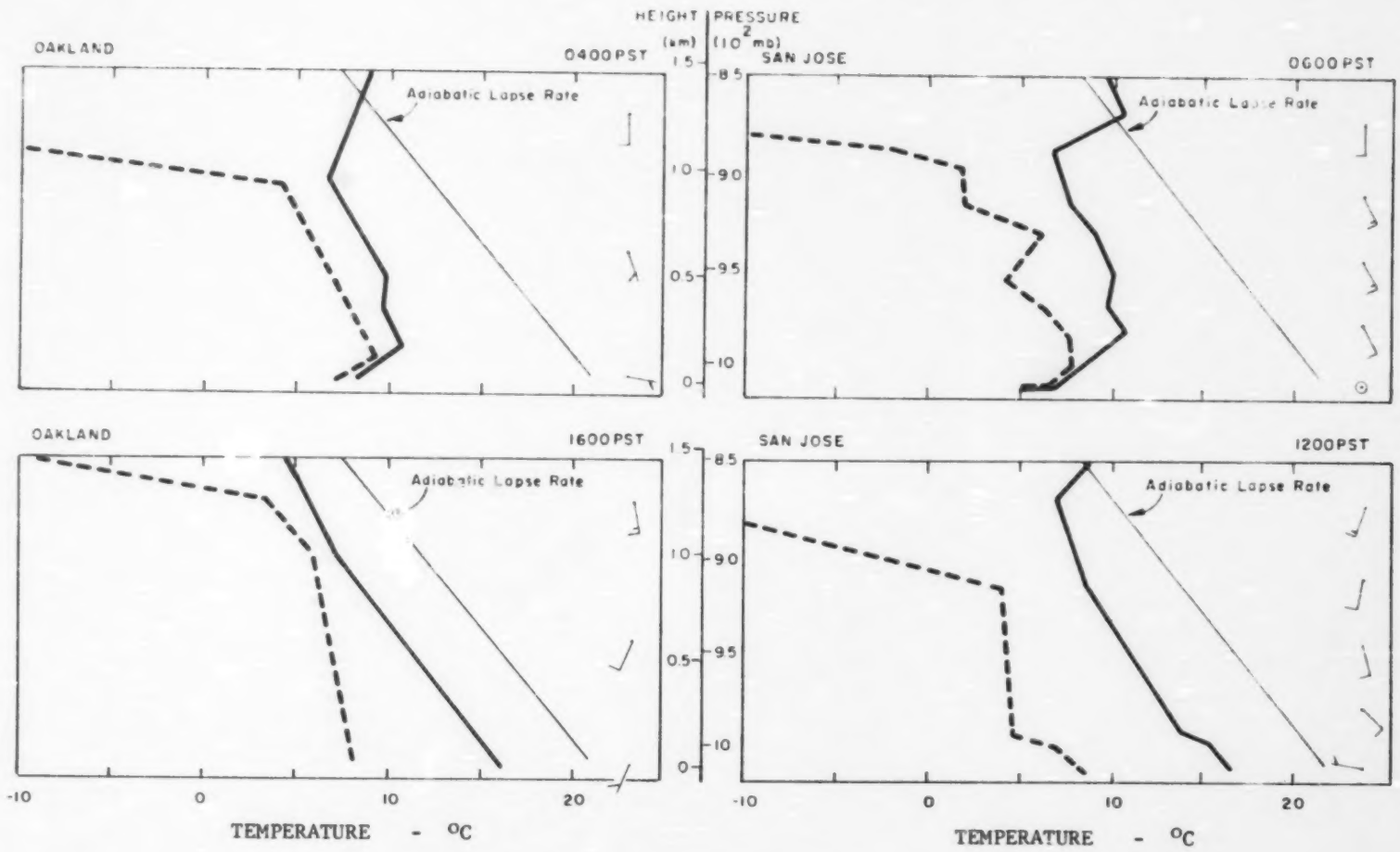

FIGURE C-9 RAWINSONDE TEMPERATURE AND DEW POINT OBSERVATIONS, 6 NOVEMBER 1972
(Temperature ——— , Dew Point - - - -)

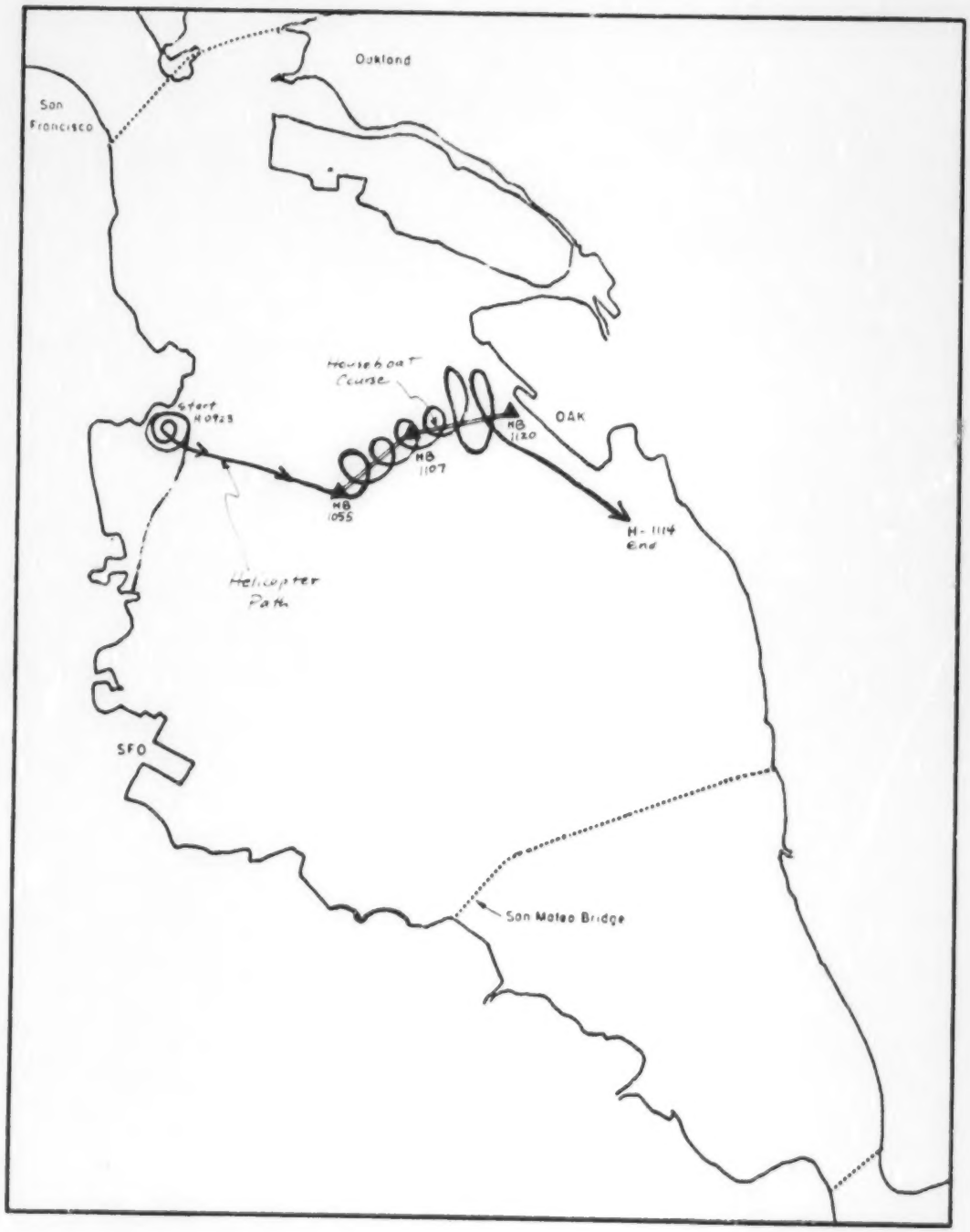

FIGURE C-10 SAMPLING PATHS OF MOBILE LABORATORIES ON 19 OCTOBER 1972
(HB - houseboat, H - helicopter)

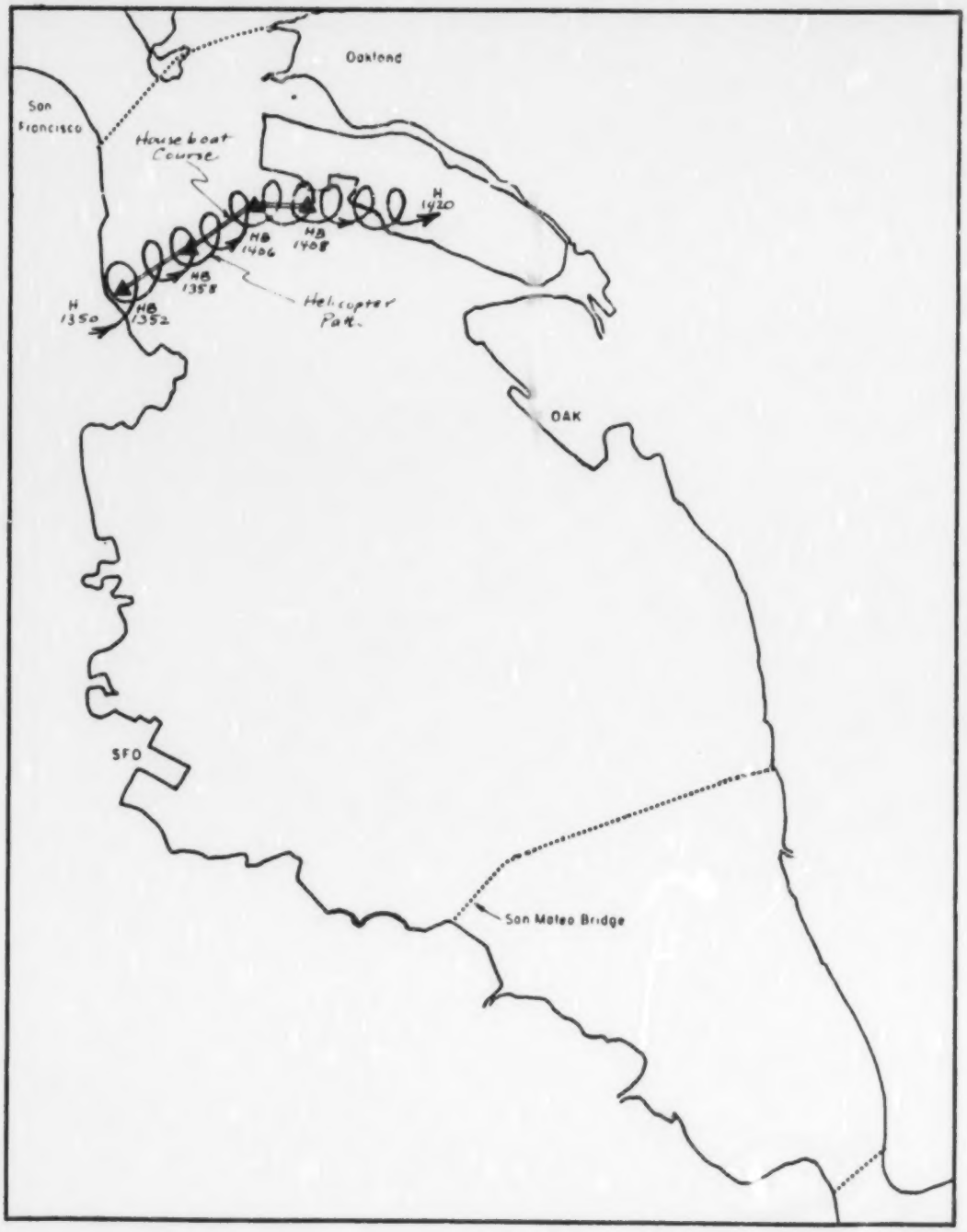

FIGURE C-11 SAMPLING PATHS OF MOBILE LABORATORIES ON 31 OCTOBER 1972
(HB - houseboat, H - helicopter)

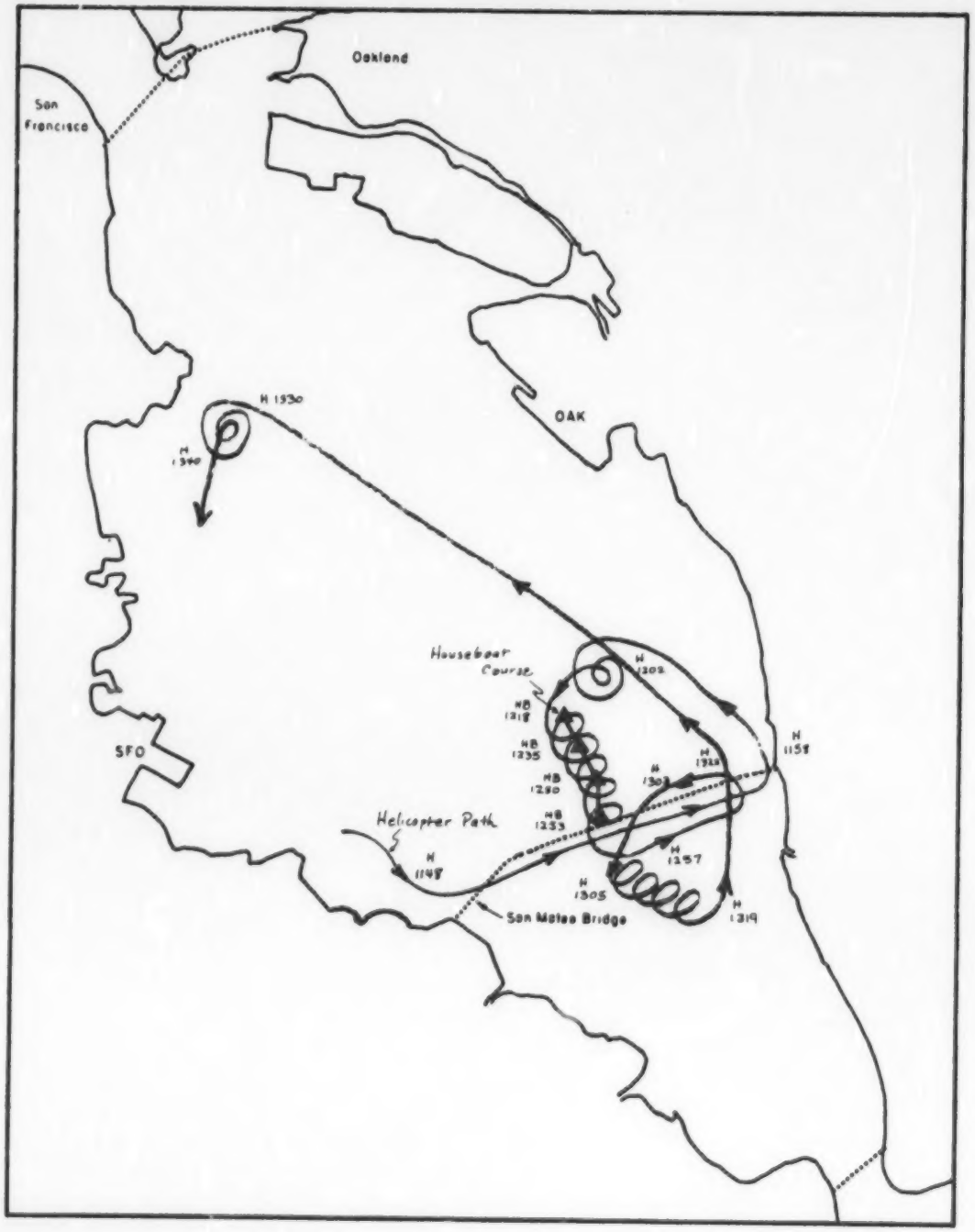

FIGURE C-12 SAMPLING PATHS OF MOBILE LABORATORIES ON 6 NOVEMBER 1972
(HB - houseboat, H - helicopter)

Table C-1

HELICOPTER MEASUREMENTS FOR 19 OCTOBER 1972

Time (PST)	Altitude (ft)	CO* (ppm)	Ox (pphm)	Temp (°C)	NO (pphm)	NO_x (pphm)
Vertical concentration gradient measurements off Hunters Point:						
0923	100		12.3	15.7	15	15
0927	200		10.3	15.6	11	15
0930	300		9.2	15.2	15	15
0932	400			14.8	11	15
0934	500			14.5	11	15
0936	600			14.1	11	15
0938	700			13.8	11	15
0939	800		8.1	13.5	11	15
0941	900			13.2	11	15
0943	1000			12.8	11	15
0945	1100		8.0	12.5	11	15
Measurements made while following tetroon:						
1050	200		2.2	24.4	15	22
1053	580	+1		23.6	11	18
1055	250		2.1	23.6	15	15
1058	260	-1		24.8	11	15
1100	550		2.1	23.8	15	
1103	800			22.7	15	15
1105	400	±0.5	2.2	23.3	15	15
1108	300			24.0	11	15
1110	300		2.1	24.3	11	--
1112	200		2.1	24.6	--	--

*The number is the CO concentration change over the indicated time interval.

Table C-2

HELICOPTER MEASUREMENTS FOR 30 OCTOBER 1972

Time (PST)	Altitude (ft)	Ox (pphm)	Temp (°C)	NO (pphm)	NO_x (pphm)
Measurements made while following tetroon:					
1251		1.8	14.4	6	8
1253	100		15.1		
1255	600	1.7	14.6		14
1257	900		14.2	9	14
1300	900	1.5	14.2	8	12
1303	500		14.5	9	11
1306	150	1.4	15.1	6	10
1309	500	1.6	14.5	6	6
1311	500		14.8	6	12
1315	500	1.7	14.4	9	11
1318	500		14.6	11	16
1320	400		14.6	10	12
1322	600		14.7	10	13
1325	600	0.2	14.7	9	12
1327	600		14.6	8	12
1330	500	3.1	14.6	8	11
1332	500	2.2	15.0	8	11
1340			14.8	8	10

Table C-3

HELICOPTER MEASUREMENTS FOR 6 NOVEMBER 1972

Time (PST)	Altitude (ft)	CO (ppm)	Ox (pphm)	Temp (°C)	NO (pphm)	NO_x (pphm)
Horizontal concentration gradient measurements:						
1150	450			13.1	23	30
1155	450			13.0	16	26
1157		+1		13.0	14	15
1159				13.6	16	25
1201				13.5	18	24
Vertical concentration gradient measurements:						
1202	50			13.6	25	27
1203	120			13.6	28	29
1205	270			13.0	28	29
1206	330			13.0	28	29
1208	400			12.9	26	24
1209	530			12.9	14	22
1210	730			13.0	15	22
1211	930			12.7	16	22
1212	1700			12.0	10	21
Measurements made while following tetroon:						
1220	< 400		1.8	12.9	12	21
1222	< 400			13.2	14	21
1224	400		1.4	13.0	16	23
1226	~ 450			13.4	16	22
1228	500	±0.3	1.7	13.1	18	23
1233	500			13.2	14	21
1235	500		1.9	13.2	15	22
1238	500	±1		13.2	14	22
1239	500			13.1	14	22
1240	~ 425		1.9	13.0	14	23
1242	450	±0.5		13.1	15	22
1246	200		1.9	13.1	14	20
1248	100			13.6	15	21
1251	350		1.9	13.1	16	21

Table C-3 (Concluded)

Time (PST)	Altitude (ft)	CO* (ppm)	Ox (pphm)	Temp (°C)	NO (pphm)	NO_x (pphm)
Horizontal concentration gradient measurements:						
1255			1.9	13.2	15	20
1300			2.0	13.2	16	21
1303	400			13.2	16	22
Measurements made while following tetroon:						
1305	400		2.0	13.2	16	22
1308	800			13.0	15	20
1310			2.0	12.9	14	20
1315	400	-1	1.9	12.7	12	18
1320			1.8	13.0	14	18
Vertical concentration gradient measurements off Hunters Point:						
1340	100		2.2	14.0	6	18
1342	200			14.0	8	20
1344	300			14.0	9	19
1345	410			13.8	8	20
1347	640			13.2	8	20
1349	1580			12.4	8	19
1351	2620		6.4	11.1	8	19

*The number is the CO concentration change over the indicated time interval.

Table C-4

CHEMICAL ANALYSES OF PARTICULATE MATTER
COLLECTED ON GLASS FIBER FILTERS

Time (hr:min)	Mass Loading ($\mu g/m^3$)	Chemical Composition ($\mu g/m^3$)			
		Nitrate	Sulfur*	Chloride	Lead
October 19					
11:41-12:20	109	0	7.9	5.2	0.61
October 24					
12:53-13:16	225	0	4.6	31.5	0
October 25					
8:00-11:04 12:35-13:20	108	9.6	3.7	2.5	2.7
October 26					
10:06-10:50 October 31 13:52-14:07	90	0	11.1	6.9	1.1
November 2					
8:33-11:20 11:23-13:17	108	10.8	6.0	1.0	2.4
16:33-17:45	194	24.7	17.3	3.1	2.6
November 6					
10:38-12.01	173	29.8	9.4	4.5	3.8
12:10-14:05	202	0	7.0	1.0	0.33
November 17					
11:05-11:20 13:17-13:47	325	0	7.1	9.9	0.56

* All water-soluble sulfur compounds are included as sulfate.

Table C-5

GAS CHROMATOGRAPH DATA-CRYOGENIC TRAP SAMPLES

Hydrocarbon Class	25 October, 0845		26 October, 0929		31 October, 1346		2 November, 0925		2 November, 1100		6 November, 1220		Typical Exhaust
	ppb C	%	ppb C	%	ppb C	%	ppb C	%	ppb C	%	ppb C	%	Range (%)
Olefins													
Ethylene	18	1.2	21	1.3	< 1	< 0.1	127	4.4	141	10.8	675	26.0	12-13
Acetylene	21	1.4	< 1	0.1	< 1	< 0.1	31	1.1	36	2.8	< 1	< 0.1	9-11
C_3-C_5	23	1.6	7	0.6	387	12.2	36	1.3	4	0.3	19	0.7	4-6
C_6-C_7	13	0.9	46	3.7	< 1	< 0.1	61	2.1	17	1.3	106	4.1	1
C_8-C_{10}	2	0.1	< 1	0.1	< 1	< 0.1	1	0.1	< 1	< 0.1	< 1	< 0.1	1
Subtotal	77	5.3	76	6.0	498	15.7	256	9.0	199	15.2	801	30.9	25-30
Paraffins													
Ethane	18	1.2	23	1.8	< 1	< 0.1	136	4.8	77	5.9	111	4.3	0-2
Propane	15	1.0	< 1	0.1	< 1	< 0.1	18	0.6	42	3.2	< 1	< 0.1	1-2
C_4-C_5	523	35.9	398	31.9	868	27.4	189	6.6	178	13.6	208	8.0	8-12
C_6-C_7	274	18.8	200	16.0	728	23.0	250	8.7	58	4.4	359	13.8	6-14
C_8-C_{10}	179	12.3	199	16.0	303	9.6	453	15.8	103	7.9	225	8.7	7-13
Subtotal	1009	69.3	821	65.8	1901	60.0	1046	36.6	458	35.1	904	34.9	30-40
Aromatics													
Benezene	34	2.3	56	4.5	106	3.3	47	1.6	10	0.8	131	5.0	2-3
Toluene	80	5.5	88	7.1	207	6.5	144	5.0	27	2.1	205	7.9	5-6
Ethyl Benzene	20	1.4	24	1.9	39	1.2	169	6.0	17	1.3	53	2.0	1-2
m-,p-Xylene	71	4.9	78	6.2	138	4.4	130	4.6	53	4.1	137	5.3	6-8
o-Xylene	38	2.6	5	0.4	87	2.7	54	1.9	29	2.2	107	4.1	3-7
C_9-C_{10}	127	8.7	100	8.0	194	6.1	1012	35.4	512	39.2	255	9.8	14-18
Subtotal	370	25.4	351	28.2	771	24.3	1557	54.5	648	49.7	888	34.2	30-45
TOTAL	1456		1247		3170		2859		1305		2593		

Appendix D

DESCRIPTION OF EDITED DATA TAPE

Appendix D

DESCRIPTION OF EDITED DATA TAPE

The thousands of individual observations made during this project have been consolidated, edited, and recorded at high-density, odd-parity mode on a single reel of seven-channel magnetic tape. In this consolidation, all the primary data were retained. Each record of the summary tape corresponds to a record as originally recorded by the data collection during a 5-minute period.

All the data have been converted to engineering units. The units used for the various parameters are shown in Table D-1. Missing data are marked by the number -99.9. Each record contains 340 words. Table D-2 shows the organization of the records. The first 30 words are devoted to averages and other items that apply to the entire 5-minute period. The next 200 words give the data collected at 15-second intervals. Another 100 words are used for the 30-second data. The last 10 words, and several spaces among the first 30 words are listed as spares. These locations can be used for derived quantities of special interest, without requiring a reorganization of the record. For example, one of the locations that was designated as spare in the original formatting has subsequently been used for relative humidities. Another space has been used to indicate periods of tetroon tracking.

Preceding page blank

Table D-1

UNITS USED IN DATA SUMMARY

Parameter	Unit
Date	Year-month-day, e.g., 720911 is 11 September 1972
Time	Hours (decimal) Pacific Standard Time
Location	Kilometers - See Figure D-1 for coordinate system
Particle concentration	Number cm^{-3} per channel
Carbon monoxide concentration	Parts-per-million-by-volume (ppm)
Total hydrocarbon concentration	ppm carbon (ppm C) as hexane
Nitric oxide concentration	parts-per-hundred-million (pphm)
Nitrogen dioxide concentration	pphm
NO_x concentration	pphm
Ozone condentration	pphm
Total sulfur concentration	pphm
Condensation nuclei	Thousands per cm^3
Scattering coefficient	$m^{-1} \times 10^4$
Solar radiation	cal $cm^{-2}min^{-1}$
Temperature	degrees centigrade
Relative humidity	percent

Table D-2

ENGINEERING UNIT MAGNETIC TAPE RECORD FORMAT

First three lines of data	Date	Record time (decimal hours PST) Start	End	X at Start (km)	Y at Start (km)	X at End (km)	Y at End (km)	Particle Count During Period Chan.1($No.cm^{-3}$)	Chan.2($No.cm^{-3}$)	Chan.3($No.cm^{-3}$)
	Particle Count During Period Chan.4($No.cm^{-3}$)	Chan.5($No.cm^{-3}$)	Average CO (ppm) *	Average Hydrocarbons (ppm C)	Average O_3 (pphm)	Average Sulfur (pphm)	Av. Scattering Coefficient ($km^{-1} \times 10^3$)	Av. Condensation Nuclei ($cm^{-3} \times 10^{-3}$)	Average CO (ppm) +	Error Code ‡
	Spare	Average NO (pphm)	Average NO_2 (pphm)	Average NO_x (pphm)	Average Temperature (°C) Dry Bulb	Wet Bulb	Average Radiation ($cal\ cm^{-2}\ min^{-1}$)	Av. Reference Voltage (V)	Av. Relative Humidity (%)	Spare
Typical data	7?1025.000 .087 -99.900	13.183 .060 8.492	13.263 -99.900 8.547	12.522 1.711 13.815	22.307 5.078 30.736	12.847 8.169 25.949	23.324 .438 2.124	.299 8.508 .961	.372 3.216 74.888	.120 -99.900 -99.900
A'	Time (hours PST)	X (km)	Y (km)	CO (ppm) *	Hydrocarbons (ppm C)	O_3 (pphm)	Sulfur (pphm)	Scattering Coefficient ($km^{-1} \times 10^3$)	Condensation Nuclei ($cm^{-3} \times 10^{-3}$)	CO + (ppm)
	13.183 13.187 13.192 13.196 13.200 13.204 13.208 13.212 13.217 13.221 13.225 13.229 13.233 13.237 13.242 13.246 13.250 13.254 13.258 13.262	12.522 12.539 12.556 12.573 12.590 12.607 12.624 12.641 12.658 12.675 12.692 12.710 12.727 12.744 12.761 12.778 12.795 12.812 12.829 12.846	22.307 22.360 22.413 22.467 22.520 22.573 22.627 22.680 22.733 22.787 22.840 22.893 22.947 23.000 23.053 23.107 23.160 23.213 23.267 23.320	-99.900 -99.900 -99.900 -99.900 -99.900 -99.900 -99.900 -99.900 -99.900 -99.900 -99.900 -99.900 -99.900 -99.900 -99.900 -99.900 -99.900 -99.900 -99.900 -99.900	1.719 1.719 1.719 1.719 1.719 1.719 1.719 1.719 1.719 1.641 1.719 1.719 1.719 1.719 1.719 1.797 1.641 1.719 1.719 1.641 1.641	5.078 5.078	9.288 8.105 8.105 8.105 9.288 8.105 3.474 9.288 9.288 8.105 9.288 8.105 8.105 8.105 8.105 8.105 8.105 8.105 8.105 8.105 8.105	.469 .469 .547 .469 .469 .469 .391 .469 .391 .469 .391 .469 .313 .469 .391 .469 .469 .469 .313 .469 .391	9.844 8.906 8.672 8.906 7.266 9.141 7.969 8.203 7.969 7.969 7.969 8.438 7.969 6.906 7.266 8.438 7.969 9.375 7.969 9.141 9.844	3.563 3.000 3.750 2.813 3.000 3.563 3.188 2.813 2.813 2.813 2.813 2.625 4.500 3.563 3.563 3.375 2.625 3.188 3.375 2.625 3.563
B'	Time (hours PST)	X (km)	Y (km)	CO (ppm)	NO_2 (pphm)	NO_x (pphm)	Temperature (°C) Dry Bulb	Wet Bulb	Radiation ($cal\ cm^{-2}\ min^{-1}$)	Reference Voltage (V)
	13.184 13.192 13.200 13.209 13.217 13.225 13.234 13.242 13.250 13.259	12.523 12.557 12.591 12.625 12.659 12.694 12.728 12.762 12.796 12.830	22.310 22.417 22.524 22.630 22.737 22.844 22.950 23.057 23.164 23.270	17.359 17.359 9.938 9.938 6.813 6.813 6.813 4.469 4.469 3.688 3.688	10.328 2.906 2.906 4.469 4.469 4.078 4.469 4.859 4.078 4.078 3.684	16.430 20.219 20.219 14.914 14.914 11.883 11.883 9.609 9.609 8.473	31.125 31.281 31.437 31.437 31.125 30.656 30.500 30.500 29.875 29.906	26.437 26.594 26.437 26.281 26.125 25.812 25.656 25.500 25.500 25.344	2.119 2.078 1.931 2.161 2.454 2.203 2.119 2.098 2.057 2.015	.961 .961 .961 .961 .961 .961 .961 .961 .961 .961
Spares	-99.900	-99.900	-99.900	-99.900	-99.900	-99.900	-99.900	-99.900	-99.900	-99.900

* CO as measured by the Bacharach mercury displacement analyzer.

\+ CO as measured by the Beckman NDIR analyzer.

‡ 0.0 = yes, -99.9 = no

' Fifteen-second sampling intervals are indicated by A and 30-second sampling intervals are indicated by B.

The locations shown are referred to the coordinate system shown in Figure D-1. The coordinates are determined from landmark azimuth sightings made on the boat periodically whenever there were significant changes of course. The coordinates on the data tape for each individual time were obtained by time-based linear interpolation for all except the times corresponding to azimuth sightings. The locations shown are estimated to be accurate within about 250 m.

The records include average and summary information to facilitate selection of data sets that meet certain criteria. For instance, data could be stratified and averaged according to time of day, location, radiation intensity, or prevailing carbon monoxide concentrations. The summary data can also be used in preliminary data analysis to produce smoothed time histories.

The data for each experimental day are contained in a separate file. Two end-of-files mark the end of the data tape.

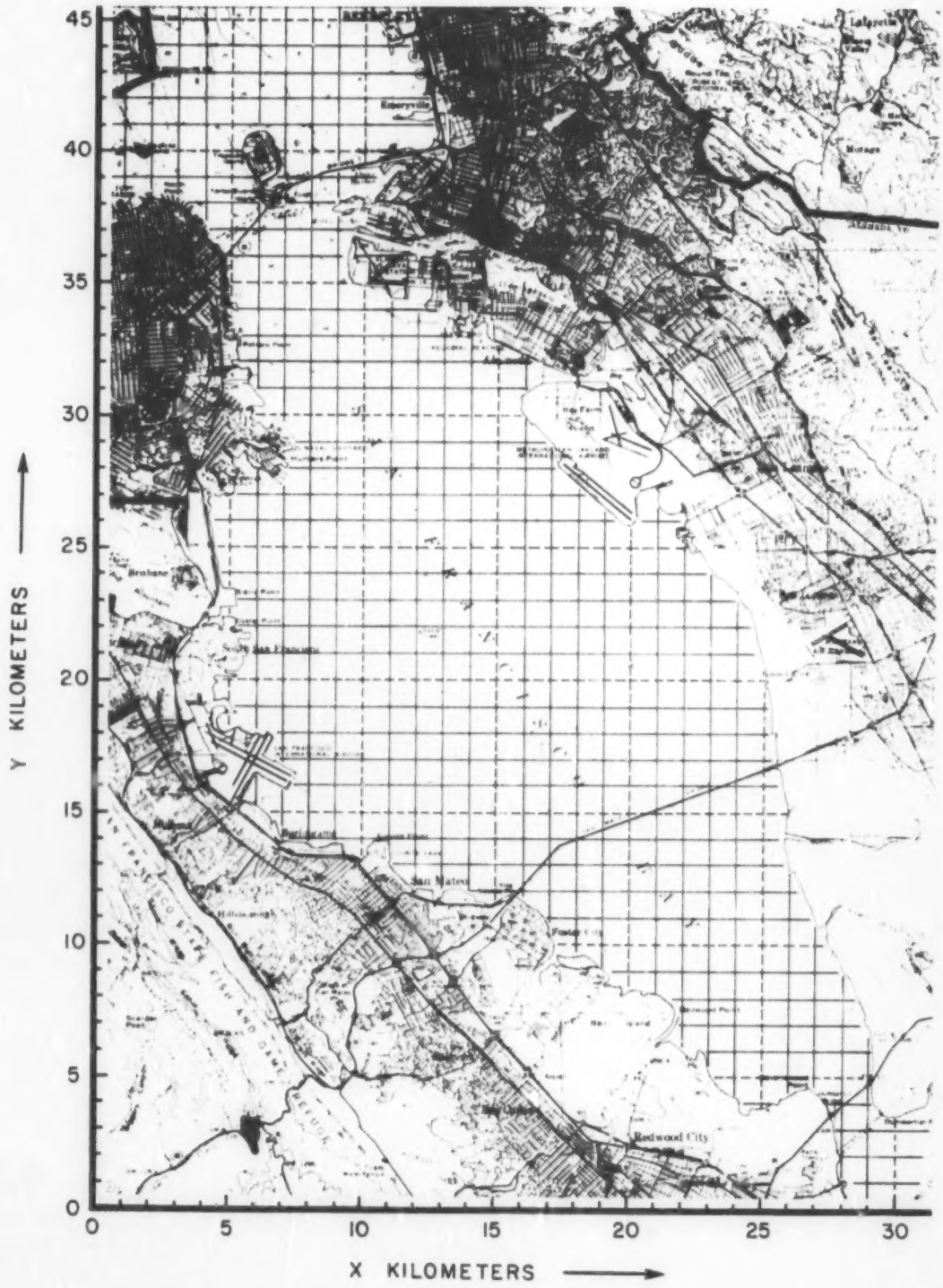

FIGURE D-1 GRID COORDINATE OVERLAY MAP OF THE BAY AREA

Appendix E

CHRONOLOGICAL SUPPORTING DATA FOR SELECTED SAMPLE DAYS

Appendix E

CHRONOLOGICAL SUPPORTING DATA FOR
SELECTED SAMPLE DAYS

The meteorological data, pollutant plots, the particulate data, and the hydrocarbon distribution data for 21 September, 25 October, 26 October, and 2 November were summarized in the Section V of this report. The following discussions are expanded analysis of the data from the four selected days.

A. 21 September

The meteorological conditions and pollutant plots for 21 September may be found in Section V.B.

The houseboat was moved from OP to a point halfway between Hunters Point (HP) and Oakland. This position was maintained for 45 minutes while the tetroon was weighed off. The data in Table E-1 are selected concentrations observed during this 45-minute interval. Two conclusions can be reached. The low values of the NO to NO_2 ratio indicate that the sampled air was well aged. The increase in O_3 concentration suggests that photochemical reactions were occurring. The houseboat proceeded to a point north of the BB where the tetroon was released at 1030. The pollutant concentrations are summarized in Figure 3. The tetroon was over San Francisco from 1037 to 1056, so that the data collected during this interval are not truly representative of the same air parcel.

While the NO concentration decreased rapidly after 60 minutes, the concentration of the other pollutants did not. However, there is a steady decrease in the concentration of CO from about 1.3 ppm to 0.8 ppm due to dilution. Since CO is essentially inert under atmospheric conditions, a

Preceding page blank

Table E-1

HOUSEBOAT DATA FOR 21 SEPTEMBER 1972, 0912 TO 1000 PST
(5-Minute Averages)

Time	NO (pphm)	NO_2 (pphm)	O_3 (pphm)	THC (ppm)	Nephelometer ($m^{-1} \times 10^4$)
0915	5.2	14.6	3.2	6.5	2.7
0930	4.6	14.9	4.5	6.9	2.1
0945*	8.0	16.2	4.3	8.4	2.2
1000	2.7	13.6	6.3	6.4	3.0

* May have some houseboat exhaust from tetroon weighoff procedure.

plot of the ratio of pollutant to CO concentrations permits the changes in pollutant concentrations to be assessed without interference or masking by dilutional effects. On the basis of pollutant to CO concentration ratios, the concentration of NO_2 decreases with a corresponding increase in O_3 concentration. The concentration of total hydrocarbons (THC) remains nearly constant. These observations are discussed in more detail in Section VI-A.

The aerosol particle counter data are summarized in Figure 6. Two features of these plots are particularly interesting. First, there is a 20-fold decrease in the aerosol concentrations from 1042 to 1226. A similar decrease was observed in the CN concentration and the nephelometer readings (by a factor of about 2) during the same time interval. Second, the number of particles in the 0.3-micron size range is nearly equal to the number in the 0.2-micron range. There may also be a peak in the size distribution in the 0.4-micron range.

The concentration decrease may be ascribed to a loss of water through evaporation from the individual particles, to coagulation, or to dilutional effects.

The dilutional effects during this period reduce concentrations by about a factor of two or three, as indicated by changes in the concentrations of CN and CO. According to theory,[30] coagulation is a process that changes size distributions only very slowly, and would in any event lead to a replenishment of the particles in the tenth micron size range. Evaporation seems the most likely cause of the reduction in the particles concentrations in the size ranges measured by the particle counter. As shown in Table E-2, the relative humidity at the stations on the perimeter of the Bay (SF and Oakland Airports) was 65 to 75 percent early in the sampling interval and decreased to about 50 to 60 percent at the end. Such changes are likely to be accompanied by evaporation of droplets containing dissolved salts.[30] Therefore, droplets of a few tenths micron diameter would shrink to dry particle sizes below the measurement range of the counter. However, the total numbers of particles would remain about the same and CN concentration would not be affected.

Table E-2

TEMPERATURE AND RELATIVE HUMIDITY
DATA FOR BAY AREA STATIONS

	San Francisco Federal Building		San Francisco Airport		Oakland Airport	
Time (PST)	Temp (°C)	RH (percent)	Temp (°C)	RH (percent)	Temp (°C)	RH (percent)
1000	23	60	19	68	19	73
1100	22	53	21	61	20	68
1200	25	54	23	53	22	66
1300	22	55	23	49	23	55

B. 25 October

The houseboat made a straight line traverse across the Bay departing from OP at 0545 and arriving at the entrance to San Leandro Harbor (SLH) at 0627. The NO concentration was 29.4 pphm at the western shore of the Bay. A gradual decrease to 0.6 pphm was observed as the houseboat approached a point about 2.5 kilometers to the west of the center of the Bay. Between this point and the SLH entrance, the concentration of NO increased to a maximum of 48.4 pphm. These measurements were made while the houseboat was at cruising speed, and exhaust gas contamination could not have occurred. A summary of the 5-minute average pollutant concentrations is shown in Table E-3.

Table E-3

HOUSEBOAT DATA FOR 25 OCTOBER 1972, 0546 TO 0636 PST
(5-Minute Averages)

Time	NO (pphm)	NO_2 (pphm)	O_3 (pphm)	CO (ppm)	THC (ppm C)	Nephelometer ($m^{-1} \times 10^4$)
0546	27.8	2.5	1.7	1.688	--	0.9
0556	11.2	1.1	2.3	1.184	3.0	0.4
0606	0.7	1.9	1.4	0.872	3.0	0.5
0616	18.4	3.5	--	1.28	3.3	0.5
0626	37.8	2.7	--	1.2	3.5	0.5
0636	26.7	8.2	--	--	4.2	1.8

Offshore breezes early in the morning probably caused encroachment of polluted air, primarily containing high NO concentrations, near the west and east shores of the Bay. The offshore advection had not advanced sufficiently to modify the very clean air present in the central Bay. While the houseboat remained near the eastern shore of the Bay from 0627 to 0754, easterly winds became established.

A tetroon was released at 0756 and drifted from east to west along essentially the identical path that the houseboat had taken from west to east 2 hours previously. The NO concentration at SLH had declined by nearly 50 percent (to about 19 pphm) from the time of arrival at 0627 until the tetroon was released at 0756. The concentration of NO in this run increased in the central Bay with some inhomogeneity to about 25 pphm; a constant decrease of NO was observed from the central Bay to the western shore. The decrease was somewhat masked by an interval of exhaust gas contamination west of the center of the Bay. The relatively high CO concentrations observed at the western shore earlier had now diminished to below 5 pphm due to advection.

During the 0756 tetroon run on this day, supplemental measurements were made by the helicopter. The helicopter circled the tetroon from 0805 until 0930. The radius of the helicopter circles, based on a constant speed and the time required for completion of a circle, varied from 225 meters to 470 meters with an average radius of about 300 meters. The tetroon was floating at an average altitude of 150 meters. The helicopter circled the tetroon in flight from an altitude of 30 meters to 180 meters. Comparison data of pollutant measurements obtained by the two mobile laboratories are shown in Table E-4.

Table E-4

DATA FOR 25 OCTOBER 1972, 0801 TO 0825 PST
(1-Minute Averages)

Houseboat					Helicopter					
Time	NO (pphm)	NO_x (pphm)	O_3 (pphm)	Temp (°C)	Time	Alt (ft)	NO (pphm)	NO_x (pphm)	O_x (pphm)	Temp (°C)
0801	19	19.1	0.8	20.2	0807	100	33	40	0.8	24.5
0812	26	2.1	0.8	20.5	0812	100	22	26	0.8	24.0
0814	21.3	25.1	0.8	26.8	0814	190	22	26	0.7	24.0
0815	23.2	25.1	0.8	21.0	0815	250	22	26	0.6	24.0
0818	14.6	19.1	0.8	21.1	0818	290	7	18	0.8	24.0
0820	14.6	17.6	0.8	21.3	0820	380	11	15	0.8	24.0
					0825	600	7	11	0.9	24.0

At 0831 the helciopter moved to a location out of the flight path of the San Francisco and Oakland Airports to obtain a vertical profile of temperature and pollutant concentrations. A spiraling ascent was performed near the San Mateo Bridge beginning at 0831. The data from this vertical profile are summarized in Table E-5.

Table E-5

HELICOPTER DATA FOR 25 OCTOBER 1972, VERTICAL PROFILE

Alt (ft)	Time (PST)	NO (pphm)	NO_x (pphm)	O_x (pphm)	Temp (°C)
100	0831	44	58	0.8	24.0
130	0832	29	51		24.0
170	0833	18	36		23.5
220	0834	11	22		23.5
300	0835	18	18	0.5	24.0
400	0837	11	15		23.9
590	0839	11	15		23.9
720	0840	7	7	0.5	24.0
900	0841	7	7		23.0
1900	0844	7	11	0.4	23.0
4800	0849	7	7	0.3	22.0

The temperatures measured during the tetroon run indicate that the atmosphere is relatively stable at the lower altitudes. As anticipated, the pollutant concentrations decreased as the measurement altitude increased.

The helicopter completed the vertical profile and returned to the houseboat to continue tracking the tetroon after the sample run was terminated by the houseboat at 0855. However, the helicopter was unable to locate the tetroon due to the lack of visual contrast between the tetroon and the background of multicolored house roofs. Due to the hilly terrain, the helicopter was unable to fly below the level of the tetroon to improve visual contrast.

The houseboat began a return trip to SLH at 0916, arriving at 0955. During the traverse from 0916 to 0955, the maximum NO concentrations (14 pphm) were observed near the western shore of the Bay. The NO concentration decreased continuously during this traverse until the NO concentrations reached a plateau of about 6 pphm near the eastern shore of the Bay. The concentration of NO_2 appeared stable at 5 pphm throughout this traverse.

The wind flow pattern changed from an east wind to onshore winds with a southerly component at about 1000. The houseboat proceeded south to the San Mateo Bridge in order to use bridge auto traffic as a pollution source. A tetroon was launched at 1135, and the run was terminated by the houseboat laboratory at 1220. The trajectory of the tetroon, as illustrated in Figure 7 (f), was to the west until a period of stagnation occurred at 1156 and lasted until 1208. When the tetroon began moving again, the wind direction had shifted, causing the tetroon to move toward the south as shown in Figures 7 (f) and 7 (g). Although short-term variations in pollutant concentrations were observed, which indicate some inhomogeneity of the air over the sample path, no gross inhomogneities were observed during this tetroon run.

A summary of 5-minute averages of pollutant concentrations observed by the houseboat during the tetroon run is given in Table E-6. The

Table E-6

HOUSEBOAT DATA FOR 25 OCTOBER 1972, 1135 TO 1215 PST
(5-Minute Averages)

Time	NO (pphm)	NO_2 (pphm)	O_3 (pphm)	CO (ppm)	THC (ppm)	Nephelometer ($m^{-1} \times 10^4$)	CN ($cm^{-3} \times 10^{-3}$)
1135	5.3	5.9	2.3	5.7	2.2	0.6	3.5
1140	4.5	5.8	2.7	5.1	2.1	0.6	5.1
1145	4.4	5.4	2.8	5.4	2.1	0.6	13.7*
1150	6.0	5.7	3.1	5.6	2.1	0.5	21.7*
1155	11.8*	7.3	3.3	5.9	2.1	0.6	19.2*
1200	22.3*	7.5	3.6	5.5	2.1	0.5	12.9*
1205	8.8	5.6	3.8	5.7	2.1	0.6	8.6
1210	4.6	4.9	3.9	5.5	2.0	0.5	6.4
1215	1.95	5.2	3.9	5.8	2.0	0.5	3.4

* Exhaust gas contamination.

relative pollutant concentrations, particularly the NO to NO_2 ratio indicate the presence of well-aged smog, even though the tetroon run was begun downwind of the San Mateo Bridge. The source of pollutants is probably auto exhaust from the East Bay or South Bay. The emissions from automobiles on the San Mateo Bridge were not great enough to significantly alter the pollutant mixture.

During the 1135 tetroon run, supplementary pollutant measurements were also obtained with the helicopter to determine horizontal and vertical concentration gradients (the flight path may be found in Figure 9). The measurements obtained by the houseboat and helicopter are summarized in Table E-7 for the first 10 minutes of the tetroon run.

Table E-7

DATA FOR 25 OCTOBER 1972, 1137 TO 1148 PST
(1-Minute Averages)

Houseboat				Helicopter					
Time	NO (pphm)	NO_x (pphm)	O_3 (pphm)	Time	Alt (ft)	NO (pphm)	NO_x (pphm)	O_x (pphm)	Temp (^oC)
1137	5.6	11.9	2.3	1137	200	4.8	9.6	1.8	24.2
1140	5.3	11.9	2.3	1140	300	5.0	10.0	1.7	24.2
1142	4.5	11.6	2.7	1142	350	2.4	4.8	2.0	24.2
1148	4.9	10.7	2.7	1148	500	1.2	4.8	1.8	24.2

The helicopter then flew in a zigzag pattern over the San Mateo Bridge at 500 feet altitude until the east shore of the Bay was reached to determine concentration gradients of the source of pollution immediately upwind of the release point of the tetroon. An increase of about 1 pphm was noted in NO concentration following the initial crossing of the San Mateo Bridge followed by a decrease of about 1 pphm. As the eastern shore was reached, the NO and NO_x concentrations had increased to 3.6 pphm and 6.0 pphm, respectively. During the return travel crossing over and nearly parallel to the San Mateo Bridge, a peak concentration of 7.2 pphm of NO and 9.6 pphm of NO_x was observed. The helicopter returned to the tetroon at 1212 and began circling the tetroon.

The houseboat and helicopter measurements for the latter part of the tetroon run are summarized in Table E-8. The helicopter continued to track the tetroon until the tetroon went aground at 1248.

The helicopter measurements correlate reasonably well with the concentrations observed on the houseboat. The gradients in pollutant concentration are not marked in either the vertical or horizontal during this afternoon run. The measurement from the helicopter indicates that the pollutant concentrations decreased until near background levels were

Table E-8

DATA FOR 25 OCTOBER 1972, 1210 TO 1258 PST
(1-Minute Averages)

Houseboat					Helicopter					
Time	NO (pphm)	NO_x (pphm)	O_3 (pphm)	Temp (^oC)	Time	Alt (ft)	NO (pphm)	NO_x (pphm)	O_x (pphm)	Temp (^oC)
1210	6.8	13	3.9	24.4	1210	500	4.8	7.2	2.2	24.4
1212	6.4	12.3	3.5	24.1	1212	500	7.2	9.6		24.4
1215	2.9	8.9	3.9	23.8	1215	500	3.6	3.6	2.8	24.4
					1225	500	1.5	7.0	3.2	24.3
					1230	500	1.0	1.5	2.2	24.3
					1235		1.0	1.5	1.8	24.3
					1240		1.0	2.0	1.7	24.3
					1245		1.0	2.0	2.0	24.4
					1258		1.5	2.5	2.0	24.4

reached after the houseboat had terminated the run. An increase in NO and NO_x occurred at the end of the helicopter track with a reduction in tetroon altitude. Helicopter measurements for 25 October are shown in Table E-9.

After termination of the tetroon run, the houseboat had proceeded northward about 1 kilometer when the NO concentrations abruptly increased from about 5 pphm to concentrations as high as 45 pphm. The 5-minute averages for NO concentrations are summarized in Table E-10. The path of the houseboat is shown in Figure 7 (f). This concentration mapping procedure again indicates the inhomogeneity of pollutant distributions over the Bay.

The relative high concentration of NO observed from 1230 to 1250 over a distance of about 5 kilometers was not accompanied by an increase in CO, THC, or CN. On the basis of meteorological observation from shore stations and the houseboat, this "pocket" of high NO concentrations could not be attributed to the emissions from the power plants located at

Table E-9

HELICOPTER MEASUREMENTS FOR 25 OCTOBER 1972

Time (PST)	Altitude (ft)	CO* (ppm)	Ox (pphm)	Temp (°C)	NO (pphm)	NO_x (pphm)
Measurements made while following tetroon:						
0808				24.0	33	40
0810				24.1	18	22
0812	100			24.0	22	26
0814	190			24.0	22	26
0818	380			24.1	11	15
0824	600			24.0	7	11
Vertical concentration gradient measurements near San Mateo Bridge:						
0831	100			24.0	44	58
0832	130			24.0	29	51
0833	170			24.1	18	36
0834	220			24.0	11	22
0835	300			24.0	18	18
0837	400			23.9	11	15
0839	590			23.9	11	15
0840	720			24.0	7	7
0843	1400			24.0	3	7
0845	2420			24.0	7	7
0849	4820			23.8	7	7
Measurements made while following tetroon:						
1137	200		6.6	24.2	5	10
1140			4.0	24.2	6	12
1142	350			24.2	2	5
1143				24.2	2	2
1148	500			24.2	1	2

Table E-9 (Concluded)

Time (PST)	Altitude (ft)	CO* (ppm)	Ox (pphm)	Temp (°C)	NO (pphm)	NO_x (pphm)
Horizontal concentration gradient measurements:						
1150	500		2.3	24.2	1	2
1155	500		2.3	24.2	2	4
1200	500		3.1	24.2	4	6
1205	500	±0.5	2.1	24.2	5	6
1210	500		2.2	24.3	5	7
1212	500			24.4	7	10
Measurements made while following tetroon:						
1216	500		2.8	24.4	4	4
1224	500		3.2	24.3	2	4
1228	500	±0.5		24.3	2	2
1233	500		1.8	24.3	2	3
1238	500			24.4	2	4
1243		+1	2.0	24.3	4	4
1247				24.4	4	4

*The number is the CO concentration change over the indicated time interval.

Table E-10

HOUSEBOAT DATA FOR 25 OCTOBER 1972, 1220 TO 1255 PST
(5-Minute Averages)

Time	NO (pphm)	Position* X	Position* Y
1220	5.2	13.366	14.132
1225	19.4	13.128	16.914
1230	28.8	12.991	15.696
1235	39.3	12.853	16.478
1240	32.4	12.716	17.260
1245	26.5	12.578	18.042
1250	17.6	12.355	18.751
1255	6.7	12.925	19.388

*The grid coordinate overlay map is found in Appendix D, Figure D-1.

Potrero Point and Hunters Point. The ozone concentrations observed in this area increased to a maximum of 5.3 pphm, an indication of aging within the air mass. A corresponding increase in NO_2 from 4.4 pphm to a maximum of 8.2 pphm confirms the aging of the air mass. The source must be attributed on a meteorological basis to auto traffic on the San Mateo Bridge, a contribution from the East Bay, or both. However, the area of this "pocket" and the concentration of pollutants (particularly NO) within it are much higher than would be anticipated. Pollutant measurements from other days, 21 September and 2 November, indicate that the emissions from the Bay Bridge and the San Mateo Bridge are observed within 1 to 2 kilometers of the line source of the bridges before dissipating to background concentrations.

Aerosol particle counter (APC) data were also collected on 25 October and are summarized in Figure 12; the chemical analyses of the particulate matter collected on a high-volume filter may be found in Table 5 or Table C-4. In contrast to the APC data for 21 September, the particle size

distribution did not change with time during the tetroon run on 25 October. However, the meteorological conditions were very different, since hot, dry air from the southeast was blowing across the Bay. On the other hand, the chemical analysis of the collected particulate is similar to that collected on other days, notably 2 November and 6 November (see Appendix C, Table C-4 for complete data) when substantial amounts of marine air were sampled.

The low molecular weight of hydrocarbon distribution for 25 October for low molecular weight nonmethane hydrocarbons is summarized as follows:

Time (PST)	Ethylene (ppb)	Ethane (ppb)
0849	23	119
1002	26	26
1035	23	21

The C_4 to C_{10} hydrocarbon distribution for 25 October at 1029 is summarized in Table E-11; a range of concentrations of typical auto exhaust is included for reference.

The cryogenic sample that was collected at 0845 on 25 October is primarily unreactive hydrocarbons. The ratio of ethylene to ethane is 1.0 in contrast to fresh exhaust where the ratio ranges from 3 to more than 10. The higher molecular weight olefins are present in low concentrations. The C_9-C_{10} aromatic fraction seems to be unusually high and probably contains unresolved higher molecular weight paraffins.

C. 26 October

October 26 was selected for analysis not because of extensive photochemical activity, but to illustrate the dispersion of pollutants and the dilutional processes that are observed in complex wind flow patterns. Measurements were made immediately downwind of San Francisco (SF) from 0816 until 0906 along a 3.7-kilometer path parallel to the shore. High

Table E-11

CRYOGENIC TRAP DATA 25 OCTOBER 1972, 0845 PST

Hydrocarbon Class	Concentration ppb C	Concentration %	Typical Exhaust Range (%)[10]
Olefins			
Ethylene	18	1.2	12-13
Acetylene	21	1.4	9-11
C_4-C_5	23	1.6	4-6
C_6-C_7	13	0.9	1
C_8-C_{10}	2	0.1	1
Subtotal	77	5.3	25-30
Paraffins			
Ethane	18	1.2	0-2
Propane	15	1.0	1-2
C_4-C_5	523	35.9	8-12
C_6-C_7	274	18.8	6-14
C_8-C_{10}	179	12.3	7-13
Subtotal	1009	69.3	30-40
Aromatics			
Benzene	34	2.3	2-3
Toluene	80	5.5	5-6
Ethyl Benzene	20	1.4	1-2
m-,p-Xylene	71	4.9	6-8
o-Xylene	38	2.6	3-7
C_9-C_{10}	127	8.7	14-18
Subtotal	370	25.4	30-45
TOTAL	1456		

pollutant concentrations were measured while stopped and headed nto the wind, and while underway; there was no evidence of exhaust contamination from the houseboat. Extreme spatial and temporal variability was observed in pollutant concentrations, particularly the nitrogen oxide concentrations downwind of San Francisco. The variability of the concentrations of the nitrogen oxides at distances up to 1 kilometer downwind of the urban source reflects the multiplicity of sources in the city and shows that mixing to a relatively homogeneous state has not yet been completed. The observed inhomogeneities indicate that sampling runs to determine mass balance must be initiated at a sufficient distance from the urban source to ensure that a homogeneous air mass is studied, or else that the measurement program should include observations spaced horizontally, vertically, and temporally so that accurate estimates can be made of pollutant fluxes.

Pollutant concentrations, other than NO_x, also varied in this area, but their variability was considerably less than the nitrogen oxides. Table E-12 indicates the range of observed concentrations at several locations and along a 1.4 kilometer-segment of the boat's path.

Small helium-filled balloons were used to determine wind direction prior to the tetroon launch. Extrapolation of the paths of the small balloons indicated a sampling track north of Treasure Island (TI) and toward San Pablo Bay. The tetroon was launched at 0906 and passed directly over TI. Figure 13 shows the streamlines during the sampling interval and the path of the mobile laboratory. The average wind velocity was from 230 degrees at 5.3 m/sec along tetroon trajectory between the point of release and TI. Over this interval the concentration of NO dropped very rapidly from 40 to 11.5 pphm.

At 0912 the houseboat began a high-speed run around TI to intercept the tetroon on the eastern side. The tetroon rapidly ascended from 75

Table E-12

HOUSEBOAT DATA FOR 26 OCTOBER 1972, 0656 TO 0704 PST

Time (PST)	Location	Houseboat Operational Mode	Pollutant Concentrations					
			NO (pphm)	NO_2 (pphm)	O_3 (pphm)	CO (ppm)	THC (ppm C)	Nephelometer ($m^{-1} \times 10^4$)
0656 to 0700	100 meters north of west end of Bay Bridge	Stopped	23-30	2.9- 8.0	0.8-2.7	1.3-2.4	--	--
0716 to 0719	200 meters south of west end of Bay Bridge	Stopped	23-50	2.9-17.0	1.6-4.7	1.3-2.4	2.6-3.4	0.7-0.9
0815 to 0817	Foot of Ferry Building, SF	Stopped	21-34	2.9-11.5	4.7-5.5	0.75-1.7	2.3-2.6	0.8-0.8
0700 to 0704		Underway	23-50	2.9-17.0	1.6-4.7	1.3-2.4	2.6-3.4	0.7-0.4

to 270 meters altitude as it passed over TI and then descended to 200 meters altitude at the point of interception. During the high-speed run around TI, exhaust gas contamination from the houseboat or from the helicopter was not possible, but the measured pollutant concentrations nevertheless varied considerably as shown in Table E-13.

Table E-13

POLLUTANT CONCENTRATIONS DURING HIGH-SPEED RUN
AROUND TREASURE ISLAND
(1-Minute Averages)

Time (PST)	NO (pphm)	NO_2 (pphm)	O_3 (pphm)	CO (ppm)	THC (ppm)	Nephelometer ($m^{-1} \times 10^4$)	CN ($cm^{-3} \times 10^{-3}$)
0911	33.4	1.7	5.1	4.17	2.3	0.7	33.4
0912	43.1	3.7	5.5	2.76	2.3	0.5	21.9
0913	15.4	3.7	5.8	1.41	2.1	0.75	15.8
0914	17.7	3.3	5.9	1.73	2.2	0.7	12.3
0915	11.3	2.9	5.9	2.25	2.2	0.7	12.5
0916	9.9	2.5	5.3	2.53	2.3	0.8	18.8
0917	11.5	4.1	4.8	1.45	2.4	0.8	32.8
0918	6.0	2.9	5.1	1.27	2.4	0.8	28.9
0919	1.3	2.7	5.1	1.27	2.3	0.8	28.6

The observed changes in pollutant concentration during this period are probably indicative of the "boundary" between the polluted air from the San Francisco urban source and the clean marine air flowing through the Golden Gate. Of course, this is not a discrete boundary, but is instead marked by irregularities and consequent concentration fluctuations.

The helicopter was in operation during 26 October; however, the nitrogen oxides instrument was damaged by the helicopter vibration. The measured changes in total oxidant and CO concentration as measured along horizontal helicopter flights did not exceed ± 1 pphm for total oxidant or ± 1 ppm for CO. This is comparable to the gradients observed on the houseboat mobile laboratory. Since minimal data were obtained on this flight, the measurements or flight path are not presented here.

A cryogenic sample for HC distribution was obtained and analyzed by high resolution gas chromatography. The concentration of HC by class is shown in Table E-14. The cryogenic sample collected at 0929 on 26 October is primarily unreactive hydrocarbons. The ratio of ethylene to ethane is about 0.9, indicating well-aged pollutants rather than fresh exhaust. The C_9-C_{10} aromatic fraction seems to be high and probably contains unresolved higher molecular weight paraffins.

D. 2 November

The tetroon release from 1123 to 1317 has been selected for additional analysis because it is an example of nearly ideal meteorological conditions. When the houseboat left OP, a slow traverse was made across the Bay to map the pollutants and winds. The houseboat was purposely sailed into the wind during the traverse,and this heading was maintained while 5-minute pollutant averages and meteorological observations were made. The NO concentrations measured during the traverse (Figure 18) were extremely high; values above 0.6 ppm were observed in the middle of the Bay. There is little chance that these measurements could result from houseboat exhaust. The NO_2 and O_3 concentrations at the same point were about 5 and 1.5 pphm and the NO to NO_2 ratio was greater than 10, suggesting that the smog was not well aged. If the pollutants had been generated at San Jose the night (or day) before and was therefore well aged, a lower NO to NO_2 ratio would be expected.

To determine the source of this air mass, the early morning meteorological observations were considered. Surface winds on the east side of the Bay were the typical light drainage type of flow -- that is, east to southeast winds from San Jose to Oakland Airport. South Bay stations observed light to calm conditions from 0000 to 1000. After 1000, the winds were north to northwest and increased until 2100 that evening. The west side showed light easterly onshore winds that persisted through the

Table E-14

CRYOGENIC TRAP DATA, 26 OCTOBER 1972, 0929 PST

Hydrocarbon Class	Concentration ppb C	Concentration %
Olefins		
Ethylene	21	1.3
Acetylene	< 1	0.1
C_3-C_5	7	0.6
C_6-C_7	23	1.8
C_8-C_{10}	< 1	0.1
Subtotal	53	4.3
Paraffins		
Ethane	23	1.8
Propane	< 1	0.1
C_4-C_5	398	31.9
C_6-C_7	223	18.0
C_8-C_{10}	199	16.0
Subtotal	844	67.8
Aromatics		
Benzene	56	4.5
Toluene	88	7.1
Ethyl Benzene	24	1.9
m-,p-Xylene	78	6.2
o-Xylene	5	0.4
C_9-C_{10}	100	8.0
Subtotal	351	28.2
TOTAL	1247	

night and morning hours. The winds were calm or light in the Oakland area; northwesterly winds at Alameda and northeasterly winds at Oakland were observed. In San Francisco the winds were also calm or light, with the general northerly direction characteristic of marine air flow. The Oakland rawinsonde for 0400 shows a light north wind at 600 meters and northeast winds above. The San Jose rawinsonde for 0700 showed light variable winds; the 1200 release showed uniformly northerly winds. In summary, there was a general counterclockwise air circulation around the South Bay and a clockwise circulation in the North Bay.

The cloud cover (stratus) observations are the most revealing of the available data. The overcast layer of stratus -- typical in the Bay Area of strong marine air flow -- moved southward through San Francisco during the previous evening and the early morning hours to an area immediately south of a line between San Francisco and Oakland Airports. This is the approximate sample path of the houseboat transect (0830 to 0954). South of this line the Bay was clear throughout the period. These data are evidence of a general northwesterly air flow on the upper half of the Bay. Therefore, the source of the high NO concentrations is most likely San Francisco, and not San Jose.

The possible contribution from the PG&E power plants emissions was calculated using the method described for 21 September. These calculations showed that the maximum concentration of NO attributable to the stacks in the middle of the Bay is about 5 pphm.* Based on the meteorological data, the source of the pollution observed in the early morning is probably San Francisco, but the very high NO levels cannot be satisfactorily explained.

At 1124 a tetroon was released from a point midway between the Oakland Airport and San Francisco Airport. The surface wind was NNW at 2.2 m/sec. The

*This calculation assumed a mixing height of 150 meters, stability class 2, and a 4-mph northwest wind.

tetroon rose to an estimated altitude of 150 meters but scarcely moved for about 40 minutes. The winds throughout the Bay Area shifted suddenly and the stronger marine air flow carried the tetroon south of the San Mateo Bridge. Selected 5-minute averages are tabulated in Table E-15.

Table E-15

HOUSEBOAT DATA FOR 2 NOVEMBER 1972, 0846 TO 1244 PST
(5-Minute Averages)

Time	NO (pphm)	NO_2 (pphm)	O_3 (pphm)	CO (ppm)	THC (ppm)	Nephelometer ($m^{-1} \times 10^4$)	CN ($cm^{-3} \times 10^{-3}$)
0846	4.5	4.2	4.4	1.9	2.8	1.7	13.1
0911	50.8	3.5	1.2	1.5	2.7	1.2	23.5
0926	60.7	5.2	1.5	1.2	3.0	1.3	23.4
0941	20.3	6.0	1.3	2.1	3.4	1.2	29.8
0956	16.5	9.9	1.5	1.1	2.7	0.9	28.9
1006	20.6	6.8	1.6	3.7	2.9	1.1	34.4
1026	14.6	9.1	1.9	4.0	2.7	1.1	34.0
1036	10.4	8.9	2.3	2.3	2.7	1.2	29.4
1109	3.6	7.0	3.5	3.7	3.3	1.3	15.4
1114	2.9	7.1	3.5	3.7	2.8	1.1	11.5
1119	7.0	7.8	3.8	2.9	2.8	1.4	16.2
1124*	9.6	7.9	3.8	5.1	3.3	1.5	29.2
1128	15.1	7.9	3.8	4.5	3.2	1.4	16.4
1154	35.2	6.8	5.0	5.4	3.6	1.3	12.8
1219	4.3	7.8	5.0	5.2	4.5	1.3	18.3
1244	1.0	5.2	5.9	3.4	4.2	1.2	11.3

*Tetroon release

The wind measurements made on board between 0830 and 1043 were used in an attempt to determine the original of the air mass into which the 1124 tetroon was released. The best estimate is that the houseboat circled around this air mass between 0944 and 1040 but did not pass directly through it. The 5-minute averages in Table E-15 from 0846 to 1036 were obtained while the houseboat was in motion, thereby minimizing the chances of exhaust contamination. The variability of NO, NO_2, THC, and CO suggests that the pollutant mixture is by no means homogeneous.

The rise of NO concentration immediately following the tetroon release (1124) was accompanied by an increase in CO concentration and sporadic increases in CN concentration. The presence of all three components are strong evidence of contamination due to houseboat exhaust. In an attempt to avoid the exhaust, a helium-filled balloon was tethered at the base of the sample inlet mast. By its position relative to the houseboat's path, the vector sum of the surface wind and the relative wind due to the boat's motion could be estimated by the position of the tethered balloon. The tethered balloon was kept on the side or stern of the boat so that raw exhaust was not pulled into the sampling lines. However, it was not possible to avoid passing through old exhaust because it was necessary to sail in circles or figure eights to stay under the tetroon. Thus, fresh but not raw exhaust was sampled from about 1130 to 1210. Therefore, the NO concentrations observed during the experiment (Figure 14, from 0 to 30 minutes) are not representative of polluted air during that interval.

The data collected immediately prior to the tetroon release (1109 to 1119, Table E-15) are probably representative of the NO concentrations that would have been measured if the houseboat exhaust had not contaminated the air. The data suggest that, based on the low NO to NO_2 ratio, the air mass was well aged.

A limited amount of hydrocarbon distribution data are available for the tetroon release. The C_2 data are summarized in Table E-16; the concentration of propylene was below the detectability limit.

Table E-16

ETHANE, ETHYLENE, AND ACETYLENE CONCENTRATIONS,
2 NOVEMBER 1972

Time (PST)	Concentration (ppb) C_2H_6	C_2H_4	C_2H_2	C_3H_8
0848	22	47	< 1	< 1
0901	38	< 1	< 1	< 1
0946	136	127	31	18
0959	106	117	< 1	< 1
1030	77	141	36	42
1120	187	527	38	37

A leak in the sampling line occurred between 1030, the end of the run, which permitted the HC inlet system to sample some cabin air which was contaminated with ethylene from the O_3 analyzer. It was not discovered and stopped until after the run. The C_2-C_3 hydrocarbon data are not reliable after 1030 on 2 November 1972. Cryogenic samples were also collected at 0925 and 1100 (Table E-17). The 0925 sample is mainly unreactive hydrocarbons. The ratio of ethylene to ethane is 0.84 whereas typical ratios for fresh exhaust range from 3 to more than 10. The percentage of higher olefins is also relatively low. The C_9-C_{10} aromatic fraction seems to be too high since these compounds are generally more reactive than the C_6-C_8 aromatics. The fraction probably contains some higher paraffins that were not separated by our GC method. The 1100 hydrocarbon sample is also suggestive of partially aged smog. The ethylene to ethane ratio is 1.8. The biggest change is the 5 percent shift from aromatics to olefins plus the lower overall concentration (THC analyzer values averaged 3.0 and 2.4 ppm C, respectively). We conclude that the 1100 sample is fresher and more reactive than the 0925 sample.

The particulate data are discussed in the text of this report.

Table E-17

CRYOGENIC TRAP DATA, 2 NOVEMBER 1972

Hydrocarbon Class	Concentration 0925 PST ppb C	%	1100 PST ppb C	%
Olefins				
Ethylene	127*	4.44	141†	10.80
Acetylene	31*	1.08	36†	2.75
C_4-C_5	36	1.26	3.5	0.31
C_6-C_7	61	2.13	17	1.30
C_8-C_{10}	1	0.05	< 1	0.08
Subtotal	265	8.97	199	15.24
Paraffins				
Ethane	136*	4.76	77†	5.90
Propane	18*	0.63	42†	3.22
C_4-C_5	189	6.61	178	13.64
C_6-C_7	250	8.74	58	4.44
C_8-C_{10}	453	15.84	103	7.89
Subtotal	1046	36.59	458	35.10
Aromatics				
Benzene	47	1.64	10	0.77
Toluene	144	5.04	27	2.07
Ethyl Benzene	170	5.95	17	1.30
m-,p-Xylene	130	4.55	53	4.06
o-Xylene	54	1.89	29	2.22
C_9-C_{10}	1012	35.40	512	39.23
Subtotal	1557	54.46	648	49.66
TOTAL	2859		1305	

* C_2-C_3 data from 0946

† C_2-C_3 data from 1030

Appendix F

AIHL REPORT NO. 148 BY THE AIR RESOURCES BOARD

CHEMISTRY OF THE AEROSOL FOR THE SRI HOUSEBOAT PROJECT

Final Report

June 1973

AIHL Report No. 148

Prepared by:

S. Wall
J. J. Wesolowski

Supported by:

Air Resources Board
Contract 2-442

Air and Industrial Hygiene Laboratory
California State Department of Public Health
2151 Berkeley Way, Berkeley, CA 94704
June 1973

Preceding page blank

I. Introduction

This is the final report of the aerosol chemistry work carried out by AIHL in cooperation with the Stanford Research Institute as part of the SRI Houseboat feasibility study. This report details AIHL's role in the experiment, and presents and discusses the aerosol chemical data obtained.

II. The Role of AIHL in the Sampling Scheme

AIHL provided consultation, technical assistance, gas analyzer calibrations and performed chemical analysis of aerosols collected by SRI as part of the Houseboat Project. Dr. James Hart Smith of SRI consulted with the AIHL gas calibration group concerning calibration of their gas analyzers. AIHL calibrated the houseboat gas instruments on the day of the final SRI run. Dr. Smith and others of the SRI staff consulted with AIHL to learn the procedures for preparing and loading the Lundgren Impactor foils provided by AIHL. All filters and foils were washed and handled by SRI personnel subsequent to their return to AIHL for chemical analysis. Drs. Wesolowski and Appel participated in a houseboat run as observers and consultants.

III. Sampling Configuration on the Houseboat

The aerosol was collected by a probe separate from the gas probe. The flow characteristics were similar to probes used in the 1972 Aerosol Characterization Study (ACHEXI). The aerosol collection probe had a Reynolds number of 8,900 at 13 CFM and consisted of PVC tubing two and one-half inches in diameter. The Lundgren Impactor was mounted at a 45° angle to the inlet probe. This rather large angle was

necessary because of physical constraints on the boat. The impactor consisted of five stages and an after filter. Four stages, 1A, 2, 3 and 4, had impaction surfaces of two-inch strips of Teflon over which one-inch Mylar strips were placed. The stage 1B foil was sticky polyethylene. The after filter was Gelman GA-1 cellulose acetate. The theoretical cut-off points for the stages (cf. AIHL Report No. 137[1]) were as follows:

Lundgren Stage	Effective 50% Cut-Off Diameters in Microns
1-A	8
1-B	8
2	4
3	1.5
4	0.5
AF	< 0.5

IV. Aerosol Chemical Analysis Scheme

AIHL provided SRI with five sets of Lundgren foils, and ten after filters for the houseboat experiment. Various problems, including mechanical failures of the impactor and unusual weather, restricted the number of useful runs to those of November 2, November 6 and November 17, 1972. No chemical analysis was performed on the November 17 samples because the sampling was conducted for only one hour. Thus, the area over which the aerosol was collected was too small to be easily handled with the present analytical schemes. The most emphasis is placed on the November 2 run since this is the only day where more than one two-hour size cut was available for analysis.

V. Validation of Chemical Data Reported to SRI by AIHL

In order to determine the validity of the elemental data, inter-method comparisons were carried out on after filters and foils collected during this study.

a. After Filters: Neutron Activation Analysis (NAA) and X-ray Excited X-ray Fluorescence[2] Analysis (XRFA).

Bromine concentrations were compared on a series of eight randomly selected after filters from the houseboat experiment. There is reasonable agreement between NAA and XRFA (cf. Figure 1A). A regression line was fitted to the points. The slope of this dashed line, shown in Figure 1A, is 0.91 which is not significantly different from 1, i.e., equal concentrations. The largest discrepancy, HB1100 AF, is 15%.

b. Foils: Alpha X-ray Emission Analysis (α-XREA)[3] vs X-XRFA

Four elements were compared; bromine, zinc, calcium and iron. Three impactor runs were used for the comparison. For each run, one 2-hour sample was selected from each stage with a Mylar impaction surface. Thus, the comparison was based on 12 foils. For bromine and zinc, lower limits of detection were reported for many samples. For those cases where the results could be compared, the concentrations reported by the two methods agreed within experimental errors. The results for Ca and Fe are shown graphically in Figures 1B and 1C. For these elements the degree of agreement is not acceptable. α-XREA has in

the past had difficulty with calcium and iron, reporting values higher than those obtained by NAA and XRFA.[4] However, revisions in the α-XREA prior to analysis of the houseboat samples have greatly improved the agreement between α-XREA and other methods. Thus, we would have anticipated better agreement.

VI. Concentrations

Twenty-three chemical species were detected (see Table 1). For consistency in data evaluation XRFA concentrations are reported here. The sulfur, nitrogen and carbon analyses reported were performed by ESCA.[5] Since total filters were not available to AIHL, the total concentrations of chemical species had to be calculated by summing the species concentration for each of the Lundgren stages plus the after filter for each 2-hour sampling segment (see Table 2). Because of small loadings, many lower limits were reported for foil determinations. In calculating the total concentration for a species, lower limits were included in the summations as 1/2 the limit of detection ± 100%. The values listed in Table 2 are from three Lundgren runs: 0833 to 1120 and 1123 to 1317 on November 2, 1210 to 1405 on November 6. ESCA sulfur analysis was routinely reported as S^{+} (oxidized) and S^{-} (reduced) to reduce the time required to interpret typically complex spectra. However, a more detailed study indicated SO_4^{-2} to be more than 70% of the S^{+} listed in Table 2.[11] Analysis for nitrogen and carbon are excluded from this table since ESCA determinations for these species on the after filters is impractical due to the high background of the sampling substrate.

The concentrations for V, Cr, Mn, Fe, Cu, Zn, Se, Br, and Hg can be compared with a nine station study of San Francisco Bay Area aerosols conducted in July 1970.[6] Agreement between the houseboat data and the average for the nine stations of the 1970 study was within a factor of two except for Fe and Cu. Values for Fe listed in Table 2 were at least a factor of six lower and for Cu a factor of three lower than those reported for the 1970 San Francisco Bay Area study. These differences could be the result of a serious impactor bounce-off problem to be discussed in Section VII.

For the houseboat study correlation coefficients were calculated for pairs of the 20 species for the three houseboat sampling periods. The concentrations for each species were ranked and non-parametric correlation coefficients calculated.[7]

Because of the small number of sampling periods, conclusions concerning species pairs with correlation coefficients with absolute value < 1 are not drawn. From Table 3 correlated species fall into three groups as follows:

1. K, Ti, Cr, Mn, Ni
2. Fe, Ca, Zn, Cu
3. Pb, Br

Similar groupings of trace elements have been noted in previous aerosol studies. The cluster analysis used to interpret the data collected in the 1970 San Francisco Bay Area study determined Mn, Cr, and Fe to be

grouped with Al, Se, Ba, La and Sm with high intercorrelations among the group members. Since in the 1970 study these elements exhibited the same diurnal pattern as wind speed and were present in the relative abundances calculated for crustal rock, it was inferred that they were in the particles generated from the soil by the wind. The 1972 Aerosol Characterization Study (ACHEX) Phase 1 report[8] noted similarities in the diurnal pattern of Cr, Mn and Fe concentrations for samples collected at the San Jose BAAPCD station on days when the site was downwind of the San Francisco Bay. Less often, similar diurnal patterns were also reported for Ti, K, Mn, Cr, and Fe.

These elements, with the exception of Fe, are included in Group 1 listed above. The possibility that these elements are found in wind-blown soil particles is reinforced by the lack of positive correlation between elements of Group 1 and the combustion products Br and Pb (Group 3). It is interesting that the houseboat data indicated Fe correlated with other members of Group 2 such as Zn, when both the 1970 San Francisco Bay and 1972 ACHEX studies conclude Fe to be associated with the soil derived elements of Group 1. However, a similarity in the diurnal patterns for Fe and Zn was observed at the ACHEX Harbor Freeway site on particles less than 0.6 microns.[8] This could indicate that the apparent correlation of Fe and Zn seen for houseboat data was due to large wall losses because of the failure of the large soil derived particles, containing the majority of Fe, to stick on the Lundgren stages.

Correlations of Br and Pb (Group 3) concentrations in ambient particles has been well documented.[8,9] Consistencies in diurnal patterns for

these elements where noted for every ACHEX sampling site. Br/Pb ratios have been suggested as a means of distinguishing between aged and fresh automobile combustion aerosol.[8] Br/Pb ratios near 0.39 have been considered fresh aerosol while lower values represent progressively more aged particles based on the removal of bromine from the lead halides found in automobile exhaust. Br/Pb ratios less than .25 and wind patterns for houseboat sampling periods on the afternoon of the second and sixth of February indicate aging aerosol carried by northwesterly winds from the San Francisco vicinity to the south bay.

VII. Particle Size Distributions

Particle size distributions for Fe, Ca, Zn, Pb, Br, C, S^+ are shown in Figures 2A through 2F. Distributions for other chemical species were not included because the concentrations were below the limits of detection on most of the Lundgren impactor stages. With the exception of S^+ and C, the species concentrations plotted at "XA+ST" is the sum of the concentrations determined on stages 1A and 1B. The sticky polyethylene substrate used on stage 1B was not analyzed for C or S^+, thus, the concentrations plotted for C and S^+ at "XA+ST" does not include the contribution from stage 1B. From Figures 2A, 2C and 2E, Pb, Br, C, and S^+ were detected primarily on sub-micron particles for the three sampling periods. This is characteristic of combustion derived aerosol and was observed for Pb and Br in both the 1970 San Francisco Bay Area study and the 1972 ACHEX. The Pb and Br particle distributions are similar (Figures 2A, 2C, 2E). This was also observed in the San Francisco study.

Detailed analysis of the ESCA spectra for S indicates S^{+} to be primarily (~ 70%) sulfate on the after filter and almost entirely sulfate on the impactor stages. When S^{-} was present in levels above the limit of detection, it was reported to consist of equal amounts of elemental sulfur and sulfide.

Fe and Ca are most often described as soil derived elements to be found on larger particles corresponding to the first stages of the Lundgren impactor. This is considered generally true for San Francisco Bay aerosols.[10] Zn distributions, however, display both large and sub-micron particle concentration maxima.[10] Houseboat distributions (Figures 2B, 2D and 2F) show serious deviations from these findings. No concentration maxima on large particles was observed for Zn, Fe, or Ca. Because of the good correspondence of Br and Pb distributions with previous studies, it is doubtful that analytical errors can be a cause for the discrepancies. It is probable that the bounce-off problem for large particles discussed in AIHL Report No. 138 is of importance here. This problem is inherent in the use of dry impaction surfaces such as those employed for the houseboat sampling and indeed would cause the distributions to be skewed toward the small particle sizes.

VIII. Conclusions

The validation study results indicate that quality chemistry was possible on the particulate samples collected on the SRI Houseboat. Although there were only a small number of houseboat samples available to AIHL, agreement with previous S. F. Bay aerosol studies was obtained

for total concentrations for most chemical species measured and for many of the size distributions. The lack of heavy smog days reduced the number of chemical species which could be discussed. Nevertheless, the fact that the concentrations of many species could be obtained and some interpretation given, although very tentative, demonstrates the feasibility of obtaining significant data on the chemical composition of aerosol collected over two-hour intervals using the SRI Houseboat approach. Of course, the lack of secondary aerosol days during the last "smog" season precludes any comments about the feasibility of obtaining information about secondary aerosol formation using this approach.

Suggested changes which could improve the probability of collecting significant data during future houseboat sampling episodes include:

1. The use of sticky surface foils on all stages of the Lundgren impactor in order to substantially reduce the bounce-off of particles.

2. Total filters as well as after filters and impactor foils should be provided for elemental chemical analysis in order to obtain information on wall losses and also to obtain total particulate concentration data of higher accuracy than obtained by summing the stages and after filters.

3. Of course the main improvement is beyond our control, namely an increase in the number of days having significant secondary aerosol.

References

1. AIHL Report No. 137, B. R. Appel, J. J. Wesolowski, Calibration and Sampling Media Selection Studies with the Lundgren Impactor, Feb. 1973.

2. The NAA was carried out at Lawrence Livermore Laboratory by R. Ragaini and R. Kaifer, and the X-XRFA at Lawrence Berkeley Laboratory by R. Giauque.

3. α-XREA was performed at the Crocker Nuclear Lab., University of California, Davis by T. Cahill.

4. AIHL Report No. 134, J. J. Wesolowski, S. Wall, and S. Twiss, Interlaboratory Comparisons of Chemical Determinations from Aerosols Collected on Cellulose Filters, Feb. 1973.

5. Electron spectroscopy chemical analysis performed at Lawrence Berkeley Laboratory by T. Novakov.

6. "Trace Element Concentrations in Aerosols from the San Francisco Bay Area", W. John, R. Kaifer, K. Rahn, and J. J. Wesolowski, Atmospheric Environment, Vol. 7, p 107-118 (1973).

7. Spearman's rank order correlation.

8. Characterization of Aerosols in California Interim Report for Phase 1, G. Hidy *et al*.

9. "Lead and Bromine Particle Size Distributions in the S. F. Bay Area," C. Martens, J. J. Wesolowski, R. Kaifer, W. John. UCRL 74349.

10. Particle Size Distributions of S. F. Bay Area Ambient Air Trace Elements (Private communication with J. J. Wesolowski and R. Rogaini).

11. Detailed Study of ESCA Spectra (Private communication with A. Harker, Lawrence Berkeley Laboratory).

Table 1

CONCENTRATIONS OF CHEMICAL SPECIES FOR HOUSEBOAT SAMPLING
SAMPLES LISTED WERE FOILS AND FILTERS USED AS COLLECTION MEDIA IN THE HOUSEBOAT LUNDGREN IMPACTOR
(Values in $\mu g\ m^{-3}$)

SPECIES	DATE AND TIME 11-2-72 - (0833-1120)						DATE AND TIME 11-2-72 (1123-1317)						DATE AND TIME 11-6-72 - (1210-1495)					
	HB1001EA		HB1002E2	HB1003E3	HB1001E4	HB1103AF	HB1001EA		HB1002E	HB1003E3	HB1004E4	HB1104AF	HB1005EA		HB1006E2	HB1007E3	HB1008E4	HB1108AF
C	< .20	–	< .20	.25 (.12)	1.5 (.70)	–	< .20	–	< .20	.20 (.01)	.60 (.30)	–	< .20	–	< .20	.20 (.10)	.20 (.10)	–
S+	< .20	–	< .20	< .20	.20 (.10)	1.4 (.30)	< .20	–	< .20	< .20	.20 (.10)	.55 (.15)	< .20	–	< .20	< .20	< .20	1.7 (.50)
S–	< .20	–	< .20	< .20	< .20	< .20	< .20	–	< .20	< .20	< .20	< .15	< .20	–	< .20	< .20	< .20	< .20
N+	< .40	–	< .40	< .40	.45 (.20)	–	< .40	–	< .40	< .40	< .40	–	< .40	–	< .40	< .40	< .40	–
N–	< .40	–	< .40	< .40	.75 (.35)	–	< .40	–	< .40	< .40	.45 (.20)	–	< .40	–	< .40	< .40	< .40	–
	HB1001XA	HB1011ST	HB1002X2	HB1003X3	HB1004X4	HB1103AF	HB1001XA	HB1011ST	HB1002X2	HB1003X3	HB1004X4	HB1004AF	HB1005XA	HB1012ST	HB1006X2	HB1007X3	HB1008X4	HB1104AF
K	< .057	< .146	< .091	< .087	< .087	.217 (.036)	< .088	< .146	< .087	< .086	< .090	.255 (.050)	< .058	< .087	< .057	< .056	< .054	.211 (.063)
Ca	< .038	< .076	.046 (.014)	.119 (.215)	.075 (.014)	.050 (.021)	< .039	< .079	.042 (.014)	.056 (.014)	.020 (.013)	.073 (.029)	< .025	< .047	.015 (.009)	.043 (.028)	.024 (.008)	< .165
Ti	< .017	< .026	< .017	< .017	< .017	.013 (.005)	< .017	< .027	< .018	< .017	< .017	.021 (.012)	< .011	.009 (.006)	< .019	< .011	< .011	< .044
V	< .013	< .020	< .012	< .012	< .012	< .019	< .013	< .021	< .013	< .012	< .012	< .026	< .008	< .013	< .008	< .008	< .008	< .034
Cr	< .010	< .014	< .009	< .009	< .010	< .015	< .010	< .015	< .010	< .009	< .010	< .021	< .006	< .009	< .006	< .006	< .006	< .027
Mn	< .005	< .011	< .008	< .008	< .008	< .012	< .008	< .012	< .008	< .008	< .008	.010 (.006)	< .005	< .007	< .005	< .005	< .005	< .020
Fe	< .006	< .010	.006 (.002)	.109 (.010)	.095 (.010)	.065 (.003)	< .007	.031 (.004)	.012 (.003)	.031 (.003)	.043 (.004)	.113 (.007)	.015 (.002)	.009 (.002)	< .004	.026 (.003)	.012 (.002)	.041 (.007)
Ni	.003 (.002)	< .006	.005 (.002)	< .004	.003 (.002)	.005 (.002)	.007 (.002)	< .006	.003 (.002)	.004 (.002)	< .004	.033 (.003)	< .003	< .004	< .003	.005 (.001)	< .003	.006 (.003)
Cu	.003 (.002)	< .006	< .005	.003 (.002)	.005 (.002)	< .009	.004 (.002)	< .006	< .005	< .004	< .005	< .012	< .003	< .004	< .003	< .003	.002 (.001)	< .014
Zn	< .006	.013 (.008)	< .006	.013 (.005)	.053 (.005)	.020 (.002)	< .006	< .024	< .006	.003 (.002)	.039 (.004)	.041 (.003)	< .004	.033 (.005)	< .004	.003 (.002)	.008 (.002)	.013 (.003)
Ga	< .003	< .005	< .003	< .003	< .004	.007 (.003)	< .003	< .005	< .003	< .003	< .003	< .007	< .002	< .003	< .002	< .002	< .002	< .010
As	< .003	< .005	< .003	< .006	< .010	< .021	< .003	< .005	< .003	< .004	< .007	< .026	< .002	< .003	< .002	< .003	< .004	< .025
Se	< .003	< .006	< .003	< .003	< .004	< .006	< .004	< .006	< .004	< .003	< .004	.011 (.003)	< .002	< .004	< .002	< .002	< .002	< .009
Br	< .004	.005 (.003)	< .004	.030 (.003)	.050 (.005)	.244 (.010)	< .004	< .007	< .004	.005 (.002)	.021 (.002)	.210 (.008)	< .003	.003 (.002)	< .003	.006 (.001)	.008 (.001)	.220 (.010)
Rb	< .006	< .012	< .006	< .006	< .007	< .010	< .006	< .012	< .006	< .006	< .006	.009 (.005)	< .004	.004 (.003)	< .004	< .004	< .004	< .017
Sr	< .003	< .015	< .008	< .008	< .008	< .011	< .008	< .015	< .008	< .008	< .008	.012 (.005)	< .005	< .009	< .005	< .005	< .005	.017 (.007)
Hg	< .005	< .009	< .006	< .006	< .006	< .010	< .006	< .009	< .006	< .006	< .006	< .013	< .004	< .006	< .004	< .004	< .004	< .016
Pb	< .006	< .009	< .005	.081 (.005)	.239 (.024)	1.95 (.040)	< .007	< .010	.006 (.002	.029 (.003)	.099 (.010)	1.10 (.040)	< .004	< .006	< .004	.025 (.003)	.048 .005	1.250 .050
Br/Pb	–	–	–	.357	.209	.232	–	–	–	.172	.212	.191	–	–	–	.270	.167	.198

Key:

< Species concentration below the limit of detection.
– No data available.
( ) Error limits enclosed.

Reproduced from best available copy.

TABLE 2

TOTAL CONCENTRATION BASED ON* SUMS OF IMPACTOR STAGES AND AFTER FILTER
(Values in $\mu g/m^3$)

Date (Time PST)	11-2-72 (0833-1120)	11-2-72 (1123-1317)	11-6-72 (1210-1405)
S^+	1.90 ± .36	1.05 ± .25	2.10 ± .54
$S^=$	.50 ± .22	.48 ± .21	.50 ± .22
K	.46 ± .12	.50 ± .12	.37 ± .09
Ca	.345 ± .054	.25 ± .057	.21 ± .055
Ti	.060 ± .023	.070 ± .025	.053 ± .025
V	.039 ± .014	.048 ± .021	.039 ± .020
Cr	.034 ± .014	.038 ± .016	.030 ± .016
Mn	.028 ± .012	.032 ± .012	.024 ± .012
Fe	.272 ± .016	.234 ± .011	.105 ± .008
Ni	.021 ± .005	.052 ± .006	.018 ± .004
Cu	.021 ± .006	.020 ± .009	.016 ± .007
Zn	.105 ± .011	.101 ± .014	.061 ± .007
Ga	.016 ± .004	.013 ± .006	.011 ± .006
As	.024 ± .012	.024 ± .014	.020 ± .013
Se	.012 ± .005	.022 ± .006	.010 ± .005
Br	.333 ± .012	.244 ± .010	.270 ± .010
Rb	.024 ± .010	.027 ± .010	.021 ± .009
Sr	.030 ± .013	.036 ± .012	.033 ± .010
Hg	.021 ± .009	.023 ± .010	.019 ± .009
Pb	1.38 ± .050	1.24 ± .050	1.34 ± .050

* In calculating the total concentration the determinations below the limit of detection were included in the summations as 1/2 the limit of detection ± 100%.

The sums of the errors were calculated as the square root of the sum of the squares of each error.

TABLE 3

NON-PARAMETRIC CORRELATION COEFFICIENTS* FOR PAIRS OF CHEMICAL SPECIES - HOUSEBOAT STUDY

Samples Collected Nov. 2 and Nov. 6, 1972

	K	Ti	Cr	Mn	Ni	Se	Rb	Hg	Fe	Ca	Zn	Cu	Ga	Pb	Br	S^+	$S^=$	Sr	As	V
Ti	1																			
Cr	1	1																		
Mn	1	1	1																	
Ni	1	1	1	1																
Se	1	1	1	1	1															
Rb	1	1	1	1	1	1														
Hg	1	1	1	1	1	1	1													
Fe	.50	.50	.50	.50	.50	.50	.50	.50												
Ca	.50	.50	.50	.50	.50	.50	.50	.50	1											
Zn	.50	.50	.50	.50	.50	.50	.50	.50	1	1										
Cu	.50	.50	.50	.50	.50	.50	.50	.50	1	1	1									
Ga	.50	.50	.50	.50	.50	.50	.50	.50	1	1	1	1								
Pb	-.50	-.50	-.50	-.50	-.50	-.50	-.50	-.50	.50	.50	.50	.50	.50							
Br	-.50	.50	-.50	-.50	-.50	-.50	-.50	-.50	.50	.50	.50	.50	.50	1						
S^+	-1	-1	-1	-1	-1	-1	-1	-1	-.50	-.50	-.50	-.50	-.50	.50	.50					
$S^=$	-.62	-.62	-.62	-.62	-.62	-.62	-.62	-.62	.12	.12	.12	.12	.12	.87	.87	.87				
Sr	.50	.50	.50	.50	.50	.50	.50	.50	-.50	-.50	-.50	-.50	-.50	-1	-1	-.50	-.62			
As	.87	.87	.87	.87	.87	.87	.87	.87	.87	.87	.87	.87	.87	.12	.12	-.62	-.12	.12		
V	.87	.87	.87	.87	.87	.87	.87	.87	.12	.12	.12	.12	.12	-.62	-.62	-.62	-.50	.87	.62	
TOTAL	-.50	-.50	-.50	-.50	-.50	-.50	-.50	-.50	.50	.50	.50	.50	.50	1	1	.50	.87	-1	.12	-.50

* Spearman's ρ

Figure 1A

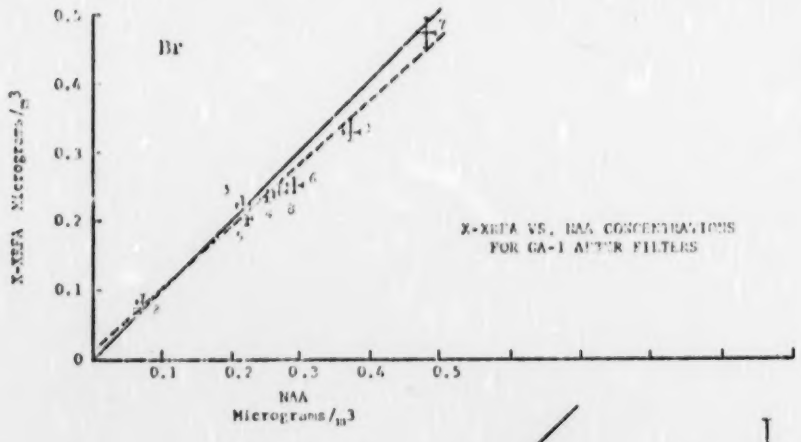

1. HB1100AF
2. HB1101AF
3. HB1102AF
4. HB1103AF
5. HB1104AF
6. HB1105AF
7. HB1106AF
8. HB1108AF

Figure 1B

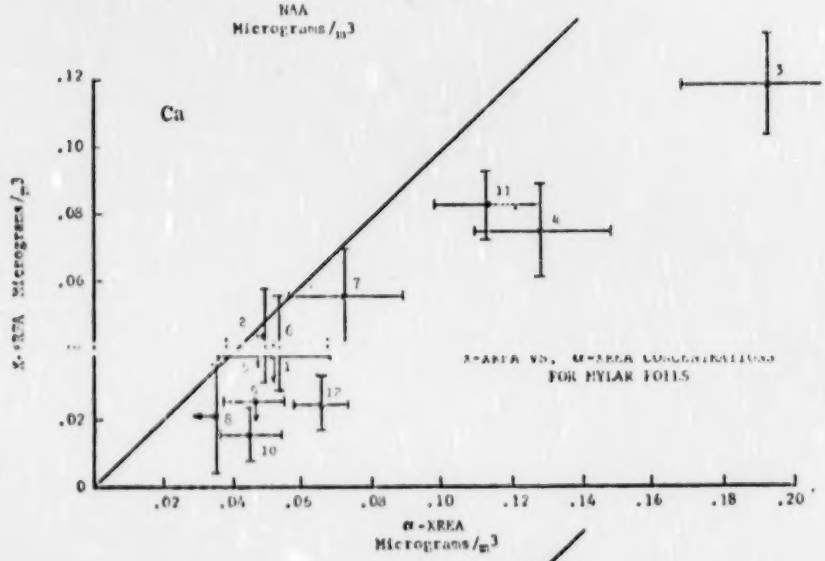

0910-1100

1. HB1001XA
2. HB1002X2
3. HB1003X3
4. HB1004X4

1117-1317

5. HB1001XA
6. HB1002X2
7. HB1003X3
8. HB1004X4

1210-1405

9. HB1005XA
10. HB1006X2
11. HB1007X3
12. HB1008X4

Figure 1C

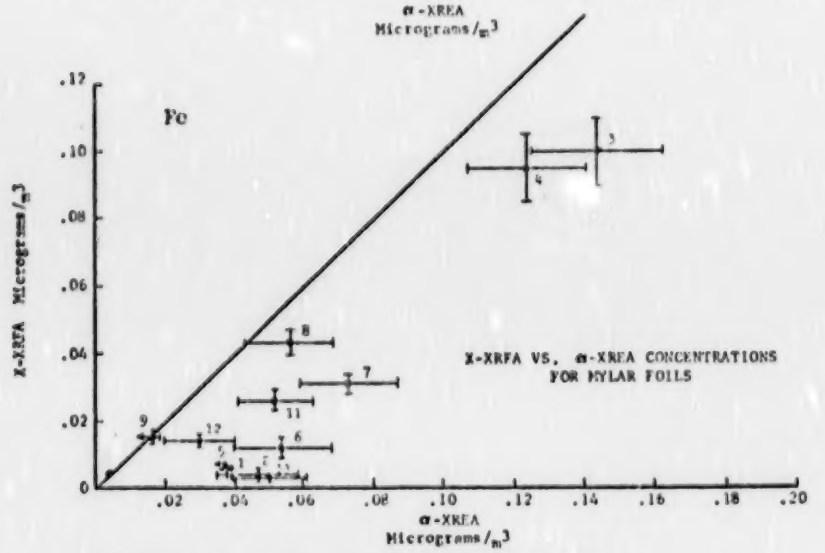

0910-1100

1. HB1001XA
2. HB1002X2
3. HB1003X3
4. HB1004X4

1117-1317

5. HB1001XA
6. HB1002X2
7. HB1003X3
8. HB1004X4

1210-1405

9. HB1005XA
10. HB1006X2
11. HB1007X3
12. HB1008X4

(↓ indicates concentration below the limit of detection)

PARTICLE SIZE DISTRIBUTIONS FOR ROVERBOAT SAMPLING

(↓ Indicates concentration below the limit of detection)

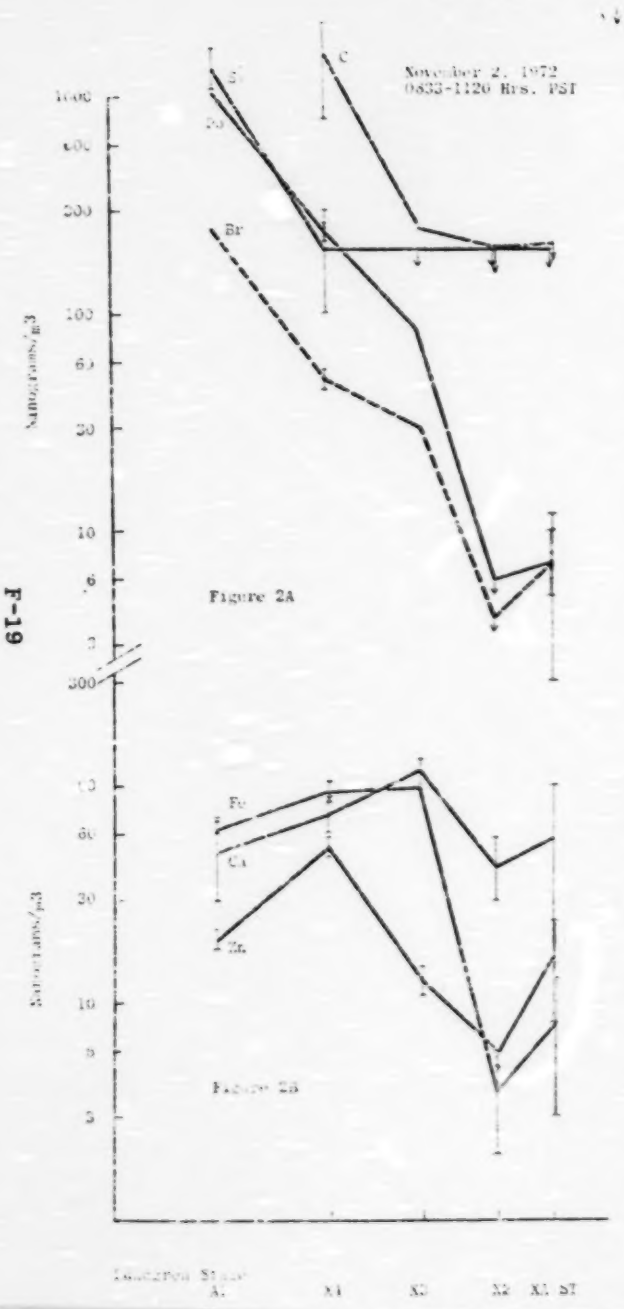

Figure 2A

Figure 2B

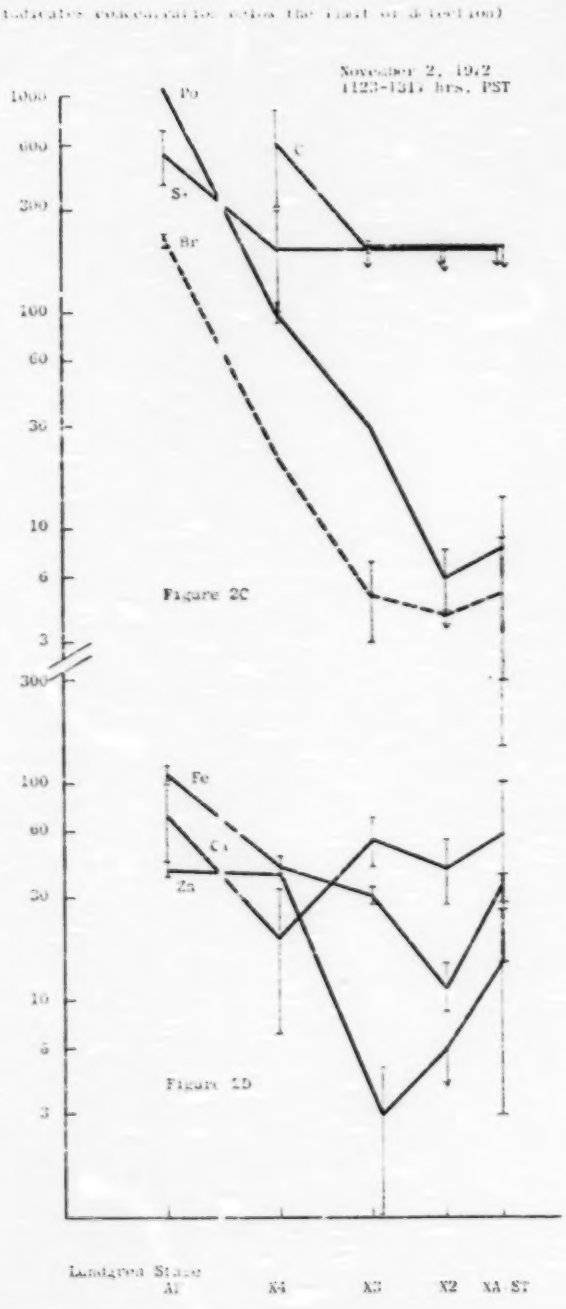

Figure 2C

Figure 2D

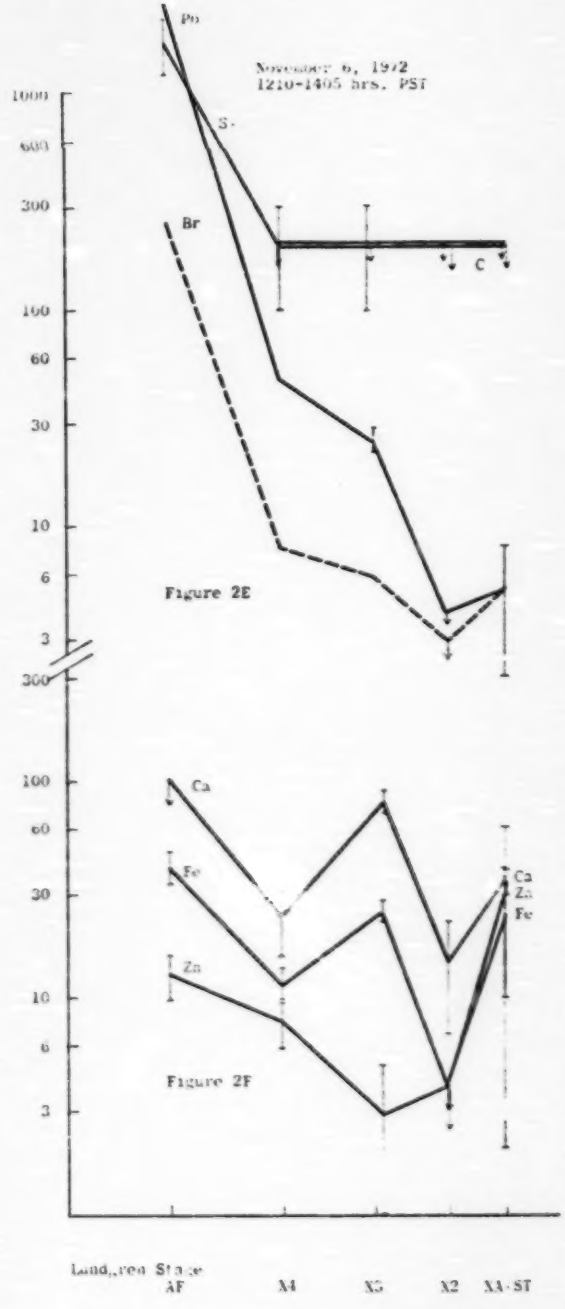

Figure 2E

Figure 2F

REFERENCES

1. A. Q. Eschenroeder, J. R. Martinez, and R. A. Nordsieck, "Evaluation of a Diffusion Model for Photochemical Simulation" Final Report, Environmental Protection Agency Contract No. 68-02-0336, General Research Corporation, Santa Barbara, California (1972).

2. J. H. Seinfeld, P. M. Roth, and S. D. Reynolds, "Simulation of Urban Air Pollution", Manuscript to be published in Advances in Chemistry.

3. L. R. Wayne, M. Danchick, M. Weisburd, A. Kokin, and A. Stein, "Modeling Photochemical Smog on a Computer for Decision Making," J. Air Poll. Contr. Assoc., Vol. 21, pp. 334-340 (1971).

4. M. C. McCracken, T. V. Crawford, K. R. Peterson, and J. B. Knox, "Development of a Multibox Air Pollution Model and Initial Verification for the San Francisco Bay Area" Report No. UCRL 73348, Lawrence Radiation Laboratories, Livermore, California (1971).

5. Bay Area Air Pollution Control District, "Contaminant and Weather Summary" (September 1972).

6. Bay Area Air Pollution Control District, "Contaminant and Weather Summary" (October 1972).

7. Bay Area Air Pollution Control District, "Contaminant and Weather Summary" (November 1972).

8. C. L. Smalley, "A Survey of Air Flow Patterns in the San Francisco Bay Area," Mimeographed paper published by U.S. Weather Bureau, S.F. International Airport (1957).

9. D. L. Blumenthal, and T. B. Smith, "Aerosol Characterization Program, Preliminary Airborne Sampling Program", Monthly Report No. 4, Contract No. ARB-358, North American Rockwell Science Center, Thousand Oaks, California (1972).

10. Bay Area Air Pollution Control District, "Air Pollution and the San Francisco Bay Area," (1972).

11. D. H. Slade, "Meteorology and Atomic Energy", U.S. Atomic Energy Commission, Oak Ridge, Tennesse (1968).

12. J. H. Smith, "Motor Fuel Composition and Photochemical Smog," a report to American Petroleum Institute, SRI Project 8558, Stanford Research Institute, Menlo Park, California (October 1971).

13. P. A. Leighton, Photochemistry of Air Pollution, pp 152-157, Academic Press, New York (1961).

14. K. L. Demergian, J. A. Kerr, and J. G. Calvert, "The Mechansim of Photochemical Smog Formation," The Chemistry Department, The Ohio State University, Columbus, Ohio (1972).

15. W. A. Williams, and R. E. DeMandel, "Land-Sea Boundary Effects on Small-Scale Circulation," Progress Report No. 2, National Science Foundation Grant GP-4248, San Jose State College, San Jose, California (1966).

16. U.S. Weather Bureau, "Climatography of the United States No. 86-4, Decennial Census of United States Climate, Climatic Summary of the United States--Supplement for 1951 through 1960, California," Washington, D.C. (1966).

17. C. P. Patton, "Climatology of Summer Fogs in the San Francisco Bay Area," University of California Publications in Geography, University of California Press, Berkeley, Vol. 10, pp. 113-200 (1959).

18. G. B. Bell, "The Use of Meteorological Data in Large Scale Air Pollution Surveys," Bureau of Air Sanitation, State of California, Berkeley, SRI Project 2238, Stanford Research Institute, Menlo Park, California (1958).

19. D. Ahrens, and A. Miller, "Variations of the Temperature Inversion over the San Francisco Bay Area," Department of Meteorology, San Jose State College (February 1969).

20. J. S. Sandberg, and R. H. Thullier, "Oxidant Levels Over San Francisco Bay and Adjacent Land Stations," J. Air Pollution Control Association, Vol. 20, pp. 599-602 (1970).

21. U.S. Department of Health, Education, and Welfare, Publication No. 999-AP-38.

22. D. A. Levaggi, Environ. Sci. and Tech., Vol. 6, pp. 250-252 (1972).

23. Annual Book of ASTM Standards No. 23, "Proposed Method of Test for Sulfur Dioxide Content of the Atmosphere (West-Gaeke Modification of the Kozlyaeva Method)," pp. 964-970 (1970).

24. C. T. O'Konski and G. J. Doyle, Anal. Chem., Vol. 27, pp. 694-701 (1955).

25. R. D. Cadle, Particle Size, p. 33 (Reinhold Publishing Corp., New York, 1965).

26. L. Kahn and F. T. Brezenski, "Determination of Nitrate in Estuarine Waters," Environ. Sci. and Tech., Vol. 1, pp. 488-491 (1967).

27. F. Ludwig, et. al., "Size Determination of Atmospheric Sulfate and Organic Particulates," SRI Interim Report Project PAU-4748, Stanford Research Institute, Menlo Park, California pp. 30-34 (December 1964).

28. D. M. Coulson and L. A. Cavanagh, "Automatic Chloride Analyzer," Anal. Chem., Vol. 32, pp. 1245-1247 (1960).

29. D. M. Coulson and D. L. Haynes, "Survey of Manual Methods of Measurements of Lead, Cadmium, Mercury, Selenium, Asbestos, and Beryllium," Final Report for Phase 1, SRI Project SCU-1374, Stanford Research Institute, Menlo Park, California, Section C of Appendix I (December 1972).

30. C. E. Junge, Chapter 2, Air Chemistry and Radioactivity, (Academic Press, New York, 1963).

31. D. B. Turner,"A Diffusion Model for a Urban Area," J. Appl. Meteorol., Vol. 3, pp. 83-91 (1964).